MOLECULAR MECHANISMS OF STRESS TOLERANCE IN PLANTS

A Dissertation
Presented to
The Faculty of the Graduate School
At the University of Missouri-Columbia

In Partial Fulfillment
of the Requirements for the Degree

Ph.D. in Plant, Insect and Microbial Sciences

By

CATHERINE G. ESPINOZA

Dr. Gary Stacey, Dissertation Supervisor

DECEMBER 2015

The undersigned, appointed by the Dean of the Graduate School,

have examined the Dissertation entitled

MECHANISMS OF STRESS TOLERANCE IN PLANTS

Presented by CATHERINE G. ESPINOZA

A candidate for the degree of

Ph.D. in Plant, Insect and Microbial Sciences

And hereby certify that, in their opinion, it is worthy of acceptance.

_____

Dr. Gary Stacey

_____

Dr. Walter Gassmann

_____

Dr. James Schoelz

_____

Dr. John Walker

DEDICATION

This dissertation is dedicated in loving memory of my grandmother, the kindest and strongest woman I ever knew and a genuine plant scientist

Isolina Figueroa Martinez

December 3, 1928 – December 21, 2010

ACKNOWLEDGEMENTS

First of all, I would like to thank my advisor, Dr. Gary Stacey, for giving me the opportunity to complete my Ph.D. degree in his lab

I will be forever thankful to Drs. James Schoelz and Mannie Liscum for his enormous support while confronting difficult times in the middle of my degree.

Many thanks to my Graduate Committee members, John Walker, Walter Gassmann and Jim Schoelz for their suggestions and support throughout my graduate career.

I would like to express my appreciation to the former and current lab members of the Stacey lab for all their guidance and moral support, especially, Drs. Kiwamu Tanaka, Yan Liang, Katalin Tóth, Yanrong Cao and Sung-hwan Cho. I would also like to acknowledge the funding support from USDA CSREES-NRI grant to Dr. Mel Oliver (USDA-ARS-PGRU) and Robert Sharp, and from the Division of Plant Sciences and the Graduate school to support my studies. I would also like to extend my appreciation to the faculty, post-docs, staff and graduate students of the Division of Plant Sciences, the Life Sciences Center and the Interdisciplinary Plant Group who provided assistance and friendship during these years.

Lastly, but not least, I would like to express my heartfelt gratitude to Rahul Patharkar and my family for their unconditional love and support during my time at MU.

TABLE OF CONTENTS

LIST OF FIGURES

LIST OF TABLES

Chapter 2

Chapter 3

Appendix 1

ABSTRACT

Environmental stress conditions such as drought, salt stress and pathogenic fungi affect negatively plant growth and productivity. Therefore, it is necessary to search for new genetic components and strategies for improving resistance and tolerance in crops. In the present thesis, we describe two different approaches that increase our understanding of mechanisms of stress tolerance in plants. The first approach is to study an extreme adaptation to dehydration tolerance from a plant than can "resurrect" after being completely dried. The second study addresses how plant might respond to two different stresses simultaneously, and how one stress can enhance the response to the other.

In Chapter 2, we investigate the dehydration tolerance mechanism in the model resurrection grass species *Sporobolus stapfianus* using a large scale expression profiling of leaf tissues at full hydration, during drying and after re-watering. This study provides some important insights into the gene regulatory mechanisms used by this interesting plant during severe vegetative desiccation and subsequent recovering during re-watering. We also found some genes that are differentially expressed between *S. stapfianus* and its desiccation sensitive sister species *S. pyramidalis*. These genes are considered potential candidates for engineering drought tolerant crops.

Previous studies have shown a positive effect of chitin (released from the fungal cell wall) on salinity tolerance. In Chapter 3, we explore the cross talk between salt stress and chitin-triggered immune responses. Our results demonstrate a physiological and biochemical link between salinity stress and chitin-triggered innate immunity. Chitin receptors, CERK1 and LYK4, and ANN1, a NaCl- induced calcium permeable channel, interact physically at the plasma membrane and are necessary to modulate early responses (e.g. Ca^{2+} signaling) to both stresses. Understanding these layers of cross-talk may lead to more sustainable methods to employ innate immunity to protect against both biotic and abiotic stress induced crop losses.

Chapter 1

General Introduction

Environmental stress conditions such as drought, salinity or pathogen infection can have devastating impacts on plant growth and yield. For example, in 2012, the impact of drought in the US affected 80% of farmlands and caused 31 billions of dollars in agricultural-related losses (http://www.ers.usda.gov ; http://www.ncdc.noaa.gov/billions/events). Likewise, salinity of soils has a negative impact on plan growth and yield. Salinity is a serious problem in Australia, where 60% of farmland is affected, and also in the US where 30% of all irrigated land is affected [1]. Unfortunately, these environmental constraints do not seem to be improving. Global climate change predicts increased temperatures and decreased rainfall, and is expected to exacerbate the negative effects of water deficit on agriculture. Decreased rainfall will increase the area of irrigated land, which will result in soil salinization. In addition to abiotic stresses, plants face the threat of infection by pathogens (bacteria, fungi, viruses and nematodes) and attack by herbivore pests. A recent study showed that the number of reported plant infecting fungi has increased dramatically in the last decade causing very dramatic crop yield losses [2]. Rice blast, for example, causes 10-35% crop losses and wheat stem rust can destroy up to 100% of the wheat fields. Therefore, it is necessary to study the plant mechanisms of stress tolerance in plants to search for new genetic components and strategies for improving resistance and tolerance in crops.

Dehydration tolerance mechanisms

Plants have developed different strategies to cope with loss of water. Drought tolerance can be defined as tolerance to sub-optimal water availability, and drought tolerant plants use strategies to maintain water in the cell, e.g. stomatal closure or osmotic adjustment. Dehydration tolerance is defined as tolerance of water loss from the cell.

Only very few plants exhibit desiccation tolerance, which is defined as the tolerance to drying to equilibrium with air.

In order to assess dehydration stress, it is necessary to measure accurately the water status of the plant. Water status is described in scientific reports in different ways, as water potential, relative water content (RWC) or water content of tissues. Water potential is defined as the chemical potential of water in a system, compared to a standard of pure water (0 MPa) at the same temperature. Most plants tolerate dehydration levels of 0 to -4 MPa. RWC relates to the amount of water remaining after dehydration in the tissues in comparison to the water when at full turgor, and is expressed as percentage (% RWC). Water content describes the amount of water as a fraction or percentage of the sample fresh or dry weight, e.g. H_2O per g DW (dry weight)[3].

Desiccation tolerance (DT) is a complex trait that is present in reproductive structures (pollen and seeds) of vascular plants. DT in vegetative tissues is also relatively common in less complex plants such as bryophytes and lichens but rare in pteridophytes and angiosperms and absent in gymnosperms [4, 5]. It is estimated that 275 to 325 desiccation-tolerant species of vascular plants exist: 9 families of pteridophytes and 7 families of angiosperms contain desiccation-tolerant sporophytes. Ferns and allies seem relatively rich in desiccation-tolerant species, including the family Pteridaceae and the genera *Cheilanthes* and *Selaginella*. Monocotyledonous families Velloziaceae and Poaceae have 200 and 39 desiccation tolerant species, respectively. Among the angiosperms, one small family, Myrothamnaceae is entirely desiccation-tolerant [6].

Phylogenetic studies suggested that the initial evolution of DT in aerial tissues was crucial in the colonization of the land by primitive plants. DT in earlier plants might resemble the DT found in modern day DT mosses. As plants evolved and acquired more complex morphologies and structures to avoid water loss, vegetative DT was lost in most plants but was recruited and maintained in reproductive organs like seeds and pollen. Vegetative DT in angiosperms subsequently re-evolved independently at least eight times as an adaptation of seed desiccation tolerance DT [6, 7].

Different mechanisms of desiccation tolerance have been described. In less complex plants, like mosses, DT is constitutive coupled with an inducible repair mechanism after rehydration of the tissues. Club mosses, e.g. *Selaginella lepidophylla*, have both constitutive and inducible DT. Ferns possess a seasonally regulated desiccation tolerance mechanism and angiosperms have an inducible mechanism [6].

Our model plant, the South African resurrection grass *Sporobolus stapfianus* Gandoger (Family Poaceae), is capable of surviving equilibration with air at 2% relative humidity (RH) (equal to -540 MPa), which is a hundred times lower compared to what most crop plants can tolerate [8, 9]. Proteome analysis in *S. stapfianus* dehydrated leaves (30% RWC) revealed the possible role of protein kinase-based signaling cascades and the brassinosteroid hormones in regulating mechanisms of cellular protection [10]. Metabolome analysis, using a sister-group comparison of *S. stapfianus* and its desiccation sensitive sister species *S. pyramidalis,* was used to compare metabolites in responses to different levels of dehydration [11]. *S. stapfianus* appeared to be primed metabolically for dehydration tolerance by accumulating osmolytes, such as sugar alcohols and amino-acids under well-watered conditions. Initial responses to dehydration were different in these sister species. The DT sensitive *S. pyramidalis* showed little metabolic response with a modest increase of proline, fructose and glucose that helped to maintain cell turgor and slow water loss. Meanwhile, *S. stapfianus* responded quickly to produce osmolytes (amino-acids, carbohydrates, sugar alcohols) and antioxidants (β-tocopherol) to delay the loss of water and to protect cell membranes from lipid peroxidation. Further dehydration of the leaves (between 50% RWC to 20% RWC) resulted in leaf senescence in *S. pyramidalis*, while *S. stapfianus* stayed green and its metabolome was characterized by antioxidant production (such gluthatione and tocopherol), nitrogen remobilization, ammonia detoxification and soluble sugar production (such sucrose, raffinose and stachyose).

Chitin-triggered innate immunity

Bacteria, fungi, oomycetes and viruses attack plants to gain energy sources from them. During evolution, plants and pathogens have developed adaptations to combat each other. This so called “arms race” between plants and pathogens has been described as a “zigzag model”, which proposes that plant immune responses consist of two branches [12]. These two forms are defined as MAMP-triggered immunity (MTI) and effector-triggered immunity (ETI). The first line of defense in plants is the recognition of conserved molecules characteristic of many microbes known as microbe- or pathogen-associated molecular patterns (MAMPs or PAMPs). In addition, endogenous molecules and fragments from damaged cells and tissues, known as damage-associated molecular patterns (DAMPs) can also be recognized as danger signals. MAMPs and DAMPs are recognized by pattern recognition receptors (PRR) localized on the cell surface to activate immune responses. In order to suppress these immune responses pathogens evolved protein effectors as virulence factors. In turn, the plants adapted by producing proteins that either directly or indirectly recognize these effectors restoring plant immunity. These plant proteins are termed ‘resistance’ (R) proteins that promote effector triggered immunity (ETI). ETI leads to a very strong defense reaction, often associated with localized cell death, known as the hypersensitive response.

During fungal attack the plants defend themselves by producing chitinases that can degrade the fungal cell wall releasing chitin oligosaccharides. Chitin is an insoluble β1-4 linked polymer of N-acetyl-D-glucosamine (GlcNAc) and a major component of fungal cell walls. Chitin oligomers are recognized by specialized PRRs localized at the plasma membrane. Some fungal pathogens are equipped with effector proteins that can inhibit plant chitinases or can associate with chitin to block recognition by plant cells and suppress chitin-triggered immunity [13].

Chitin receptors belong to the lysin (LysM)-domain protein family, whose name derives from the Lysin motif, an ancient and conserved 40 amino acid motif that recognizes N-acetylglucosamine. LysM-containing cell surface receptors are either LysM-containing receptor-like kinases (LYKs) or LysM-containing receptor proteins (LYPs). Arabidopsis has

five LYKs (AtCERK1/AtLYK1 and AtLYK2-5) and three LYPs (AtLYP1-3) [14]. CERK1 has the ability to bind chitin directly [15, 16], which results in CERK1 dimerization [17]. Mutations in CERK1 result in the complete loss of chitin-triggered innate immunity [18, 19]. More recently, it was shown that two other LysM-RLK proteins, AtLYK4 and AtLYK5 are also required for chitin signaling. Single mutations of LYK5 or LYK4 result in decreased chitin signaling, and simultaneous mutations in both genes are necessary for complete loss of chitin-triggered immunity [16, 20]. Structurally, LYK4 and LYK5 are similar to CERK1 but they lack the critical residues necessary for kinase catalytic activity. The ectodomains of LYK4 and LYK5 bind chitin [16], with LYK5 having much higher affinity than CERK1 (LYK5 Kd=1.7 μM in comparison to CERK1 Kd=45 μM) [20], indicating that LYK5 is the primary chitin receptor with CERK1 functioning as a co-receptor. For example, dimerization of CERK1 was shown to be dependent on the ability of LYK5 to bind chitin. It was proposed that LYK5 forms a chitin-inducible receptor complex with CERK1 leading to CERK1 phosphorylation which initiates the signal for downstream immune responses [20].

AtLYM2, a LYP protein which lacks the intracellular kinase domain, also showed high affinity binding of chitin [15]. However, LYM2 is not necessary for CERK1-mediated chitin responses but contributes to disease resistance against fungal pathogens *Botrytis cinerea* and *Alternaria brassicicola* [21]. More recently, LYM2 was found to be required for chitin-induced suppression of molecular flux through plasmodesmata (specifically they measured the flux of monomeric red fluorescent protein (mRFP)), a response that does not require CERK1 [22].

CERK1 is required for innate immunity in response to peptidoglycan (PGN), a bacterial MAMP, but does not bind PGN itself [23]. Other LysM receptors, LYM1 and LYM3, bind directly to PGN [23]. LYM1 and LYM3 lack a significant cytoplasmic domain and, therefore, it is likely that CERK1 provides the necessary cytoplasmic kinase function that allows downstream signaling in response to PGN binding. More recently, ectodomain shedding of CERK1 was reported to be important for cell death during pathogen attack and senescence, a process that did not require a chitin stimulus [24].

Upon chitin recognition, the host elicits a series of cellular responses and physiological changes that include $[Ca^{2+}]_{cyt}$ increases, extracellular alkalinization, membrane potential depolarization, ion effluxes, increase in reactive oxygen species (ROS), activation of a MAP kinase (MPK) cascade, ethylene biosynthesis, callose deposition and gene transcriptional changes, which collectively result in resistance to pathogen attack [25]. Upon chitin elicitation, there is a rapid and transient increase of cytosolic Ca^{2+} levels [16] that involves ionotropic glutamate receptor (iGluR)-like channels [26].These iGluR-like channels are also involved in the generation of flg22- and elf28-triggered Ca^{2+} transient [26]. Inhibition of iGluR-like channels resulted in decreased MAPK activation and defense gene transcripts [26].

Chitin induces strong MAPK activation within 5 minutes after elicitation. In particular, MAPK3 and MAPK6 were shown to be activated by chitin in a MKK4/5 dependant manner, indicating a chitin-induced MAPK cascade consisting of MKK4/5-MPK3/6 [25, 27]. Chitin elicitation causes a reprogramming of gene expression, including many transcription factors (TF) ([16, 28]). A more recent study found MPK3 and MPK6 can physically interact and phosphorylate chitin-responsive TFs ETHYLENE RESPONSIVE ELEMENT BINDING FACTOR (ERF)5 and EFR6 [29, 30]. Moreover, phospho-mimicking ERF6 is able to activate fungal resistance-related genes and conferred enhanced resistance to *Botrytis cinerea* [30]. Together, these studies suggest a MPK3/MPK6 cascade that activates ERF6 and, in turn, regulates plant defense against fungal pathogens. ROS production is one of the earliest responses, starting only a few minutes after chitin treatment. ROS have been proposed to act as antimicrobial compounds, cross-linkers of the plant cell wall to block pathogen entry and as a secondary messenger in innate immune responses. ROS production depends on NADPH oxidase (RBOHD). It was shown that RBOHD associates with the PRR complex FLS2/BAK1/BIK1 *in vivo*, where BIK1 phosphorylates RBOHD, which is required for MTI responses [31, 32]. Interestingly, BIK1 also interacts with CERK1 and plants defective in BIK1 showed a reduction in chitin responses [33]. However, further studies are necessary to elucidate

the role of the interaction of CERK1 and BIK1, and if this complex associates with RBOHD to control chitin-triggered immunity.

Salt stress tolerance

Soil salinity has a negative impact on plant growth and yield affecting agriculture worldwide. Salt accumulation in farmland is mainly derived from irrigation water that contains trace amounts of sodium chloride (NaCl) and from seawater. Increased soil salt concentration decreases the ability of the plant to take up water (dehydration). The accumulation of Na^+ and Cl^- in tissues negatively affects growth by impairing photosynthesis and other metabolic processes. Therefore, salinity stress has both osmotic and ionic stress components. Plants have evolved mechanisms to mitigate osmotic stress by accumulating osmolytes (ions, solutes or organic compounds) to lower the osmotic potential and reduce water loss. In addition, plants can counteract the effects of ionic Na^+ toxicity by exclusion of Na^+ from leaf tissues and by cellular compartmentalization of Na^+ mainly into vacuoles [34].

Plant roots are the first organs to sense the hyperosmotic component and the ionic Na^+ increases. It is suggested that plants have two different sensory mechanisms to deal with both stress components, since some response to NaCl are different from those to osmotic stress. However the molecular identities of a plant osmotic sensors or Na^+ sensor remain unknown [35]. Plant osmotic sensors are likely to be localized closely to Ca^{2+} channels because $[Ca^{2+}]_{cyt}$ increases in response to NaCl are very rapid within seconds. Therefore, it is thought that an osmosensor may be closely coupled to Ca^{2+} channels. Even more, in bacteria and animals, osmosensing Ca^{2+} channels serve as osmosensors. Recently, a previously unknown plasma membrane protein, OSCA1, was proposed to be an osmosensor. OSCA1 is capable of forming hyperosmolality-gated calcium permeable channels responsible for $[Ca^{2+}]_{cyt}$ increases induced by osmotic stress [36]. Other candidates to play a role as osmosensors are the mechanosensitive (MS) channels. Osmotic stress disrupts the plasma membrane causing mechanical stress that

may be sensed by MS channels, but to date no MS channel has been confirmed as a osmosensor, perhaps due to high functional redundancy in this family [37].

Elevated cytosolic Ca^{2+} leads to the activation of various Ca^{2+} sensor proteins including calcineurin B-like proteins (CBLs), CBL-interacting protein kinases (CIPKs) and calcium-dependent protein kinases (CDPKs). Ca^{2+} increases also activate RBOHD to produce ROS, which in turn may activate Ca^{2+} permeable channels like annexins [38] to sustain further Ca^{2+} mobilization. This Ca^{2+}- and ROS-dependent signaling network plays a role in regulating detoxification mechanisms such as the Ca^{2+}-dependent activation of Na^+/H^+ exchangers, SOS1 (SALT OVERLY SENSITIVE 1) and NHX1 (Na^+/H^+ exchanger 1), Na^+ efflux from the cytosol, regulation of xylem loading of Na^+, Na^+ exclusion from leaves, and induction of osmoprotective proteins and osmotyles (reviewed by [35, 39]). Plants also possess a rapid stress signaling system based on Ca^{2+} waves that propagate the signal through the cortex and endodermal root cell layers to the aerial tissues. These Ca^{2+} waves elicit systemic molecular responses in target organs and may contribute to whole plant salt stress tolerance [40].

Cross tolerance between biotic and abiotic stresses

While most of the current research has studied one stress in isolation, under natural conditions, plants are exposed to combinations of environmental abiotic stresses and often need to battle biotic stresses caused by pathogens. Plants have to respond quickly and efficiently to these different stress combinations. Therefore, it is not surprising that many regulatory systems are part of larger, intertwined networks that allow integration of a number of environmental responses. This “crosstalk” occurs in a complex regulatory network, including Ca^{2+} fluxes, oxidative burst, kinase cascades, and an overlapping set of stress response genes [41].

Abiotic stress often affects the tolerance to biotic stress and vice versa. There are two possible mechanisms by which abiotic stress affects the interaction between plants and pathogens. One possibility is that the negative effects of pathogens and abiotic stress can be additive. For example, tomato plants pre-irrigated with saline water were more

severely affected with crown and root rot disease (*Fusarium oxysporum* f. sp. *radicis-lycopersici*) [42], and drought-stressed Arabidopsis plants showed severe susceptibility to the bacterial pathogen *P. syringae* [43].

The other possibility is that abiotic stress enhances plant pathogen resistance, or vice versa. This phenomenon is also known as cross-tolerance, cross-resistance or multiple-stress resistance and was demonstrated for different types of stress [44]. For instance, tomato and barley plants exposed to drought and salt stress developed increased tolerance to barley powdery mildew fungus (*Blumeria graminis*) and to *B. cinerea* and *Oidium neolycopersici*, respectively [45, 46]. Interestingly, drought stress exerted tolerance to both the necrotrophic fungus *B. cinerea* and the biotrophic fungus *O. neolycopersici*, while salt stress only increased tolerance to the latter, suggesting that drought and salt stress stimulate different pathogen-defense pathways [46]. Similarly pathogen infection can enhance tolerance to abiotic stresses. For example, infection of Arabidopsis with the soil borne fungal pathogen *Verticillium longisporum* (thale cress wilt) resulted in *de novo* xylem formation, enhancing drought tolerance [47].

Some signaling components play a dual role in response to abiotic and biotic stresses. For example BOS1, a R2R3 MYB transcription factor, and its interactor BOI, an E3-ligase, are required for the response to the necrotrophic fungal pathogen *Botrytis cinerea* and to salinity stress [48, 49]. Interestingly, some LysM-RLKs have been suggested to play a role in a crosstalk between abiotic and biotic stresses. AtLYK3 was reported to be important for the crosstalk between signaling pathways activated by pathogens and abscisic acid (ABA) [50]. AtLYK3 negatively regulates basal expression of defense genes and resistance to *B. cinerea* and *Pectobacterium carotovorum* infection. Plants lacking a functional LYK3 resulted in reduced physiological responses to ABA and reduced ABA-induced inhibition of PHYTOALEXIN-DEFICIENT3 (PAD3) expression [50]. Previous research implicated LYK3 in suppression of plant innate immunity in response to short chain chitin oligomers [degree of polymerization (dp) <6] [51]. An interesting study reported that treatment with chitin improved the salinity stress tolerance in Arabidopsis plants. Similar results were found when ectopically expressing fungal chitinases in

Arabidopsis, increased tolerance to salinity during germination and enhanced tolerance to *B. cinerea* infection [52]. Interestingly, ectopic expression of chitinase in *cerk1* mutant plants did not increase tolerance to salinity and necrotrophic fungus, suggesting a role for AtCERK1 in the crosstalk between salinity stress and fungal infection [52].

Although the number of studies is limited, some transcriptome, metabolome and proteome analyses of plants in response to different stress combinations revealed several signaling pathways specifically activated, including different transcription factors, defense responses, hormone signals and osmolyte synthesis (reviewed in [53]). These studies indicated that the plant response to two or more stresses simultaneously is different to the response to a single stress [53, 54]. Therefore, further studies are required to address the molecular and biochemical mechanisms that regulate the response to stress combinations found in nature. This information will help us to design strategies to improve tolerance in plants and crops.

Chapter 2

Large-scale mRNA expression profiling in the resurrection tolerant grass *Sporobolus stapfianus* during dehydration and rehydration

Abstract

Studying plant adaptations to tolerate dehydration is necessary to develop novel strategies for improving drought tolerance in sensitive crops. To investigate the dehydration tolerance mechanism in the model resurrection grass species (*Sporobolus stapfianus*), we compared the mRNA expression profiling of leaf tissues using a *S. stapfianus* specific Nimblegen oligonucleotide based microarray at full hydration, during drying and after re-watering. A total of 4,751 transcripts were found to be differentially expressed across the eight conditions. Hierarchical clustering of these data revealed 177 clusters of co-expressed genes at an average pairwise correlation of 0.85. Dehydration resulted in a progressive decrease in the abundance of transcripts encoding proteins with functions related to photosynthesis, reflecting its inhibition during desiccation. In contrast, transcript abundance increased for genes involved in biosynthesis of raffinose-like sugars, lipid biosynthesis and turnover, and protection against oxidative stress. Other abundant groups of genes expressed in response to desiccation included late embryogenesis abundant (LEA) proteins, transporter proteins, and kinases and phosphatases.

Keywords: Resurrection plants, Sporobolus stapfianus, Dehydration tolerance, mRNA expression profiling

Mel Oliver (USDA-ARS-PGRU, Columbia MO) designed the experiment. Jim Elder (USDA-ARS-PGRU, Columbia MO) performed the drying experiment, collected the tissues and isolated the RNA. The expression profiling data was generated at Mel Oliver Lab and was statistically evaluated and processed by John Cushman and Karen Schlauch at the

University of Nevada, Reno. Catherine Espinoza performed the bioinformatic analysis of the expression profiling data, the verification of the array data by qRT-PCR, and the comparison of gene expression between *S. stapfianus* and its sensitive sister species *S. pyramidalis*.

Introduction

Drought or water scarcity represents a major threat to agriculture and is the most common cause of severe food shortages, because it drastically reduces seed and biomass yield ([55, 56]. Global climate change, which predicts increased temperatures and decreased rainfall, is expected to exacerbate the negative effects of water deficiency on agriculture unless new heat- and drought-tolerant crop varieties and more efficient irrigation systems are developed [57]. Therefore, there is a need to study plants that have developed natural adaptations to withstand dehydration in order to search for novel genetic components and strategies for improving crop production under water scarcity.

Terrestrial plants have developed several different strategies to solve the problem of living in dry environments. Most angiosperms cannot survive dehydration of their vegetative tissues to water potentials of -5 to -10 MPa, but there are some plants that can survive levels of -100 MPa and lower [58]. Plants that tolerate almost complete loss of protoplasmic water are termed desiccation tolerant and if the plant is an angiosperm it is referred to as a "resurrection plant". The mechanism of desiccation tolerance is observed throughout the microbial, fungal, animal and plant kingdom. In plants, desiccation tolerance is common to reproductive structures in plants (pollen, spores, and seeds), but rarely observed in vegetative tissues, as in bryophytes, club mosses, ferns and a resurrection plants [5, 6].

Resurrection plants represent a model to study how cells survive and repair the damage caused by water loss from the cytoplasm or water influx during rehydration. Over the past decade some progress has been made in elucidating the mechanism of desiccation tolerance in different resurrection plants, including the dicots, *Craterostigma plantagineum, C. wilmsii, Lindernia brevidens, Myrothamnus flabellifolia, Haberlea rhodopensis, Boea hygrometrica, Ramonda serbica*, and the monocots, *Xerophyta viscosa, X. humilis, Eragrostis nindensis,* and *Sporobolus stapfianus* [7, 59-61]. Resurrection plants have to deal with different problems during the processes of drying and rehydrating. Loss of water in the cells causes membrane and protein damage, and

mechanical stress due to changes in cell osmotic pressure is detrimental to cell wall integrity. Adjustment of carbohydrate metabolism and induction of late embryogenesis abundant (LEA) and heat shock proteins, have been proposed to be important for the conservation of membranes and proteins during dehydration. Accumulation of amino acids, such as arginine and asparagine derived from protein breakdown during drying, is also common in *S. stapfianus* [11, 62]. These amino acids could act as osmolytes and also may be used later on during the recovering of growth upon rehydration. Morphological changes (e.g. leaf rolling), and changes in cell wall properties (e.g. expansins) have been also observed in response to desiccation [63, 64]. While dehydration continues, plants experience oxidative stress. Disruption of electron transport increases the production of reactive oxygen species (ROS), superoxide and hydroxyl radicals that accumulate in the cell, which are detrimental to nucleic acids, proteins and membrane lipids. Glutathione and enzymes involved in glutathione metabolism are involved in the oxidative stress responses in nearly all desiccation-tolerant plants examined (reviewed by [65, 66]. For example, the accumulation of γ-glutamyl peptide conjugates was reported in the moss *Tortula ruralis*, the grass *S. stapfianus* and the lycophyte *S. lepidophylla* [11, 67]. Ophthalmate, an analog of glutathione never reported before in plants, was found to increase in *S. stapfianus* during desiccation [11]. Regulatory molecules like CDT1, a retrotransposon, and phopholipase D, were found to be abundant during desiccation in *C. plantagineum* [68-70].

The South African grass *Sporobolus stapfianus* Gandoger (Poaceae) is capable of surviving equilibration with air at 2% relative humidity (RH), equivalent to a leaf water potential of -540 MPa (more than hundred times lower than most crop plants) [8, 9]. In its natural habitat, plants equilibrated to 30-40% RH (-120 to -150 MPa) [8, 71] can remain viable in a desiccated state for several months [72]. Desiccated leaves of *S. stapfianus* can resume normal growth within hours of re-watering. A time-lapse video of *S. stapfianus* being re-watered and recovering within 24 hours, after 1 week of being desiccated to 10% RWC can be viewed at the following website (See video at

http://www.youtube.com/watch?v=BINkhNNpYvc, credits: Dr. Oliver Lab, USDA-ARS). This resurrection grass is also salt tolerant [72]. *S. stapfianus* has many advantages for use as a model for desiccation tolerance research. It is a grass (Poaceae) and, therefore, research on this plant may be relevant to other, closely related crop species such as wheat, barley, maize and rice. Furthermore, as a perennial grass, *S. stapfianus* has the potential to be used for forage and biomass production. The existence of a sensitive sister species, *Sporobolus pyramidalis*, provides the opportunity to perform comparative studies to investigate the role of adaptive genes important for desiccation tolerance. A recent study comparing the metabolome of *S. stapfianus* and its sensitive sister species *S. pyramidalis* revealed adaptive metabolic responses to dehydration [11].

The lack of a full genome sequence for a resurrection plant has limited the application of modern functional genomic tools to study these species. However, the recent boom of high-throughput sequencing and "omics" technologies provides an opportunity to expand gene discovery efforts to several resurrection species. Thus, transcriptomic studies have been carried out in the desiccation tolerant plants T. *ruralis* [73], *C. plantagineum* [74], *X. humilis* [75], *S. lepidophylla* [76], and *H. rhodopensis* [77]. These transcriptome studies have shown similarities and unique features of these plants during desiccation and rehydration, and have provided us with large and valuable data sets of novel genes.

Using Roche/454 Life Sciences pyrosequencing, 490,144 high quality ESTs were obtained using mixed cDNA libraries prepared from dehydrating and rehydrating aerial tissues in an effort to capture the full repertoire of expressed genes in *S. stapfianus*. These ESTs were used to fabricate a custom oligonucleotide microarray that was used for this study. Here, we report on large scale mRNA expression profiling of the resurrection grass *S. stapfianus* during six incremental drying stages and after 12 and 24 hours of rehydration. The expression of a total of 4,751 transcripts was significantly different across two or more of the eight conditions. The gene expression analysis revealed novel and unique genes potentially important for the dehydration tolerance phenotype. A gene expression comparison between *S. stapfianus* and its desiccation sensitive sister

species, *S. pyramidalis*, was used to further highlight genes responding to dehydration. These adaptive genes can be used for further functional studies with the aim to improve drought tolerance in dehydration sensitive plants.

Results and Discussion

Sequencing and assembly of ESTs

Three month-old plants were subjected to a drying event by withholding water until desiccation. Young leaf tissues were collected at eight conditions: at full hydration (water content of 3 g H_2O/g Dry Weight (DW)) and at incremental dehydration stages (2, 1.5, 1, 0.75, and 0.5 g H_2O/g DW; which corresponds to 60, 50, 40, 20 and 5 % relative water content (RWC) [11]), and after rehydration at 12 and 24 hours (Figure 2.1).

The 454 pyro-sequencing of cDNA populations from dried and rehydrated tissues resulted in 408,458 ESTs, and, after the trimming process, 349,334 high-quality ESTs were returned. These high quality ESTs averaged 215 nucleotides in length and totaled 648 Mb. High quality ESTs were assembled into 50,690 contigs with an average length of 384 bp. We submitted the 50,690 ESTs sequences to search for similarity against the NCBI non-redundant (nr) protein database using BLASTX [78]. A total of 18,332 sequences (36%) matched known proteins ($E>10^{-5}$). This low percentage of BLAST hits could be due to the reads obtained with 454-pyrosequencing technology being much shorter than traditional Sanger reads and also can present some base-calling error [79], or a reflection of the relatively few plant genome sequences fully annotated at the time of our analysis (year 2010). Nevertheless, 454 sequencing is a very powerful tool for high throughput sequencing and makes it possible to obtain transcripts of thousands of genes from non-sequenced plant species, like *S. stapfianus*. BlastX analysis revealed that translated proteins from most of the *S. stapfianus*'s transcripts were similar to the protein sequences of *Oryza sativa* and *Zea mays*. This result is not surprising since the three species belong to the group of grasses (Family Poaceae) and rice and maize genomes have been fully sequenced. Phylogenetically, *S. stapfianus* (sub-family

Chloridoideae) is closer to maize (sub-family Panicoideae) than to rice (sub-family Ehrhartoideae) [80].

The 18,322 ESTs contigs with BLAST hits were mapped to retrieve gene ontology (GO) terms using the program BLAST2GO [81]. 9,667 EST contigs (53%) retrieved mapping results. Representation of GO mapping results (Figure 2.2) showed a diversity of categories assigned for *S. stapfianus* EST contigs, suggesting that our cDNA libraries were able to collect a wide range of transcripts.

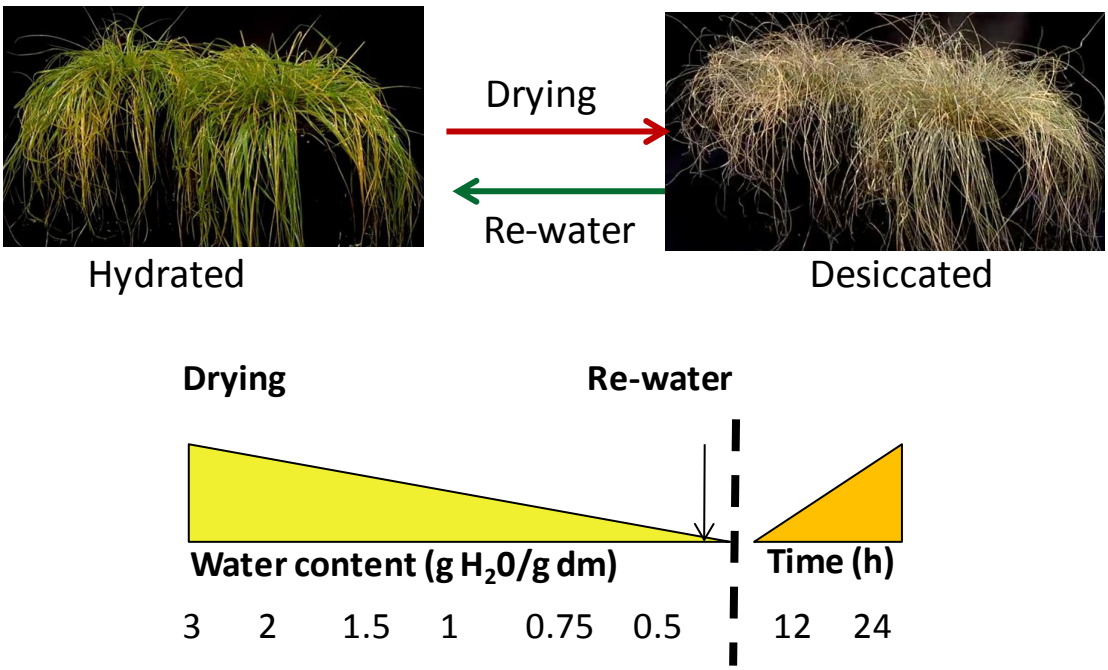

Figure 2.1. Drying and rehydration in the resurrection grass *Sporobolus stapfianus*

Leaf tissues were collected when the leaf water content (as g H_2O/ g dry matter) reach the indicated dryness and after 12 and 24 h after re-watering. Pictures were taken from http://youtu.be/BINkhNNpYvc (Mel Olivers's Lab).

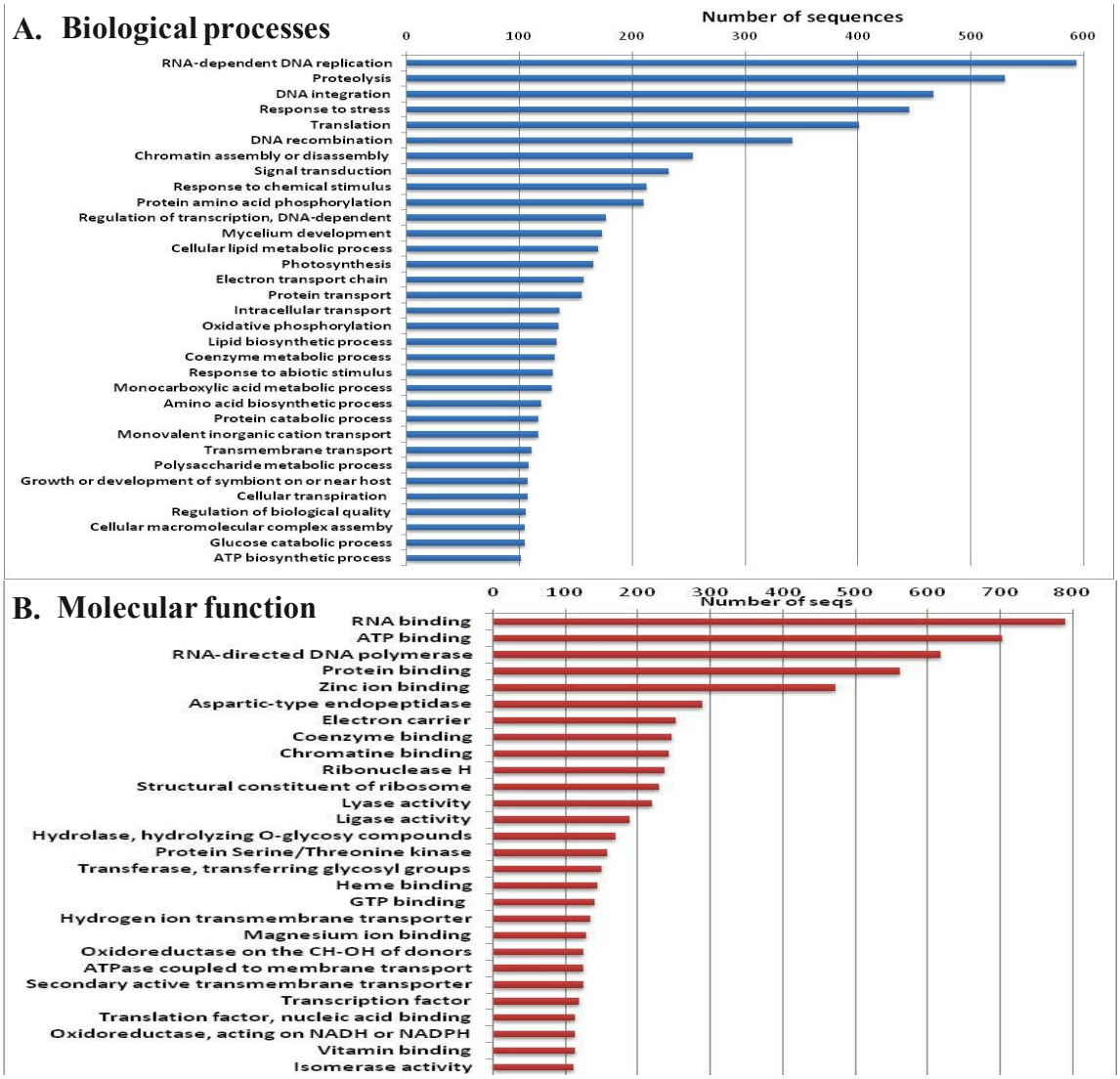

Figure 2.2. Representation of Gene Ontology (GO) mapping results for *S. stapfianus* ESTs

ESTs were mapped to retrieve GO terms using the program BLAST2GO (v.1.2.7). GO terms are only given for categories with more than 100 sequences.

Identification and clustering of differentially expressed genes during dehydration and rehydration

After performing an ANOVA and a multiple testing correction (FDR) [82], 4,751 transcripts (9.37% of total ESTs present in the microarray) were found to be differentially expressed ($p \leq 0.05$) in at least one of the eight conditions. Hierarchical clustering of these data revealed 177 clusters of co-expressed genes at an average pairwise correlation of 0.85.

In order to monitor transcriptional profiles during dehydration and rehydration in *S. stapfianus*, we graphed the nine clusters that contained 56% of the differentially expressed genes (2,666 genes; Figure 2.3). Clusters 1, 2 and 3 (345, 308 and 212 genes, respectively) showed transcriptional profiles of genes that were found to be up-regulated progressively during drying, showing a peak at 0.75 g H_20/g dm. Cluster 17 (168 genes) showed a transcriptional profile of genes that are induced early during dehydration at 2 g H_20/g dm, and remained up-regulated during the drying period. Clusters 10 and 19 (781 and 113 genes, respectively), showed transcriptional profiles of genes that were up-regulated during rehydration. Cluster 38 (82 genes) contains genes that were down-regulated during desiccation (0.5 g H_2O/g dm) and up-regulated during rehydration. Clusters 13 and 15 (238 and 419 genes, respectively) showed genes whose expression was down-regulated progressively during drying.

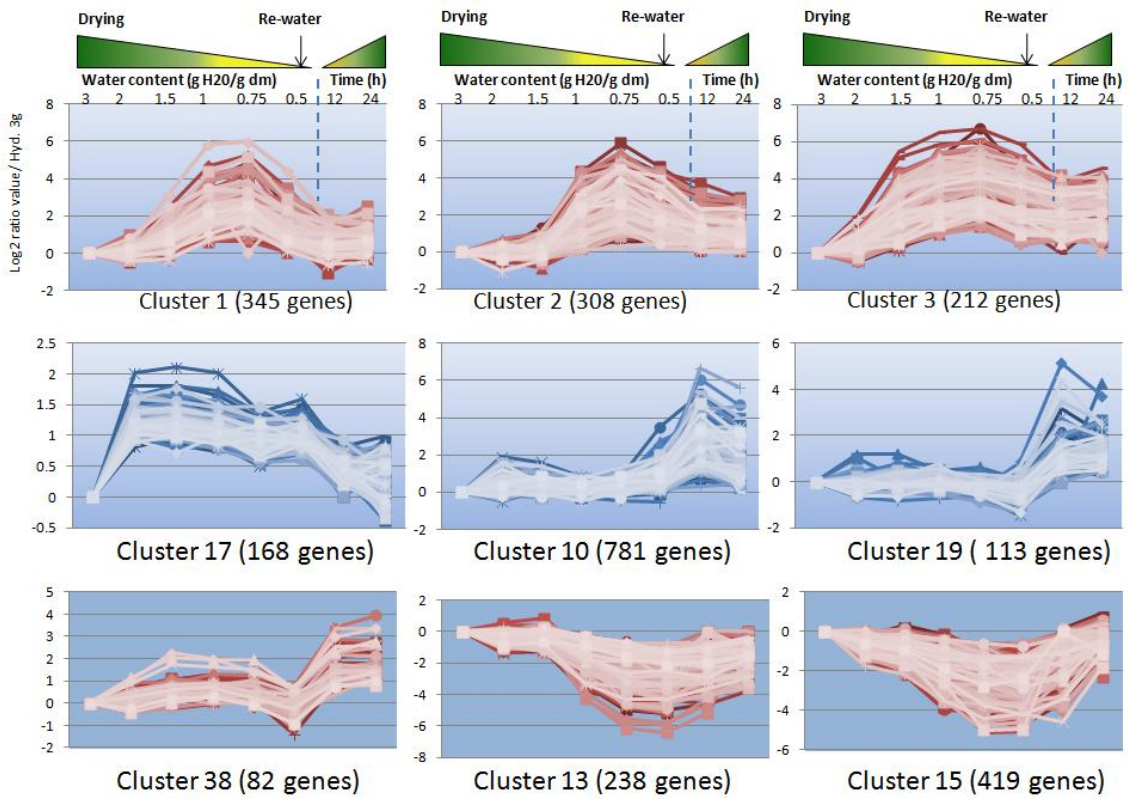

Figure 2.3. Transcriptional profiles of *Sporobolus stapfianus* genes during drying and rehydration of young leaves

We compared large-scale mRNA expression patterns of young desiccation tolerant leaf tissue at full hydration, during drying and after re-watering. Hierarchical clusters were constructed with an average pairwise correlation of 0.85. This figure shows 9 clusters (from the 177 found), which contain 56% of the differentially expressed genes. Data are expressed as the $\log^2$ values of the ratio treated/untreated.

To confirm the accuracy and reproducibility of the microarray results, sixteen genes that showed an increase in transcript abundance during dehydration and rehydration were chosen for quantitative real-time (qRT)-PCR (Table 2.1). Correlation between microarray and qRT-PCR was evaluated using fold change measurements. Scatter plots were generated using the $\log^2$ ratio value determined from the microarray analysis and the $\log^2$ fold change determined by qRT-PCR, calculated with ΔΔCT (comparative threshold cycle) method. As shown in Figure 2.4, qRT-PCR results showed that expression trends of these genes showed significant similarity (r^2=0.85) with the microarray data.

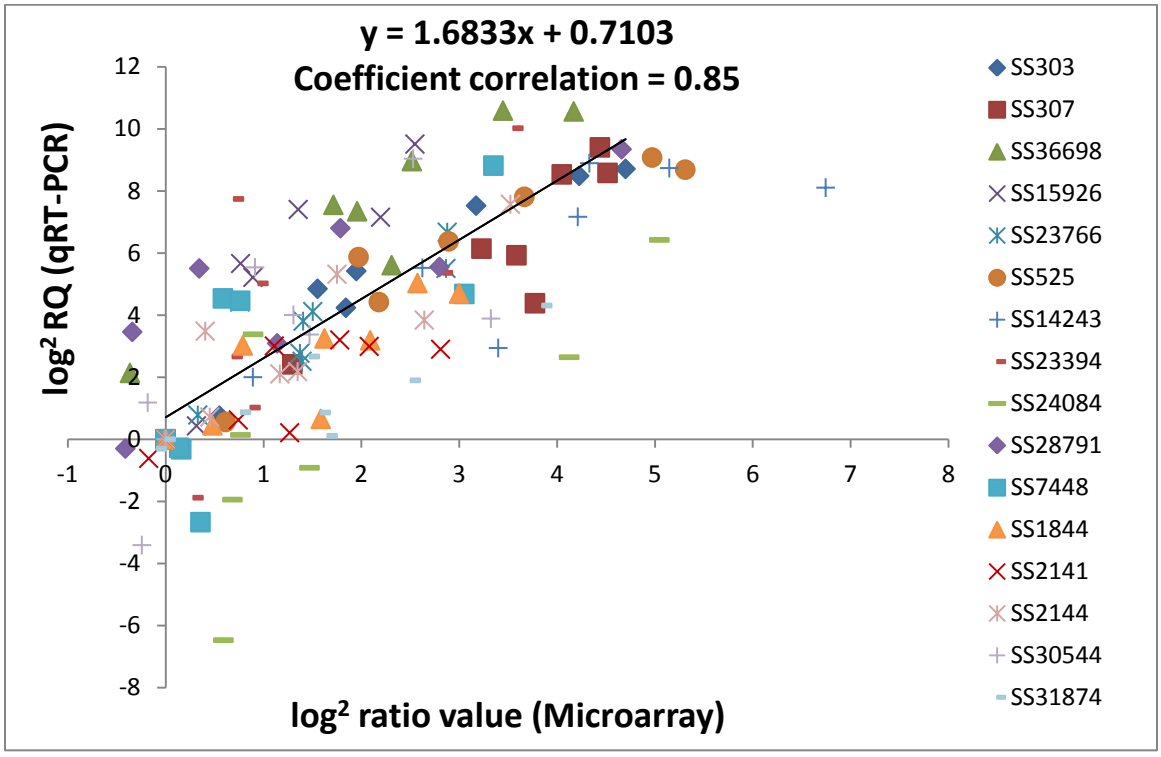

Figure 2.4. Validation of microarray by qRT-PCR

RNA was extracted from leaf tissue taken at six different dehydration stages and 12 and 24 h after rehydration (See Figure 2.1 for details). Same RNA was used for microarray and qRT-PCR analysis. Each symbol indicates a different gene and the graph shows eight different points per symbol corresponding to the eight treatments described above. The results are the means of three biological replicates.

Functional assignment of differentially expressed genes during dehydration and rehydration.

We used BLASTX [78] to annotate the 4,751 differentially expressed *S. stapfianus* ESTs against the green plant subset from the non-redundant (nr) NCBI database, the rice peptide database OsGDB_OSpepV 6.1 (http://www.plantgdb.org/OsGDB), the maize peptide database ZmB73_5a_WGS (http://maizesequence.org) and Arabidopsis peptide database TAIR10 (http://www.arabidopsis.org) using a e value of 10^{-5}. From this list, 2,680 ESTs (56.4%) could be assigned a green plant annotation; 2,623 (55.2%) could be assigned a maize annotation; 2,598 (54.7%) could be assigned a rice annotation, and 2,187 (46%) can be assigned an Arabidopsis annotation.

To further delineate the metabolic pathways participating in the dehydration and rehydration responses, we used the Mercator web application [83] to assign a functional description to the 4,751 differentially expressed ESTs for subsequent use in the program Mapman. Most of the differentially expressed ESTs correspond to unknown or unclassified genes (67%, 3,185 of 4,751 ESTs). From these, 1,425 ESTs had no Mercator results and no annotation. 1,369 ESTs (28.8% of total clustered ESTs) had no Mercator results but did have an annotation. 391 ESTs (8.2%) had Mercator results and annotation, but corresponded to genes with unknown function (Table 2.1).

Table 2. 1 . Functional categorization of genes from the most populated clusters of genes

Functional category	Early Drying	Drought	Dehydration	Desiccation	Rehydration			Down-regulated during drying	
	Cluster 17	Cluster 3	Cluster 1	Cluster 2	Cluster 10	Cluster 19	Cluster 38	Cluster 15	Cluster 13
Photosynthesis			1	1	8	1	1	79	9
Major CHO metabolism		1	5		3			2	9
Minor CHO metabolism		1	4	2	1			1	1
Glycolysis			1		3				
Fermentation			3	2	3		1		
Gluconeogenesis					1			5	4
OPP pathway					2	1	1		
TCA			5		10			7	4
Mitochondrial electron transfer			1		6	1		1	1
Cell wall		1	2		2	1		3	1
Lipid metabolism			9	1	3		2	5	4
N-metabolism			1		2	1		5	1
Amino acid metabolism		1	1		1	1		6	6
S-assimilation									
Metal handling		1	1						
Secondary metabolism					2	1		6	5
Hormone metabolism		2	1	1		2	1	8	7
Co-factor and vitamin metabolism					1			1	
Tetrapyrrole synthesis							1	8	
Stress	4	5	12	10	4	3	3	6	5
Redox		1	9	5	4	1	2	4	3
Polyamine metabolism									1
Nucleotide metabolism			1	1	1			4	
Xenobiotics				2					
C1-metabolism					1	1			1
Miscellaneous		1	7	9	7			7	7
RNA	20	3	2	5	3	8	10	7	16
DNA	4		1		2				1
Protein	1	4	19	5	50	15	26	13	10
Signaling	4		3	12	3	2		8	10
Cell		3	3		5	1			2
MicroRNA									
Development		7	8	9	1	1	2	5	4
Transport		2	21	1	11	4	2	16	14
Not assigned/Unknown	137	182	224	242	641	68	30	212	112
Sub-total	**170**	**215**	**345**	**308**	**781**	**113**	**82**	**419**	**238**

We used the Mercator web application (http://mapman.gabipd.org/web/guest/aap/mercator) to assign a functional category. Abbreviations: CHO: carbohydrate, OPP: oxidative pentose phosphate, TCA: tricarboxylic acid cycle, N: nitrogen, S: sulfur, C1: one carbon.

Retrotransposons are potential regulators at early events of drying

Our study found a unique cluster of genes induced during early drying (60% RWC) after which gene expression progressively returned to basal levels (Cluster 17 in Figure 2.3). Interestingly, 47% of these genes were annotated as Retrotransposons (79 out of 168 transcripts). Most of these retrotransposons were annotated as unclassified, but 5 were annotated as Ty3-gypsy sub-class, a long terminal repeat (LTR) retrotransposon, and 8 were annotated as LINE (long interspersed nuclear elements) sub-class, a non-LTR retrotransposon.

These findings suggest that both a network of retrotransposon transcripts and controlled retrotranspositions might serve important functions during the rapid response to early drying in the resurrection grass *S. stapfianus*. One possible role of these retroelements would be to control the expression of genes involved in dehydration tolerance. Retrotransposons are transcriptionally activated under abiotic or biotic stress conditions [84]. The mechanisms of how retrotransposons control gene regulation under abiotic stress are recently being addressed. One hypothesis is that insertions of the retrotransposon make the adjacent genes stress inducible creating new regulatory networks. Two studies, one in rice under cold and salt stress [85]and the other in Arabidopsis under heat stress [86], have shown evidence for this hypothesis. In the resurrection plant *Craterostigma plantagineum*, a retrotransposon-like CDT1 is involved in post-transcriptional control of the expression of genes involved in desiccation tolerance, by producing siRNAs which are the direct regulators of expression [68].

Table 2. 2 Overview of the different phases of dehydration and rehydration and their molecular responses.

Leaf hydration stage	Phase	Molecular Response (Induced gene expression)	Cluster (number of genes)
60% RWC	Initial Drying	Induction of Retrotransposons	17 (168 genes)
50% RWC	Moderate dehydration	Abiotic stress-induced proteins: LEAs group 3, Dehydrins, Rab17 ABA signaling: GRAM domain protein, CIPK10	3[a] (212 genes)
40% to 20% RWC	Severe Dehydration	Most of the metabolic pathways affected: Activation of raffinose synthesis, GABA, Fermentation (ALDH) ABA-dependant regulation by HVA22E, ABA regulation by Ser//Thr Ppase Calcium signaling Phospholipase D signaling Remorins: unknown signaling Stress-response signaling: SnRK1 Dehydration-induced TFs: GBF3, Zn finger CCCH type Abiotic stress-induced proteins: LEAs group 1, Oleosin/Caleosin proteins Transporters induced: ABC transporters, TIP, aquaporins	1[b] (345 genes)
Less than 10% RWC	Desiccation	Abiotic stress-induced proteins: Dehydrins, desiccation-related proteins Detoxification: 1-Cys peroxiredoxin, Metallothioenin Cellular structural changes: cell wall hydrolases, membrane lipid changes Light signaling: ELIPs Dehydration-induced TFs: Unknown transcription factors , Oxidoreductases	2[c] (308 genes)
Rehydration	Rehydration after 12-24 h	Abiotic stress-induced proteins: Heat shock factors Metabolism comes-back: Glycolysis, TCA, Photosynthesis, Protein synthesis Cellular structural changes: Cell wall degradation, Lignin biosynthesis, regulation of Actin by cap1 Transcription factor Signaling mediated by MAP Kinase and GTP-binding proteins Rehydration-induced transcription factors: RACK1C, 14-3-3 protein Transporters activated: Inositol-, Phosphate-, Polyol/monosaccharide-, Amino acid-, Sugar-, Starch-transporters	10 (781 genes) 19 (113 genes)

RWC: leaf relative water content. Clusters correspond to those described in Figure 2.2. [a] Cluster 3: Expression of these genes was induced during moderate dehydration and continues to be up-regulated during severe dehydration, desiccation and rehydration. [b] Cluster 1: Expression of these genes is induced only during severe dehydration, and return to basal levels during desiccation and rehydration. [c] Cluster 2: These genes are induced during severe dehydration and continue to be up-regulated during desiccation.

Moderate dehydration induces ABA-related genes

Cluster 3 showed genes that were induced at moderate dehydration (50% RWC), maintaining high levels of gene expression through the drying process. Interestingly, these genes were highly induced again after 24 h of rehydration (Figure 2.3 and Table 2.3). This gene expression pattern suggests that these genes are important during early water deficit conditions, during the stressful events of desiccation, and during rehydration. This cluster of genes includes those previously reported to be ABA-induced in plants. These ABA-induced genes include a GRAM-domain protein and LEA (LATE EMBRYOGENESIS ABUNDANT) group 3 proteins.

The most abundant genes in this cluster correspond to LEA group 3 proteins. LEA 3 proteins are thought to play a protective role, by interacting alone or with disaccharides (e.g. sucrose) with membranes and/or proteins during dehydration [87, 88]. LEA 3 proteins are very diverse and are widely distributed within the plant kingdom, where transcripts have been found in algae, non-vascular plants, seedless plants and in all seed plants. LEA 3 proteins were also shown to accumulate in non-plant organisms in response to dehydration, like bacteria and nematodes [88]. In plants, the expression of LEA 3 proteins is regulated by ABA during developmental stages and upon other stress conditions like dehydration, salinity and low temperatures [87]. The functions of LEA 3 proteins during desiccation have been assessed in loss-of-function experiments with bacteria and nematodes. Mutants lacking group 3 LEA-like proteins from the extremophilic bacterium *D. radiodurans* were found to be dehydration sensitive [89], and mutants of *C. elegans* with a truncated LEA 3 protein where also found to be desiccation sensitive [90]. In plants, strong, ectopic expression of LEA 3 proteins increased tolerance to abiotic stress [91]. Collectively, these data argue that LEA 3 proteins are important for cellular protection during the drying and desiccation in *S. stapfianus*. There are no reports on the role of LEA3 proteins during rehydration in other organisms. It is tempting to speculate a role for LEA3 proteins in preventing cell damage upon rehydration.

Table 2. 3 Summary of genes induced during moderate dehydration, desiccation and rehydration (Cluster 3)

Contig number	Drying Stages (%RWC)					Rehydration		Gene description	Putative role
	60 %	50 %	40 %	20 %	Desiccat	12 h	24 h		
Ss_29715	1.96	5.13	5.83	5.98	5.23	3.39	4.12	1-Cys peroxiredoxin	R
Ss_29713	1.10	4.39	5.26	5.23	4.48	2.74	3.49	LEA group 3	P
Ss_3962	1.13	4.34	5.02	5.00	4.45	2.74	3.47	LEA group 3	P
Ss_29712	0.54	4.25	5.22	5.28	4.61	2.88	3.48	LEA group 3	P
Ss_3965	1.00	4.15	4.83	4.88	4.06	2.62	3.18	LEA group 3	P
Ss_3958	0.76	4.08	5.10	5.08	4.36	2.36	3.28	LEA group 3	P
Ss_3961	0.67	3.93	5.01	4.97	4.24	1.96	2.83	LEA group 3	P
Ss_43733	0.57	3.90	4.84	5.12	4.60	3.40	3.90	Ammodytin I2(C) variant	U
Ss_29707	0.57	3.87	4.56	4.59	3.76	2.26	3.13	LEA group 3	P
Ss_29706	0.83	3.87	4.59	4.71	4.00	2.91	3.10	LEA group 3	P
Ss_29708	0.70	3.79	4.44	4.41	3.79	2.82	3.13	LEA group 3	P
Ss_6738	0.56	3.78	4.82	5.07	4.54	3.38	3.68	Putative uncharacterized protein	P
Ss_282	0.81	3.77	4.76	5.15	4.55	3.74	3.75	RAB17 protein	U
Ss_6857	0.84	3.77	5.14	5.07	4.00	2.24	3.16	AWPM-19-like membrane family protein	U
Ss_8646	0.92	3.56	4.14	4.53	3.94	3.35	3.22	Dehydrin-/LEA group 2-like protein	P
Ss_5360	0.87	3.47	4.58	4.71	3.14	1.64	2.47	LEA group 3	P
Ss_5602	1.18	3.40	4.30	5.79	3.38	2.00	2.79	LEA group 1	P
Ss_8670	1.84	3.40	4.01	4.17	3.92	3.45	3.63	LEA group 3	P
Ss_29718	0.66	3.32	3.96	4.07	3.36	2.50	2.70	LEA group 3	P
Ss_44021	1.30	3.26	4.00	4.06	2.82	1.72	2.20	Stress-inducible membrane pore protein	T
Ss_307	1.30	3.23	4.44	4.52	4.05	3.59	3.78	LEA group 3	P
Ss_6802	-0.02	3.20	4.46	4.67	4.09	2.69	3.37	Embryonic protein DC-8	U
Ss_29709	0.16	2.94	3.52	3.51	2.63	1.17	2.09	LEA group 3	P
Ss_284	1.07	2.94	3.65	4.52	3.53	2.73	2.59	DHN4-like protein	P
Ss_3967	0.36	2.92	3.42	3.58	2.54	1.96	2.28	LEA group 3	P
Ss_311	0.83	2.74	3.52	3.63	2.99	2.92	2.89	LEA group 3	P
Ss_7044	1.15	2.70	3.31	3.58	2.95	2.42	2.72	LEA group 3	P
Ss_280	0.77	2.67	3.18	3.42	2.43	2.06	2.15	Dehydrin DHN1 (M3)(RAB-17 protein)	U
Y10779	1.09	2.57	3.66	4.06	3.56	3.07	3.27	LEA group 3	P
Ss_3964	0.32	2.54	4.13	4.54	3.52	2.74	2.73	LEA group 3	P
Ss_44088	0.81	2.51	3.49	3.78	2.60	2.69	2.54	LEA group 3	P
Ss_43693	0.04	2.43	4.40	4.74	3.41	2.66	2.85	Putative RAB protein	U
Ss_4166	0.21	2.42	4.10	4.54	3.72	2.02	2.71	Dehydrin	P
Ss_36724	0.43	2.41	4.36	5.05	4.33	3.18	3.26	LEA group 3	P
Ss_13457	0.18	2.05	3.04	3.49	2.58	2.00	2.35	GRAM domain containing protein	S
Ss_8669	0.77	2.04	2.39	2.50	2.34	2.18	2.22	LEA group 3	P
Ss_36725	0.44	1.93	3.70	4.22	3.84	3.35	3.17	LEA group 3	P
Ss_5352	0.32	1.86	4.05	4.82	4.19	2.79	2.90	LEA group 3	P
Ss_351	0.19	1.77	4.22	4.47	3.33	2.00	3.10	oxidoreductase, aldo/keto reductase	U
Ss_36698	-0.36	1.71	3.45	4.17	2.52	1.96	2.31	Peroxiredoxin	D

These genes are grouped in Cluster 3. Expression values are shown as $\log^2$ ratio of treament over fully-hydrated control. Light blue color represents 2- to 3-fold change; blue color represents 3- to 4-fold change; dark blue color represents 5-to 7-fold change. Putative roles: T, Transporters; R, redox; S, signaling; P, protection; TF, transcription factor; U, unknown; M, metabolism; C, cellular structural changes; PD, protein degradation; D, detoxification

Genes induced during severe dehydration

Cluster 1 contains 345 ESTs that were found to be up-regulated (2 to 6-fold) during severe dehydration (40 and 20 %RWC), after which expression levels decreased during desiccation (less than 10% RWC), and returned to basal levels after rehydration (Figure 2.3 and Table 2.4). This severe dehydration stage is characterized by an induction of different metabolic pathways, like activation of raffinose synthesis and GABA metabolism; induction of ABA-dependent regulatory proteins and other signaling proteins, including proteins involved in calcium signaling and stress response signaling.

LEA group 1 proteins and Oleosin/Caleosin proteins may play a specific role during dehydration

Plant LEA (LATE EMBRYOGENESIS ABUNDANT) proteins are a group of very hydrophilic proteins that accumulate to high levels in mature seeds, when seed desiccation tolerance is acquired, and in vegetative tissues during drought [87].

This severe dehydration stage (20% RWC) is highly enriched in LEA group 1 proteins, while during earlier drying (50% RWC) LEA group 3 proteins were enriched. This finding suggests that LEA group 3 proteins might be important in response to earlier drying while LEA group 1 proteins might be playing a role during late stage of drying and preparing the cells to desiccate.

Specific roles for LEA proteins were reported previously in maize where, different LEA proteins were induced in a tissue-specific manner. In maize, LEA group 2 and 3 proteins were induced in vegetative tissues in response to abiotic stresses, while LEA group 1 proteins were found exclusively in embryogenic tissues. In Arabidopsis, LEA group 1 proteins were induced exclusively during seed drying. Also, the protective roles of the three different LEA group of proteins in maize appeared to be different when assessed *in vitro* and *in vivo*. *E. coli* containing recombinant maize LEA proteins were tested for protein anti-aggregation properties and protective effects on *E. coli* growth under different stresses. LEA group 3 proteins were most efficient during dehydration and osmotic stress; LEA group 2 protein were highly efficient during dehydration, but also

during heat shock and freezing treatments; while LEA group 1 proteins were less efficient during all treatments [92].

LEA group 1 proteins appear to play important protective roles during extreme desiccation. In dehydration sensitive plants, like maize and Arabidopsis, LEA group 1 proteins localized to drying seeds, while in resurrection plants they are localized to the vegetative tissue. These observations led the authors to suggest that seed protection systems from dehydration sensitive plants evolved to provide extreme dessication resistance in the vegetative tissues of resurrection plants [4, 7].

Caleosin and oleosin proteins were also upregulated during this severe dehydration stage. Caleosin and oleosin are important in the formation of plant lipid bodies. Oleosin is a structural protein that stabilizes the lipid bodies, while caleosins are located on the surface of lipid bodies and are thought to be involved in signal transduction via calcium binding or phosphorylation/dephosphorylation. Plant lipid bodies have been intensively studied in seeds, but they are also found in the shoot apex of perennial plants during growth arrest and bud formation [93]. Possible functions of these lipid bodies would be to (i) provide energy and carbon for growth after recovery from dormancy or desiccation, (ii) to provide lipids for reconstitution of the plasma membrane, and (iii) to transport enzymes and signals to modify the plasma membrane, cell wall and plasmodesmata [93]. In Arabidopsis, the RD20 protein, a member of the caleosin family, was shown to play a role in drought tolerance through stomatal control under water deficit conditions [94]. In the resurrection plant *Craterostigma plantagineum*, a caleosin transcript was induced during early dehydration (80% RWC) and during desiccation (5% RWC) [74]. Together, these data suggest a function of caleosin and oleosin proteins during severe dehydration and desiccation. It would be interesting to investigate if *Sporobolus stapfianus* leaf tissues accumulate lipid bodies during desiccation.

Transcription Factors and Signaling-related proteins

Two transcripts annotated as transcriptions factors were up-regulated during this severe dehydration stage: a G-box binding factor 3 (GBF3) transcription factor and a Zinc finger

CCCH type transcription factor. Arabidopsis GBF3 encodes a bZIP G-box binding protein, is induced by drought [95], and activates transcription of alcohol dehydrogenase in response to ABA [96]. Interestingly, in *S. stapfianus*, genes encoding alcohol dehydrogenases were up-regulated during desiccation (Table 2.4). bZIP transcription factors were induced during desiccation in resurrection plants *C. plantagineum* and *Haberlea rhodopensis* [97, 98]. In the same way, Zinc finger CCCH transcription factors were found to play a role in response to drought and salt stress in Arabidopsis and cotton [99].

A gene similar to a remorin was induced during the late stages of dehydration, but before complete desiccation. Remorins are plant-specific proteins associated with plasma membrane domain that were hypothesized to oligomerize and act as scaffold proteins during membrane signaling and trafficking [100]. Induction of remorins was shown to be important during rhizobial infection in *Lotus japonicas* [101], to regulate bacterial infection in *Medicago truncatula* [102] and to impair a potato x virus movement protein [103]. The role of remorins in response to abiotic stress has been little studied, but two recent studies reported that remorins were induced by osmotic stress (dehydration and salt stress) in mulberry trees [104], and by salinity stress, cold stress and ABA in foxtail millet, *Setaria italica* [105]. Moreover, when the mulberry and foxtail millet remorin genes were ectopically expressed in Arabidopsis, they conferred drought and salinity stress tolerance, respectively.

Another ABA-induced protein similar to HVA22E was up-regulated (3.6-fold) during this severe dehydration stage. HVA22E is an ABA- and stress-inducible gene originally isolated from barley, where it plays a role in regulating seed germination and seedling growth by regulating vesicle trafficking [106]. In Arabidopsis seedlings, HVA22E expression is induced by ABA, dehydration, salt and cold stress. Drought stress imposed in soil-grown plants also enhanced AtHVA22E expression in rosette and cauline leaves [107].

Together, these reports suggest that the transcription factors, remorins and HVA22 proteins might be important during the drought response in desiccation sensitive

species and in response to drying in the resurrection grass *S. stapfianus.* However, their specific role in response to drying in resurrection plants still needs to be explored. We are tempted to speculate that they might be important in cellular signaling events and activation of target genes to prepare the plants to be completely desiccated.

Table 2. 4 Summary of genes induced during severe dehydration (Cluster 1)

Contig number	Drying Stages (%RWC)					Rehydration		Gene description	Role
	60 %	50 %	40 %	20 %	Desiccation	12 h	24 h		
Ss_36700	0.18	1.75	4.37	5.18	2.88	1.64	2.14	1-Cys-peroxiredoxin	R
AJ242805	0.07	2.07	3.87	4.85	2.42	1.45	1.90	Aquaporin	T
Ss_16841	0.44	1.02	3.37	3.89	2.04	0.47	0.92	Sodium/calcium exchanger family protein / calcium-binding EF hand family protein	S
Ss_36733	-0.09	2.29	3.46	3.89	2.19	1.76	2.13	LEA group 3	P
Ss_5971	0.10	1.72	2.65	3.79	1.83	0.61	1.59	DUF639	U
Ss_1940	0.04	0.33	3.56	3.67	2.16	0.61	1.06	Caleosin	P
Ss_16366	0.00	0.57	2.46	3.55	2.60	1.01	0.96	LEA-like protein	P
Ss_2144	0.45	1.35	2.64	3.52	1.75	0.41	1.17	G-box binding factor 3 (GBF3)	TF
Ss_1939	0.22	0.49	3.25	3.51	2.16	0.68	1.31	Caleosin	U
Ss_22957	0.48	1.51	2.26	3.27	1.83	1.43	1.42	zinc finger CCCH type family protein	TF
Ss_44032	0.30	0.96	2.96	3.19	2.05	0.96	1.13	HVA22	S
Ss_1742	-0.15	0.02	2.54	3.13	2.30	-0.32	0.01	1-Cys peroxiredoxin	R
Ss_6846	0.33	0.67	2.50	3.09	1.64	0.44	1.01	LEA group 1	P
Ss_6849	0.34	0.55	2.38	3.07	1.46	0.80	0.93	LEA group 1	P
Ss_6848	0.26	0.59	2.19	3.01	1.38	0.23	0.76	LEA group 1	P
Ss_2080	-0.03	0.75	2.50	2.96	1.71	0.13	0.80	ABC transporter family protein	T
Ss_37274	0.15	1.31	2.62	2.95	1.57	0.88	0.95	Aminomethyltransferase	U
Ss_22865	0.29	1.71	2.77	2.94	1.67	1.02	1.02	Cold acclimation protein COR413-PM1	U
Ss_2008	0.16	0.82	2.39	2.89	1.43	0.89	0.80	Transketolase	M
Ss_23766	0.33	1.41	2.87	2.88	1.50	1.37	1.39	NRAMP metal ion transporter 6	T
Ss_16098	0.23	1.53	2.57	2.79	1.55	1.41	1.59	Senescence/dehydration-associated protein	U
Ss_20770	0.19	0.83	2.71	2.79	1.54	0.73	0.95	Sodium/calcium exchanger family protein / calcium-binding EF hand family protein	S
Ss_5302	-0.37	0.68	2.18	2.77	0.83	0.56	0.84	LEA family protein	P
Ss_43766	-0.30	1.35	2.41	2.77	1.93	1.26	1.01	Putative gamma tonoplast intrinsic protein (TIP)	T
Ss_30431	0.01	0.57	1.97	2.70	0.97	-0.37	-0.01	SnRK1	S
Ss_25306	0.43	0.87	2.22	2.69	1.65	0.82	0.35	Phospholipase D delta	S
Ss_15926	0.32	0.89	2.20	2.55	1.36	0.77	0.76	Remorin C-terminal domain containing protein	TF
Ss_17184	-0.28	0.48	2.14	2.45	1.11	-9.10	-9.10	Dehydrin	P
Ss_32159	0.30	0.99	1.77	2.40	1.31	0.85	0.74	Embryonic protein DC-8	U
Ss_2081	-0.51	0.36	2.08	2.24	0.89	0.05	0.27	ABC transporter family protein	T
Ss_31112	-0.08	0.39	1.69	2.21	0.60	-0.55	0.14	Ser/Thr protein phosphatase family protein	S
Ss_22221	-0.15	0.39	2.05	2.18	1.25	0.82	-0.01	Oleosin family protein	U
Ss_31842	-0.60	0.13	1.72	2.04	1.02	0.23	0.28	Glutamate decarboxylase	M
Ss_46685	-0.01	0.50	1.36	2.03	0.74	0.56	0.12	Putative zinc finger protein	TF
Ss_43912	-0.07	0.31	1.51	2.01	0.87	0.30	0.33	LEA group 1	P

These genes were grouped in Cluster 1. Expression values are shown as $\log^2$ ratio of treatment over control fully hydrated. Light blue color represents 2- to 3-fold change; blue color represents 3- to 4-fold change; dark blue color represents 5-to 7-fold change. Putative roles: T, Transporters; R, redox; S, signaling; P, protection; TF, transcription factor; U, unknown; M, metabolism.

Genes induced during desiccation

Genes induced during desiccation are grouped in Cluster 2. These genes were induced during later dehydration stages (40% RWC) and continued to be expressed during further desiccation (10% RWC) (Figure 2.3 and Table 2.5). The gene expression pattern of this cluster suggests that these genes are playing a role when cells are moving to a stage of severe dehydration, perhaps involved in cellular maintenance and protection mechanisms. Indeed, this cluster was enriched in genes encoding Early Light inducible Proteins (ELIPs), dehydrins, 1-cys peroxiredoxin, metallothioenin, and oxidoreductases, all of which were previously suggested to play a protective role during desiccation. Cell structural proteins (e.g. cell wall hydrolases) and those related to membrane lipid metabolism were present in this cluster, reflecting the cell structural changes occurring during desiccation.

Protective mechanisms during desiccation: ELIPs, Cys-Peroxiredoxin, Dehydrins

During water limited conditions, photosynthesis is severely suppressed and the energy from light cannot be dissipated by the chlorophyll, leading to formation of oxygen free radicals that cause cellular damage. One of the mechanisms to deal with photooxidative stress is the accumulation of protective proteins and antioxidants. Another mechanism used by resurrection plants is the ability to retain most of their chlorophyll and thylakoid integrity during drying (termed homoiochlorophyllous). *S. stapfianus* showed an intermediate behaviour between homoiochlorophyllous species and poikilochlorophyllous species (where chlorophyll is totally lost and the thylakoids are completely degraded) [108]. Using this extraordinary mechanism, *S. stapfianus* is able to resume photosynthesis rapidly after re-watering.

ELIPs were up-regulated during desiccation in *S. stapfianus*. ELIPs are thylakoid chlorophyll binding proteins that accumulate when mature leaves are exposed to excessive light or in response to other environmental stresses. In *Arabidopsis,* a double mutant *elip1/elip2*, failed to increase photoinhibition under high light and cold stress conditions, suggesting that they are not sufficient to provide photoprotection [109]. Instead, ELIPs might bind and stabilize zeaxanthin, an antioxidant component that might

provide photoprotection [109-111]. Induction of ELIPs was reported to be involved in desiccation stress in resurrection plants like *T. ruralis* [112], *H. rhodopensis*[77] and *C. plantagineum* [110]. Strong, ectopic expression of the ELIP-like DSP22 protein from the resurrection plant *C. plantagineum* in *Medicago truncatula* plants resulted in an improved efficiency of energy conversion in photosystem 2 after recovery from water deficit conditions [111], demonstrating the photo-protective role of ELIPs from this resurrection plant.

1-cys-peroxiredoxin was also found induced in the desiccated leaves of *S. stapfianus* in this study. 1-Cys-peroxiredoxin protein is an antioxidant enzyme that is commonly found up-regulated only in seeds of desiccation sensitive plants (Buitink et al., 2006). Interestingly, 1-cys-peroxiredoxin is induced in vegetative tissues of resurrection plants during desiccation (Illing et al., 2005; Mowla et al., 2002).

The group 2 LEA proteins, commonly called dehydrins, were also induced during this desiccation stage. These proteins are exclusively found in plants, whereas other LEA groups can be found in bacteria and nematodes (see above). Dehydrins fall in the category of intrinsically disordered proteins, proteins that lack a fixed 3D structure under physiological conditions, and are thought to function as chaperonins to prevent denaturation of other proteins during stress [113]. These proteins are very abundant in desiccated leaves of several resurrection plant species and also in seeds, suggesting a role in desiccation tolerance in plants.

Table 2. 5. Summary of genes induced during dehydration and desiccation (Cluster 2)

Contig number	Drying Stages (%RWC)					Rehydration		Gene description	Role
	60 %	50 %	40 %	20 %	Desiccation	12 h	24 h		
Ss_16106	0.17	0.76	4.35	5.89	4.61	3.22	2.63	LEA	P
Ss_7107	-0.33	0.78	4.47	5.49	4.58	2.31	2.34	LEA group 1	P
Ss_29705	0.68	1.00	4.13	5.42	3.97	3.15	2.77	NA	U
Ss_15937	0.27	0.27	2.95	5.31	4.27	2.70	2.01	Early light-induced protein (ELIP)	S
Ss_1874	-0.21	0.29	4.09	5.17	3.60	2.88	1.98	Early light-induced protein (ELIP)	S
Ss_8720	0.13	1.09	4.65	5.09	3.53	1.61	2.13	Aldose reductase-related protein	M
Ss_1856	-0.02	0.64	3.46	5.08	3.56	2.73	2.18	Dehydrin	P
Ss_49936	0.19	-0.24	2.80	5.08	4.06	2.51	1.06	NA	U
Ss_359	0.53	0.08	2.97	5.02	3.93	2.16	2.47	Win1, Wound-induced protein	U
Ss_16003	0.53	1.13	3.86	4.98	4.22	2.42	2.48	NA	U
Ss_29896	0.20	0.38	3.58	4.94	4.33	3.19	2.83	Early light-induced protein (ELIP)	S
Ss_6777	0.08	1.06	3.88	4.94	3.11	1.94	1.84	Peroxiredoxin	R
Ss_44545	0.20	0.19	3.33	4.84	4.32	2.63	2.80	Early light-induced protein (ELIP)	S
Ss_17841	0.14	-0.10	3.45	4.78	4.33	3.72	2.96	Early light-induced protein (ELIP)	S
Ss_16118	0.20	0.85	3.51	4.72	3.52	2.34	2.16	Early light-induced protein (ELIP)	S
Ss_4083	-0.34	-0.26	3.11	4.68	3.57	1.69	1.60	Early light-induced protein (ELIP)	S
Ss_16311	0.05	0.49	3.58	4.60	3.16	1.31	1.75	Desiccation-related protein PCC13-62	U
Ss_31699	-0.05	0.23	2.83	4.59	2.37	0.98	1.50	Desiccation-related protein PCC13-62	U
Ss_352	0.23	1.04	3.98	4.59	3.32	1.95	1.81	Aldose reductase-related protein	M
Ss_29899	0.12	0.98	4.01	4.57	3.60	2.31	2.48	Early nodulin 20 precursor	U
Ss_37321	0.01	-0.08	2.77	4.49	3.27	1.28	1.16	Endo-Beta-Mannanase	C
Ss_36723	-0.13	0.73	2.55	4.47	2.37	1.82	2.16	LEA group 3	P
Ss_4081	0.24	-0.06	3.29	4.45	4.06	2.29	2.31	Early light-induced protein (ELIP)	S
Ss_1718	-0.11	1.14	3.65	4.45	3.37	2.17	2.19	Embryonic protein DC-8	U
Ss_15936	-0.01	-0.05	3.03	4.34	3.85	2.92	1.87	Early light-induced protein (ELIP)	S
Ss_5554	0.15	0.35	2.18	4.29	2.92	2.05	1.45	Early light-induced protein (ELIP)	S
Ss_16201	-0.19	0.81	3.33	4.24	2.66	1.89	2.05	LEA group 1	P
AJ242806	0.10	0.24	2.78	4.20	3.41	2.57	1.52	Early light-induced protein (ELIP)	S
Ss_45312	1.19	-0.04	1.63	4.16	3.42	2.42	2.40	Cysteine proteinase inhibitor 8 precursor	PD
Ss_9410	-0.17	0.13	2.27	4.00	2.95	2.35	2.02	Endochitinase	U
Ss_4412	-0.07	0.36	2.01	3.87	2.55	2.20	2.06	Osmotin 34	U
Ss_4084	0.39	0.26	2.14	3.87	3.08	1.83	1.61	Early light-induced protein (ELIP)	S
Ss_30274	-0.01	-0.65	2.48	3.82	2.09	2.23	0.92	Endo-Beta-Mannanase	C
Ss_466	-0.13	0.36	2.87	3.78	2.53	2.30	1.93	Dehydrin	P
Ss_467	-0.08	0.41	2.67	3.78	2.85	1.35	1.58	Dehydrin	P
Ss_7072	0.04	1.27	3.14	3.72	2.43	1.70	1.66	Embryonic protein DC-8	P
Ss_1713	-0.22	0.34	2.73	3.71	2.32	1.18	1.20	Oxidoreductase	U
Ss_4027	0.15	0.53	2.68	3.68	2.29	1.36	0.96	Oxidoreductase	U
Ss_5299	-0.24	0.47	3.00	3.67	2.06	1.28	1.43	LEA domain-containing protein	P
Ss_43776	-0.04	0.52	2.94	3.63	2.51	1.53	1.36	Peroxiredoxin	R
Ss_44034	-0.08	0.33	2.42	3.60	2.34	1.59	1.26	HVA22	S
Ss_4026	0.12	0.48	2.49	3.46	2.16	1.16	0.93	Oxidoreductase	U
Ss_30544	-0.24	-0.18	0.91	3.32	2.53	1.47	1.31	Regulation of transcription, unclassified	TF
Ss_23145	0.06	0.42	2.00	3.27	2.61	0.71	1.16	Alcohol dehydrogenase	M
Ss_5987	0.19	0.37	1.48	3.10	2.04	1.02	0.90	Aldehyde dehydrogenase	M
Ss_29898	0.03	-0.07	1.51	3.07	2.53	2.15	2.01	Early light-induced protein (ELIP)	S
Ss_1740	-0.02	0.08	1.64	3.02	2.36	1.14	0.78	Early light-induced protein (ELIP)	S
Ss_8719	0.08	0.79	1.64	2.90	2.10	1.45	1.32	Secretory protein	U

These genes were grouped in Cluster 2. Expression values are shown as $\log^2$ ratio of treatment over control fully hydrated. Light blue color represents 2- to 3-fold change; blue color represents 3- to 4-fold change; dark blue color represents 5-to 7-fold change. Putative roles: T, Transporters; R, redox; S, signaling; P, protection; TF, transcription factor; U, unknown; M, metabolism; C, cellular structural changes; PD, protein degradation; D, detoxification.

Transcriptional regulation during rehydration

Most research on resurrection plants has focused exclusively on dehydration. However, the rehydration process is an integral part of the desiccation tolerance mechanism in resurrection plants. Rehydration processes involve the recovery of the cellular organization and metabolic activities, but also include mechanisms for preventing and/or repairing cell damage upon rehydration.

Re-greening of leaves is observed after 24 hours of re-watering the fully desiccated plants of *S. stapfianus* (see video at http://youtu.be/BINkhNNpYvc). This rapid recovery is because *S. stapfianus* leaves retain considerable chlorophyll in the dry state (homoiochlorophyllous). This rapid recovery can be observed at the transcriptional level in our experiment. We found two clusters, one with genes whose expression was shut down during drying and after 24 hours of rehydration returned to basal levels (Cluster 15, Figure 2.3); the other cluster showed genes whose expression was shut down during drying and did not return completely to basal levels after 24 h of re-watering (Cluster 13, Figure 2.3). These results suggest that the rapid regreening of the plant during 24 hours of rehydration does not reflect a full recovery of plant metabolism to a fully hydrated state.

Our clustering analysis identified clusters that were exclusively induced during rehydration (Clusters 10, 19 and 38 in Figure 2.3).

Metabolism comes back during rehydration and this is reflected in the induction of genes involved in glycolysis, tricarboxylic acid cycle, photosynthesis and synthesis of ribosomal proteins (Tables 2.3 and 2.7). This high rate of protein translation might be achieved through the induction of RECEPTOR FOR ACTIVATED C KINASE 1 (RACK1). RACK1 is a scaffolding protein necessary for the normal production of 60S and 80S ribosomes and protein translation [114]. Cellular structural changes occur during the influx of water into the cells and this is reflected in the induction of some cell wall degradation enzymes, lignin biosynthetic genes and a CAP1 transcription factor, which regulates actin synthesis. Signaling molecules induced during rehydration include a 14-3-3 protein-like protein, a MAP Kinase (similar to MAPK6) and several GTP-binding

proteins, suggesting that several cellular signaling events are taking place during this time. An interesting group of genes induced during rehydration are those encoding transporters of inositol, phosphates, polyol/monosaccharides, amino acids, sugar and starch. This abundance of transporters might reflect the re-activation of the metabolism during rehydration. As mentioned earlier, some mechanisms of protection must be activated to prevent cell damage upon rehydration. Rehydration of *S. stapfianus* induced the expression of genes encoding heat shock proteins (HSP) (Table 2.6). HSPs were previously mentioned as providing cellular protection during drying, but we found no reports about their possible function during rehydration. Other protective molecules up-regulated during rehydration were LEA group 3 proteins. LEA group 3 proteins are thought to play a protective role by interacting alone or with disaccharides (e.g. sucrose) with membranes and/or proteins during dehydration [87, 88].

Table 2. 6. Summary of genes induced during rehydration (Cluster 10)

Contig number	Drying Stages (%RWC)					Rehydration		Gene description	Role
	60 %	50 %	40 %	20 %	Desiccated	12 h	24 h		
Ss_17444	-6.04	-6.04	0.94	0.34	-6.04	6.65	5.62	Cytochrome c oxidase subunit 3	M
Ss_3286	1.43	0.50	0.39	0.12	-7.42	5.93	4.54	Hydrophobin 3	U
Ss_8040	1.47	0.71	0.40	-0.02	1.05	5.75	3.44	NADH-ubiquinone oxidoreductase	M
Ss_46870	1.16	0.51	0.39	0.35	-5.76	5.63	3.88	UBiQuitin family member	PD
Ss_48500	1.41	1.04	0.79	0.92	1.11	5.52	4.64	Amino-acid permease inda1	T
Ss_46163	1.21	1.24	0.65	1.00	1.71	5.17	4.15	40S ribosomal protein	RS
Ss_24084	0.89	1.47	0.59	0.68	0.77	5.05	4.12	Inositol transporter 2	T
Ss_7078	1.46	1.20	0.79	1.07	1.71	4.71	3.55	60S ribosomal protein L21-A	RS
Ss_465	1.08	0.49	0.27	-0.21	-5.39	4.66	3.08	Actin	C
Ss_13136	0.76	1.01	-0.03	0.66	0.77	4.43	3.54	Translation elongation factor 1 alpha	RS
Ss_30355	0.68	0.48	0.26	0.53	0.79	4.39	3.14	Sugar transporter	T
Ss_9716	0.37	0.33	0.09	0.27	1.18	4.39	3.12	60S ribosomal protein L27	RS
Ss_23729	0.40	0.45	0.19	-0.20	1.85	4.38	3.31	40S ribosomal protein S4	RS
Ss_13041	1.13	0.72	0.63	0.67	1.47	4.38	3.39	GTPase activating protein Sec23a	T
Ss_34294	0.76	0.54	-0.23	0.41	1.15	4.37	3.30	Plasma membrane ATPase	T
Ss_48534	1.01	1.20	0.36	1.01	1.37	4.23	3.43	phosphate transporter 3;1	T
Ss_2112	0.82	0.93	0.45	0.89	1.76	4.15	3.18	60S ribosomal protein L39	RS
Ss_46793	0.90	1.29	0.01	0.88	0.99	4.15	4.35	Elongation factor 1-alpha (Fragment)	RS
Ss_12615	0.24	-0.27	-0.16	-0.03	0.31	4.01	3.74	Major facilitator superfamily protein	T
Ss_37232	1.39	0.70	0.66	1.00	1.88	3.95	4.01	Heat shock protein 17.4	P
Ss_26768	0.53	1.01	0.40	1.05	1.58	3.82	3.66	Beta-tubulin 2	C
Ss_40953	0.40	0.64	0.13	0.46	0.56	3.79	3.21	ADP/ATP carrier 3	T
Ss_34261	0.66	0.65	0.40	0.37	0.95	3.75	3.00	Mitogen-activated protein kinase sty1	S
Ss_41927	0.65	0.46	0.28	0.37	0.64	3.74	3.81	ATP synthase subunit beta	PS
Ss_42597	0.77	0.84	0.31	0.79	1.08	3.71	3.63	Endoglucanase B	C
Ss_5822	0.37	0.36	0.06	0.17	0.35	3.69	2.85	Cytochrome c	PS
Ss_23394	0.95	0.87	0.28	0.68	0.70	3.55	2.83	Receptor for activated C kinase 1C	TF
Ss_29838	0.17	0.85	0.20	0.70	1.16	3.53	2.87	Glyceraldehyde-3-phosphate dehydrogenase	M
Ss_42900	0.51	0.46	-0.22	0.89	1.01	3.50	2.97	phosphate transporter 3;1	T
Ss_7448	0.59	0.16	0.36	0.14	0.76	3.35	3.05	polyol/monosaccharide transporter 5	T
Ss_49373	-0.03	0.18	-0.19	-0.07	0.25	3.24	2.36	14-3-3 protein-like	TF
Ss_34127	1.01	0.69	0.41	0.76	0.65	3.14	2.91	Calcium pump1 (cap1), mRNA	TF
Ss_3580	1.05	1.00	0.70	0.93	1.26	2.98	2.36	Pom1 kinase homologue pomA	U
Ss_26622	0.36	0.56	0.19	0.60	1.10	2.91	3.01	OsGrx_C2.1 - glutaredoxin subgroup I	R
Ss_39214	0.32	0.55	-0.17	0.03	0.12	2.60	2.47	Heat shock protein 70 (Fragment)	P
Ss_19831	0.57	0.42	0.36	0.68	0.82	2.59	2.06	Retrotransposon polyprotein	U

These genes were grouped in Cluster 10. Expression values are shown as $\log^2$ ratio Light blue color represents 2- to 3-fold change; blue color represents 3- to 4-fold change; dark blue color represents 5-to 7-fold change. Putative roles: T, Transporters; R, redox; S, signaling; P, protection; TF, transcription factor; U, unknown; M, metabolism; C, cellular structural changes; PD, protein degradation; RS, RNA synthesis; D, detoxification; PS, photosynthesis

Comparison of *S. stapfianus* with the desiccation sensitive, sister species *Sporobolus pyramidalis*

Phylogenetic sister groups are thought to have relatively the same evolutionary age and share a common ancestor. These features are usually reflected in similar metabolism that may vary only in relatively few traits (e.g. desiccation tolerance) (Barraclough, T., et al., 1998). *S. pyramidalis* is a sister species to *S. stapfianus* but does not exhibit desiccation tolerance. The desiccation sensitive *S. pyramidalis* responds differently to dehydration when compared to *S. stapfianus* at the metabolomic level [11].

In order to investigate the differences in gene expression between *S. stapfianus* and *S. pyramidalis* in response to dehydration, we compared the expression of 16 genes. These genes were up-regulated in *S. stapfianus* during dehydration in this study. We used aerial tissues that were dehydrated at 60% RWC, because *S. pyramidalis* is wilted and further dehydration resulted in apparent cell death [11].

We identified five genes which showed differential gene expression between the two species: a LEA protein group 3-like gene, a 1-cys peroxiredoxin-like gene, a peroxygenase1-like gene, a remorin-like gene and a gene encoding a protein with unknown function (Figure 2.5). We considered them as putative adaptive genes that may be important for the desiccation tolerance phenotype of *S. stapfianus*. Expression of 3 out of 16 genes could not be detected in *S. pyramidalis*, and 8 out of 16 had a similar expression pattern than *S. stapfianus* (not shown). One caveat with this experiment is that we assumed that we are targeting the homologous gene in *S. pyramidalis*. Unfortunately, at the time (year 2011) we lacked a sequenced genome for this species.

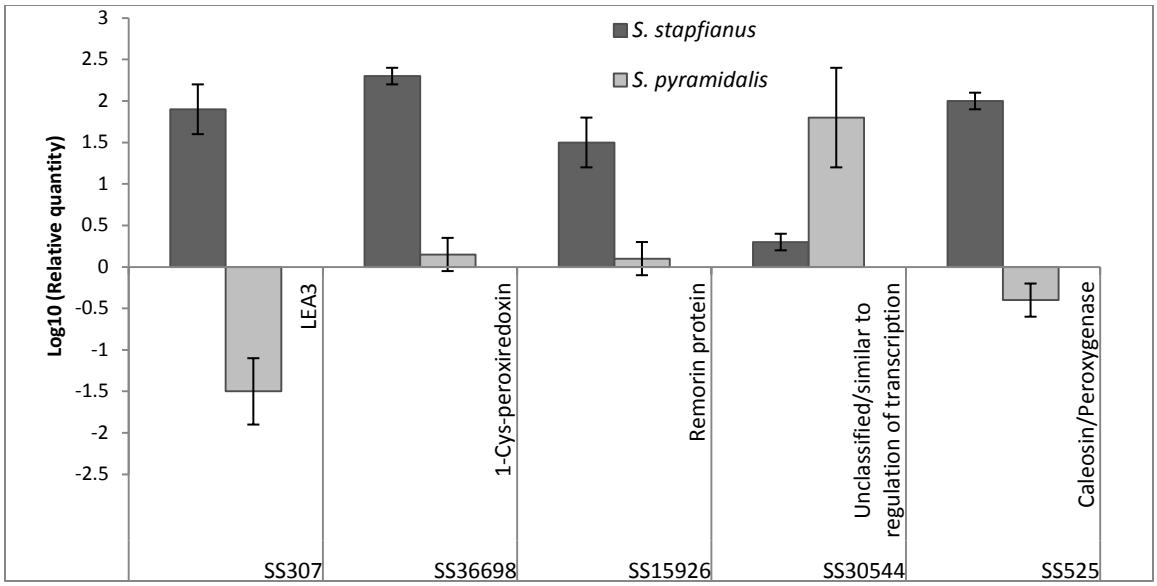

Figure 2.5. Differential gene expression between desiccation tolerant *Sporobolus stapfianus* and its sensitive sister species *S. pyramidalis*

Leaf tissues from both species were dehydrated at 1.5 g H_2O/g DW to extract RNA and perform qRT-PCR.

Concluding remarks and future directions

Our large scale gene profiling in the resurrection grass *S. stapfianus* provides some important insights into the gene regulatory mechanisms used by this interesting plant during severe vegetative desiccation and subsequent recovering during rewatering. Some important highlights of the *S. stapfianus* transcriptome are: 1) Up-regulation of retrotransposons during early drying, suggesting an important mechanism of gene regulation mediated by retrotransposons; 2) ABA-induced genes and induction of LEAs and dehydrins for cellular protection during moderate dehydration, which suggest similar mechanisms with desiccation sensitive plants in response to dehydration; 3) Up-regulation of LEA group 1 and 1-cys-peroxiredoxin during desiccation that is similar to what is seen during desiccation of seeds; and 4) Up-regulation of protective and signaling genes during rehydration, indicating the importance of cellular protection when water re-enters the cells.

Gene expression comparison between sister species differing in dehydration tolerance can be used to uncover adaptive genes important for this trait. Our data showed that five out of sixteen genes showed differential expression between *S. stapfianus* and its desiccation sensitive sister species, *S. pyramidalis*. But a large scale comparison will help us to elucidate which pathways and regulatory mechanisms are important for this dehydration tolerance trait. This could be accomplished by generating a specific *S. pyramidalis* microarray or using Next Generation Sequencing, comparing the entire transcriptomes of both species. In addition, a more extensive ancestor-descendant comparison between other desiccation tolerant species, desiccation sensitive species and desiccation tolerant seeds, would provide a rich dataset to trace gene networks through phylogenies and to explore for conserved patterns that infer adaptive value. These ancestor-descendant comparisons will add to our understanding of the evolution of desiccation tolerance in plants.

Materials and methods

Plant materials and drying conditions.

The South African grass *Sporobolus stapfianus* Gandoger was grown in one-gallon pots under greenhouse conditions of 16 h light and day/night temperatures of 28^{o}C/19^{o}C. Three month-old plants were subjected to a drying event by withholding water until desiccation. After one week of being desiccated, plants were re-watered by spraying the plants with a continuous mist. Young leaf tissues were collected at eight conditions: at full hydration (water content of 3 g H_2O/g Dry Weight (DW)) and at incremental dehydration stages (2, 1.5, 1, 0.75, and 0.5 g H_2O/g DW; which corresponds to 60, 50, 40, 20 and 5 % relative water content (RWC) [11]), and after rehydration at 12 and 24 hours (Figure 2.1). Three independent biological replicates were produced from each condition. Duplicate samples were taken to allow for the determination of the water content and RWC at the time of sampling. Water content was calculated as (fresh weight – dry weight)/dry weight. Leaf RWC was calculated as RWC(%)= [(FW-DW)/(TW-DW)]x100; where FW: fresh weight, DW: dry weight, TW: fully turgid weight [115]. Jim Elder (USDA Research Technician, Columbia MO) performed the experiment, collected the tissues and isolated the RNA.

RNA isolation.

Frozen leaf tissue was ground in liquid nitrogen using a ceramic mortar and pestle. Total RNA was isolated from the frozen powder using a Qiagen RNeasy® plant mini kit (Qiagen Inc., Valencia, CA, USA) according to the manufacturer's instructions. RNA quality was gel verified and quantified spectrophotometrically (NanoDrop ND-1000, ThermoScientific, Waltham, MA).

454 pyro-sequencing, trimming and assembly of expressed sequence tag (EST) reads.

Mixed cDNA populations representing transcripts of genes expressed in tissues collected at dehydration through rehydration time course were submitted to 454 Life Sciences Biotechnology Company (Roche, Branford, CT) for sequencing, trimming and assembly.

The 454 high throughput pyro-sequencing was performed according to the method described by Margulies et al [116]. The sequences were subsequently trimmed: poly (A/T) tails, *E. coli* contaminating sequences and cloning artifacts were removed. To identify overlapping EST sequences, reduce sequencing error and produce non-redundant EST data for further comparative analysis and functional annotation, high quality ESTs were assembled into contigs using the TGI clustering tool [117] and a modification of the protocol used by TIGR for assembling their Plant Transcript Assemblies [118].

BLAST hits were mapped to retrieve gene ontology (GO) terms using the program BLAST2GO (v.1.2.7) [81]. GO terms for each of the three main categories (biological process, molecular function, and cellular component) were obtained using a E-value-hit-filter of $1.0E^{-6}$ and a similarity cut-off of 55%.

NimbleGen microarray design.

Custom oligonucleotide microarrays were fabricated by NimbleGen Systems Inc. (Madison, WI, USA) using its proprietary Maskless Array Synthesizer (MAS) technology [119]. The custom S. stapfianus oligonucleotide microarray contained 7 probe sets for 50,152 unique EST contigs, derived from a combined EST collection obtained from a cDNA library prepared with desiccated leaf tissue (unpublished) and from the 454-pyrosequencing described above. The targets included 11 ESTs to be used as control, whose transcript abundance during drying were reported previously using Northern blots [72, 120].

Microarray analysis and clustering.

RMA (Robust Multi-Array Average; Bioconductor release package 1.2) was applied to normalize the microarray data. Expression values were computed from the raw Pairs files by first applying the RMA model of probe-specific background correction of PM (perfect match) probes. These corrected probe values were then normalized via quantile normalization, and a median polish was applied to compute one expression measure from all probe values. Expression values were $\log_2$-transformed. Pearson correlation

coefficients and Spearman rank coefficients were computed on the RMA expression values (log_2-transformed) for each set of biological replicates. Differentially expressed genes between the stress conditions and across the temporal states were determined by ANOVA on the RMA expression values. A multiple testing correction such as the Benjamini-Hochberg adjustment for the false discovery rate of Storey's q value adjustment was applied to the p-values of the F-statistics to adjust the false discovery rate. Genes with adjusted F-statistic p-values<0.05 were extracted for further analysis. Hierarchical clustering was performed using correlation between two profiles as a measure of dissimilarity, and the average agglomeration method.
Microarray data analysis and clustering was performed by Dr. Karen Schlauch at University of Nevada, with inputs from Dr. Mel Oliver (USDA, Columbia MO), Dr. John Cushman (University of Nevada, Reno) and Catherine Espinoza (University of Missouri, Columbia MO).

Functional annotation and metabolic pathway analysis using Mapman software.
The *S. stapfianus* EST contigs were annotated against the green plant subset from the non-redundant (nr) NCBI database, the rice peptide database OsGDB_OSpepV 6.1 (http://www.plantgdb.org/OsGDB), the maize peptide database ZmB73_5a_WGS (http://maizesequence.org) and Arabidopsis peptide database TAIR10 (http://www.arabidopsis.org) by using BLASTX [78] with an e-value of 10^{-5}. Manual annotation and bibliographic searches were also performed to correct annotation errors as necessary.
To assign functional plant categories, the 4,751 differentially expressed *S. stapfianus* ESTs were submitted to the Mercator web tool (http://mapman.gabipd.org/web/guest/mercator). The ESTs were functionally annotated against the Arabidopsis protein TAIR Release 9, SwissProt/UniProt plant proteins and TIGR5 rice proteins databases, using a BLAST cut-off of 80. This mapping file containing *the S. stapfianus* ESTs with their assigned "bin" was used in Mapman software [83], to show the differences in gene expression in different cellular and

metabolic processes. Ratios were expressed in $\log_2$ scale for importing into the software.

Quantitative RT-PCR.

To verify the *S. stapfianus* Nimblegen customized microarray data, quantitative RT-PCR was performed on first strand cDNA prepared from the same RNA samples used for the microarray experiments. One microgram of total RNA from leaf samples was used for reverse transcription using the SuperScript III Reverse Transcriptase (Invitrogen, Waltham, MA). The cDNA synthesis reaction was carried out using oligo-dT(12-18) primers. The resulting first strand cDNA was used for qRT-PCR experiments. Triplicate quantitative assays for each tissue were performed with the SYBR® Green master mix (Applied Biosystems) according to manufacturer's instructions. Primers for qRT-PCR were designed using the PerlPrimer v1.1.21 program to target *S. stapfianus* EST sequences that showed more than 2-fold difference during drying and rehydration (Table 2.7). To evaluate gene expression, results were normalized against a well-watered control using a housekeeping gene, EST (SS40298), annotated as a putative RNA-binding protein. We selected this EST based on its similarity to the Arabidopsis housekeeping gene (At3g01150) [121] and because microarray and qRT-PCR analyzes showed that this EST was stably expressed across the eight different conditions used in this study.

Table 2. 7. Primers used for validation of microarray with qRT-PCR

Gene type	EST name	Gene Annotation	5' -> 3' Primer sequences
Reference	SS40298	Polypyrimidine-tract-binding protein	AATGCGTTCAAAGGGTTATGGAT TACGGCCGGGATGAACAAAGC
Target	SS14243	Unknown	ATTCAGAAGGACAGAGGG GCAGATGTTGTGAATGGA
Target	SS303	Unknown	GCAACGACAAGATCCATCC AGCAAATCCCAGTCCCAG
Target	SS28791	DNA J heat shock N-terminal domain protein	TGAGGAGGATTATGGAAGAG CATCAACGCAACATTCAC
Target	SS36698	1-Cys peroxiredoxin	GGGAACATCTTCTTAGCCTC AGCTCAGCTTCCTGTACC
Target	SS31874	Aminopeptidase	GTTTGTAGGAATCTTCGCA GAACAATCTCCATATCAGCC
Target	SS2144	GBF3 (G-box binding factor 3)	TGATAAACCAAGAGAACCAG CCCTGTTTGATTGCTTCC
Target	SS30544	Regulation of transcription/ unclassified	CTTCATGTCGGAAATGTTGG ACGAGCAAAGCAAATAAGCA
Target	SS1844	Senescence/dehydration associated protein related	AGTTCTTCAAATTGATGCCC CTTGTTCGCCAAATCTGTG
Target	SS23766	Metal transporter	GCTCATCCATAACTCGCT GAAAGTGATGATTGAGTCCT
Target	SS2141	ERD7 (early-responsive to dehydration 7)	GTTCGCCTTAATAGTGGA ATCATCAACTGTAACGACC
Target	SS15926	Remorin family protein	CGGTAGACAATGATGCTG CTCTTCTCGCTTTCCTCC
Target	SS24084	INT2 (inositol transporter 2)	CTGTCTTCTCCTCTGCTC CGATGTATTGAGTGCCGA
Target	SS307	LEA-3 maize	CAATAAACAGCACGCCCT GACAAACTTCTCACGGCA
Target	SS7448	ATPLT5 (polyol transporter 5)	CCTTCCAATACTCCGCAG TTGAGACCAGCGTAGAATCC
Target	SS23394	RACK1C (Receptor for activated kinase 1C)	TGCTTGGACTCGTTCAGG ACATTGGTCACACTGGCT
Target	SS525	Caleosin/peroxygenase	GTCCACAACATCCACAAGAG TCCGTAGAAATCGAAGACCA

Acknowledgements

We would like to acknowledge the technical assistance of Jim Elder (USDA, Columbia, MO), and the assistance of bioinformaticians Christopher Bottoms at University of Missouri, and Richard Tillett at University of Nevada, Reno. This study was funded by an USDA CSREES-NRI Grant (2007-02007) to PI Mel Oliver USDA-ARS-PGRU Columbia, Co-PIs Robert Sharp, University of Missouri; John Cushman, University of Nevada, Reno; Paxton Payton, USDA-ARS-PSRU Lubbock.

Chapter 3

Chitin receptors CERK1 and LYK4, and ANNEXIN 1 regulate a crosstalk between salt stress and chitin-triggered innate immunity in Arabidopsis

Abstract

Salt stress and pathogenic fungi decrease crop yields worldwide. In nature, plants need to respond to multiple environmental stresses that require coordination and fine-tuning of different stress signaling pathways. Here, we explore the crosstalk between fungal-derived chitin and salt stress responses and how chitin receptors *CHITIN ELICITOR RECEPTOR KINASE* (*CERK1)* and *LYK4* mediate this cross-talk. Transcriptome analysis revealed that salt stress induced genes are highly correlated with chitin-induced genes. The *cerk1* and *lyk4* mutants were more susceptible to NaCl than wild type, and *cerk1* had an irregular calcium influx after NaCl treatment. The altered $[Ca^{2+}]_{cyt}$ response in *cerk1* plants was specific to the ionic component of salt stress and not the osmotic component. Bimolecular fluorescence complementation (BiFC) and co-immunoprecipitation experiments indicated that CERK1 and LYK4 physically interact with ANN1, an annexin that forms a calcium-permeable channel that contributes to the NaCl-induced $[Ca^{2+}]_{cyt}$ signal. In turn, an *ann1* mutant showed hypersensitivity to chitin-induced rapid responses, such as the production of reactive oxygen species (ROS) and MAP kinase phosphorylation. The data suggest a functional link between salt stress and fungal-triggered innate immunity. We propose the sodium ions may function as a danger signal to elicit an innate immune response in plants.

Keywords: chitin, salt stress, calcium signaling, CERK1, ANN1

Introduction

Salinity stress limits agricultural production in over 30% of irrigated crops and 7% of dryland agriculture worldwide [1]. Likewise, plant pathogenic fungi and fungal-like oomycetes also cause significant yield losses. For example, it is estimated that crop losses due to fungal infection of rice, wheat, maize, potato, and soybean between 2009 and 2010 would have been sufficient to feed 8.5% of the 7 billion humans alive in 2011 [2]. Hence, both biotic and abiotic stresses that affect food production are significant problems that we can ill afford with a rapidly growing population.

In recent years, the plant model, *Arabidopsis thaliana,* has been used to discover the mechanisms of salt stress tolerance. The plant senses NaCl through unknown sensor/sensors that result in an increase of cytosolic calcium. The increase in cytosolic calcium is sensed by the calcineurin B-like (CBL) calcium binding protein SALT OVERLY SENSITIVE 3 (SOS3). SOS3 interacts with SOS2, a CBL-interacting protein kinase, which in turn activates a plasma membrane Na^+/H^+ antiporter, SOS1, to extrude Na^+ ions out of the cell [34, 122]. However, it is not clear which components function in the early events of the salt stress signaling pathway at the plasma membrane.

Chitin, a fungal cell wall polymer, is a microbe-associate molecular pattern (MAMP) recognized by plant cells resulting in the triggering of an immune response that contributes to fungal resistance [123]. In Arabidopsis, chitin is recognized by a receptor complex comprising the lysin motif (LysM) containing proteins CHITIN ELICITOR RECEPTOR KINASE 1 (CERK1), LYSM-CONTAINING RECEPTOR-LIKE KINASE 4 (LYK4) or LYSM-CONTAINING RECEPTOR-LIKE KINASE 5 (LYK5) [16, 18-20]. The data suggest that LYK4 and LYK5 are partially redundant, with LYK5 playing the primary role in chitin recognition [20]. CERK1 also mediates perception of bacterial cell wall peptidoglycans (PGN), which also requires LYSM DOMAIN GPI-ANCHORED PROTEIN1 (LYM1) and LYM3, two LysM containing receptor proteins (LYPs) that physically interact with PGN [23]. More recently, CERK1 was reported to have a chitin-independent role in pathogen-induced cell death control [24].

While most research on plant stress has examined one stress at a time, in nature, plants are exposed to various abiotic and biotic stresses simultaneously. Abiotic stress often affects the tolerance to biotic stress and vice versa. There are two possible mechanisms by which abiotic stress affects the interaction between plants and pathogens. One possibility is that the negative effects of pathogens and abiotic stress can be additive. For example, tomato plants pre-irrigated with saline water were more severely affected with crown and root rot disease (*Fusarium oxysporum* f. sp. *radicis-lycopersici*) [42]. The other possibility is that abiotic stress enhances plant pathogen resistance [124]. This phenomenon is also known as cross-tolerance, cross-resistance or multiple-stress resistance and was demonstrated for different types of stress [44]. For instance, barley plants irrigated with saline water developed increased tolerance to barley powdery mildew fungus [45]. Additionally, in Arabidopsis, a pre-treatment with chitin improved the total chlorophyll content (by 13%) in the response to salinity [52]. Genetic studies in Arabidopsis show that some genes are important for both the response to biotic and abiotic stresses, confirming that both stresses share signaling components. For example, BOS1, a R2R3 MYB transcription factor, and its interactor BOI, an E3-ligase, are required for the response to the necrotrophic fungal pathogen *Botrytis cinerea* and to salinity stress [48, 49]. Arabidopsis plants ectopically expressing fungal chitinases (from the mycoparasite *Trichoderma asperolloides*) showed an increased tolerance to salinity during germination, and an enhanced tolerance to the necrotrophic fungus *Botrytis cinerea* [52]. Interestingly, this effect was not seen when chitinase was ectopically expressed in *cerk1* mutant plants [52]. These findings suggested a possible role for chitin signaling in mediating salinity stress signaling. Such a role was also suggested by studies of another member of the Arabidopsis LysM RLK family, LYK3, which was reported to be important for the crosstalk between signaling pathways activated by pathogens and abscisic acid (ABA) [50]. Previous research implicated LYK3 in the suppression of plant innate immunity in response to short chain chitin oligomers [degree of polymerization (dp) <6] [51].

These publications led us to examine in more detail the possibility of crosstalk between chitin and salt stress responses. The results clearly show that members of the chitin receptor complex, *CERK1* and *LYK4,* are necessary for a robust plant salt stress response. *CERK1* and *LYK4* expression is induced by NaCl treatment and *cerk1* and *lyk4* mutant plants were more susceptible to NaCl but not to osmotic stress. Previously described cross tolerance between fungal defense and salinity stress, can be explained by our finding of a highly correlated and specific set of genes whose expression responds to both chitin and NaCl treatments. Similarly, we found a relationship between chitin- and NaCl-induced $[Ca^{2+}]_{cyt}$ increases suggesting a crosstalk at early signaling events. Our results also indicate that CERK1 is necessary for the correct modulation of $[Ca^{2+}]_{cyt}$ increases when roots sense salinity stress but not osmotic stress. This role might be explained by the association and physical interaction of CERK1 with ANNEXIN1 (ANN1), a calcium permeable channel involved in salinity stress. The data suggest a model where a protein complex localized at the plasma membrane, comprised of CERK1, ANN1 and LYK4, is important for signaling after plant cells sense higher Na^+ content caused by either soil salinization or due to ion leakage after fungal attack.

Results

The LysM-containing receptor-like proteins *CERK1, LYK4* and *LYK5* are transcriptionally induced by salinity stress

The profile of CERK1 mRNA expression was examined using the AtGenExpress and eFP-Browser visualization tools with a specific focus on the response to various abiotic stresses (e.g., NaCl, osmotic-PEG, ABA, drought, heat and UVB). *CERK1* expression in roots was induced (~2-fold) with NaCl treatment, but not with the other abiotic stresses (Figure 3.1A). At the cellular level, the increase in expression of *CERK1* under salinity stress occurs mainly in the endodermis and cortical cells in roots [125] (Figure 3.1B). The two other LysM-containing receptor proteins, *LYK4* and *LYK5*, were also induced 1.7-fold and 3-fold, respectively, by salt (Table 3.1). These results suggest a role for

chitin receptors in salinity stress that is specific to the ionic stress component, since osmotic stress did not affect *CERK1* expression.

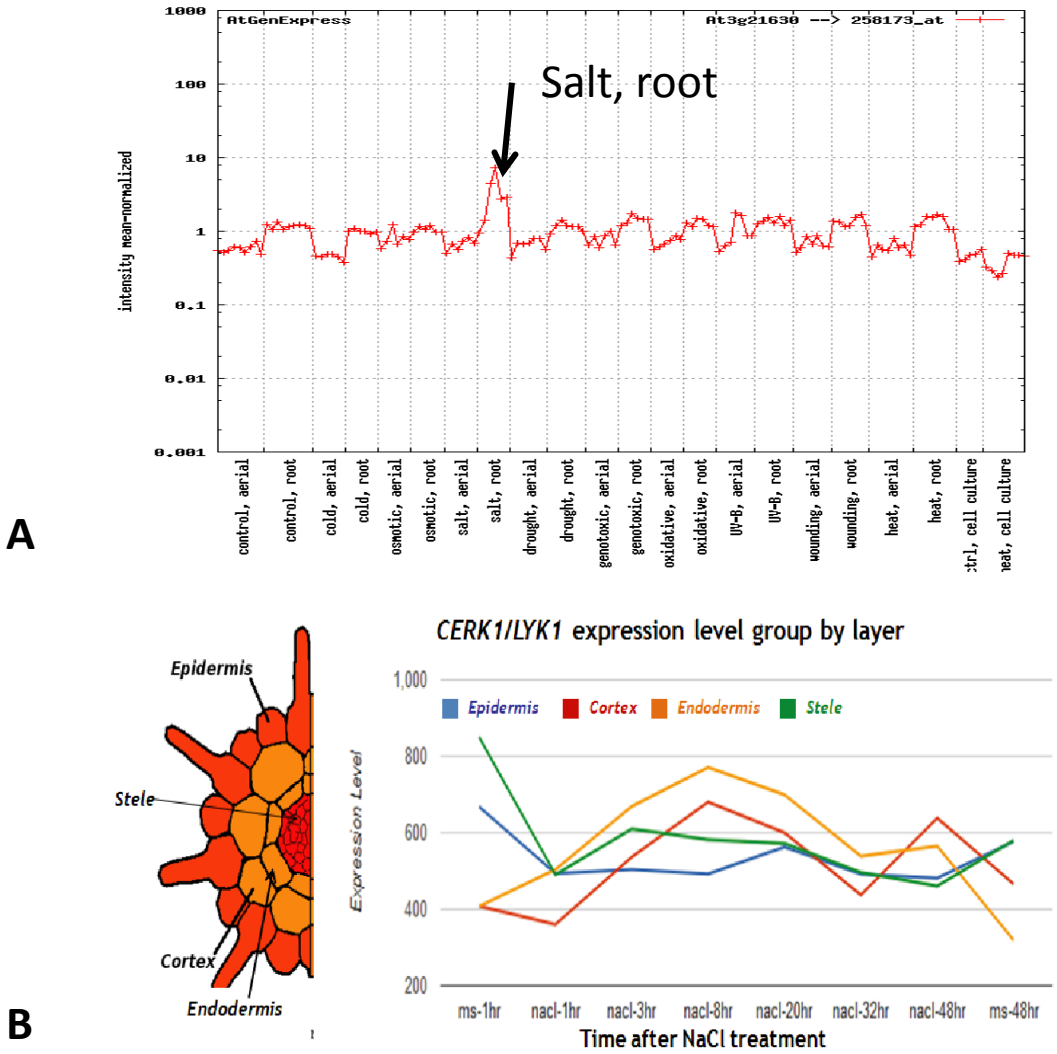

Figure 3.1. CERK1 is induced specifically by NaCl in roots
(A) CERK1 expression under different abiotic stress treatments (AtGenExpress). (B) CERK1 is induced in the root endodermis and cortical cells after NaCl treatment (Dinneny's Lab EFP Browser).

Table 3.1. Expression of LysM receptor like kinase genes in response to abiotic stress. Gene expression after treatment with osmotic stress (300 mM Mannitol), salt stress (150mM NaCl), or chitin (1uM chitooctaose) [a].

AGI	Gene name	Osmotic_shoot_6h	Osmotic_root_6h	Salt_shoot_6h	Salt_root_6h	Chitin
At3g21630	*CERK1*	0.2	-0.0	0.3	**2.0**	1.0
At2g23770	*LYK4*	-1.7	0.3	-0.8	**1.7**	1.3
At2g33580	*LYK5*	1.4	0.6	0.4	**3.0**	3.2
At1g51940	*LYK3*	-2.0	-1.8	-0.4	0.4	-0.0

Source of data: AtGeneExpress database.

[a]Fold change expressed as $\log^2$, $p<0.05$

cerk1 and _lyk4_ mutant plants are hypersensitive to NaCl

In order to better define a possible role for *CERK1, LYK4 or LYK5* in salinity stress tolerance, we assessed the response of T-DNA mutants of these genes versus the wild type (WT) Columbia (Col-0) in NaCl-containing agar plates. At 125 and 150 mM NaCl, *cerk1* seedings showed fewer green cotyledons relative to the wild type (Figures 3.2A and 3.2B). *cerk1* and *lyk4* seedlings were more susceptible to 150 mM NaCl than the wild type, while the complemented lines showed a similar or improved response compared to WT plants (Figures 3.3A, 3.3B, 3.3D and 3.3E). *lyk5* seedlings were not different than WT, but *lyk4/lyk5* double mutant was susceptible to 150 mM NaCl as *lyk4* (Figure 3.3I). *cerk1* seedlings showed no apparent differences with WT when grown on plates containing 275mM D-Sorbitol (an isosmotic control for 150mM NaCl) (Figure 3.3A and 3.3C) or 10uM ABA or KCl (Figure 3.4). This indicates that *cerk1* plants were hypersensitive to the ionic stress and not to the osmotic component of the salinity stress. *cerk1* seedlings also showed hypersensitivity when soil-grown plants were irrigated with 300 mM NaCl (Figures 3.3F and 3.3G). The NaCl hypersensitivity observed in *cerk1* can be explained by a higher accumulation of Na^+ ions in the rosettes. Plants uptake Na^+ ions from saline soils through the roots and transport the sodium to the aerial parts where they accumulate causing chlorosis. Indeed, *cerk1* rosette leaves accumulated more Na^+ than WT, measured by ICP-OES (Figure 3.3H). Together, these results suggest that chitin receptors CERK1 and LYK4, but not LYK5, might play a role in salinity stress. These data are also interesting since this is the first time that the phenotype of *lyk4* plants can be distinguished from that of *lyk5* mutant plants.

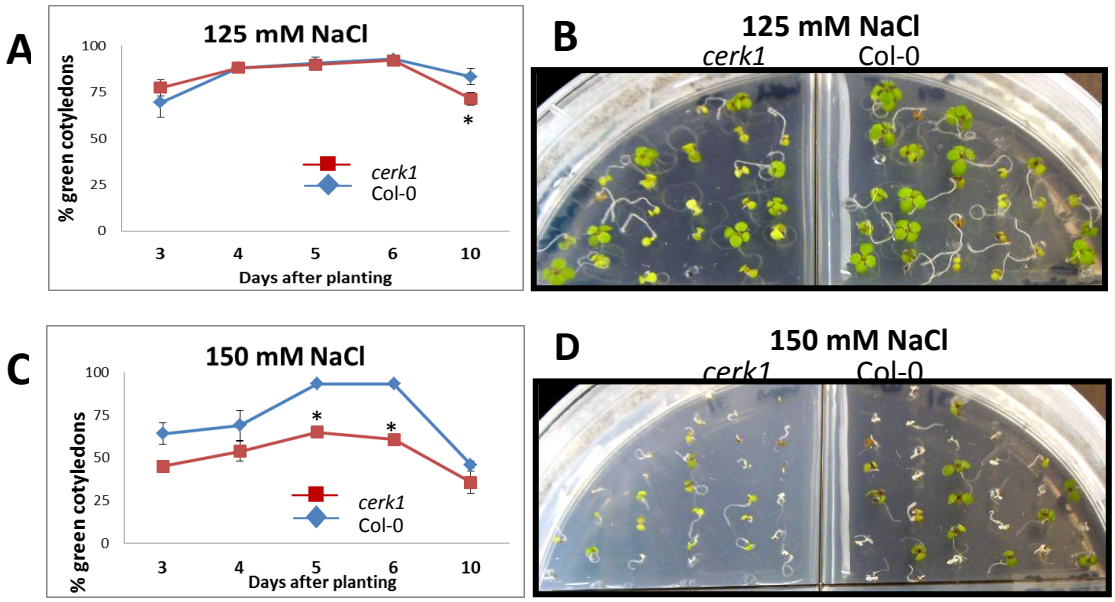

Figure 3.2. *cerk1* is more sensitive to NaCl than the WT

(A) Percentage of green cotyledons of WT and *cerk1* seedlings grown in 125 mM NaCl agar plates for indicated times. (B) A representative figure of the growth of WT and *cerk1* under 125 mM NaCl treatment after 10 days. (C) Percentage of green cotyledons of WT and *cerk1* seedlings grown in 150 mM NaCl agar plates for indicated times. (D) A representative figure of the growth of WT and *cerk1* under 150 mM NaCl treatment after 10 days. n=120 seedlings ± SE; *p<0.5. Experiments were repeated three times.

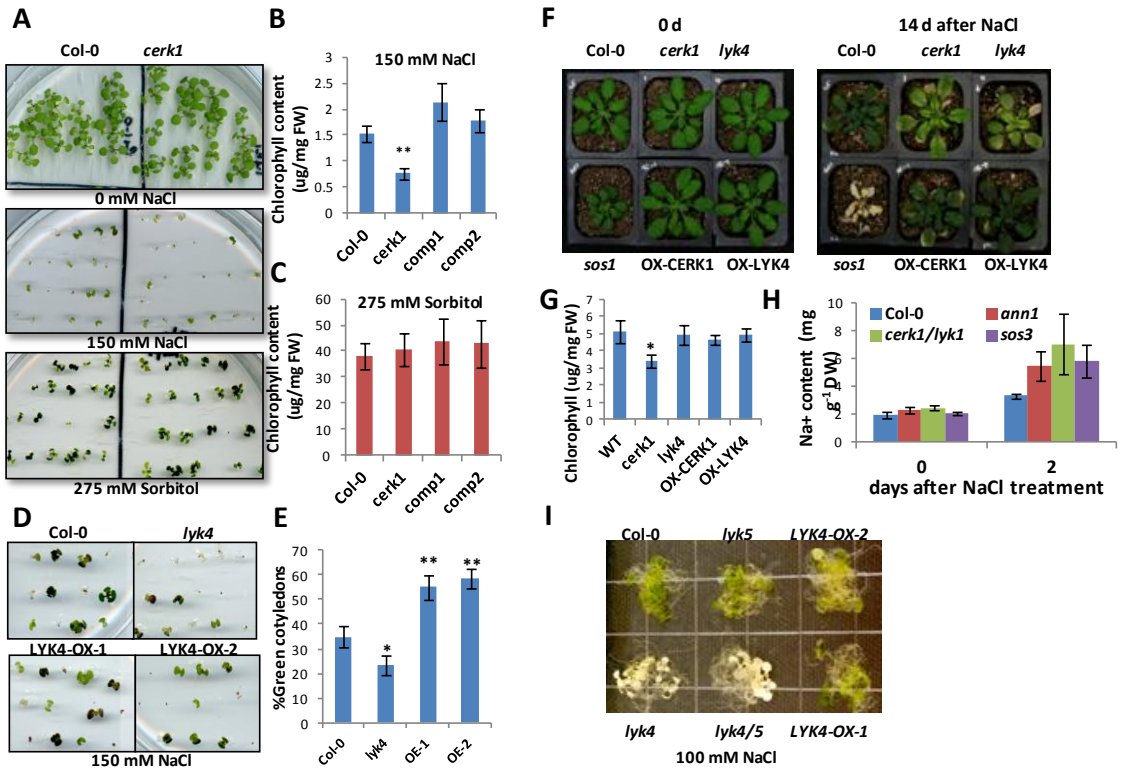

Figure 3.3. *cerk1* and *lyk4* are hypersensitive to NaCl

(A) Comparison of *cerk1* to WT when growing for 11 days on agar media containing either 0 mM NaCl, 150 mM NaCl,or 275 mM D-Sorbitol. (B) Chlorophyll quantification of seedlings grown on medium with 150 mM NaCl, or on grown on medium with 275 mM D-Sorbitol (C). FW means fresh weight. Comp1 and comp2 are complementation lines of CERK1. (D) Comparison of *lyk4* to WT when growing for 11 days on agar media containing 150 mM NaCl. (E) Percentage of green cotyledons of plants shown in (D). LYK4-OX-1 and LYK4-OX-2 are over-expressing lines of LYK4. (F) Soil-grown plants watered with 300 mM NaCl and chlorophyll content was analyzed after 14 days (G). Na^+ content in rosette leaves after watering with 300 mM NaCl (H). *lyk5* is not different than WT in response to 100 mM NaCl (I). Data shown in B, C and E are means from 12 pools of 20 seedlings each; data in G are means from 6 plants; data in H are means from 4 rosettes. Bars represent standard error (SE). Asterisks indicate statistically significant differences compared with WT:*p<0.05, **p<0.01.

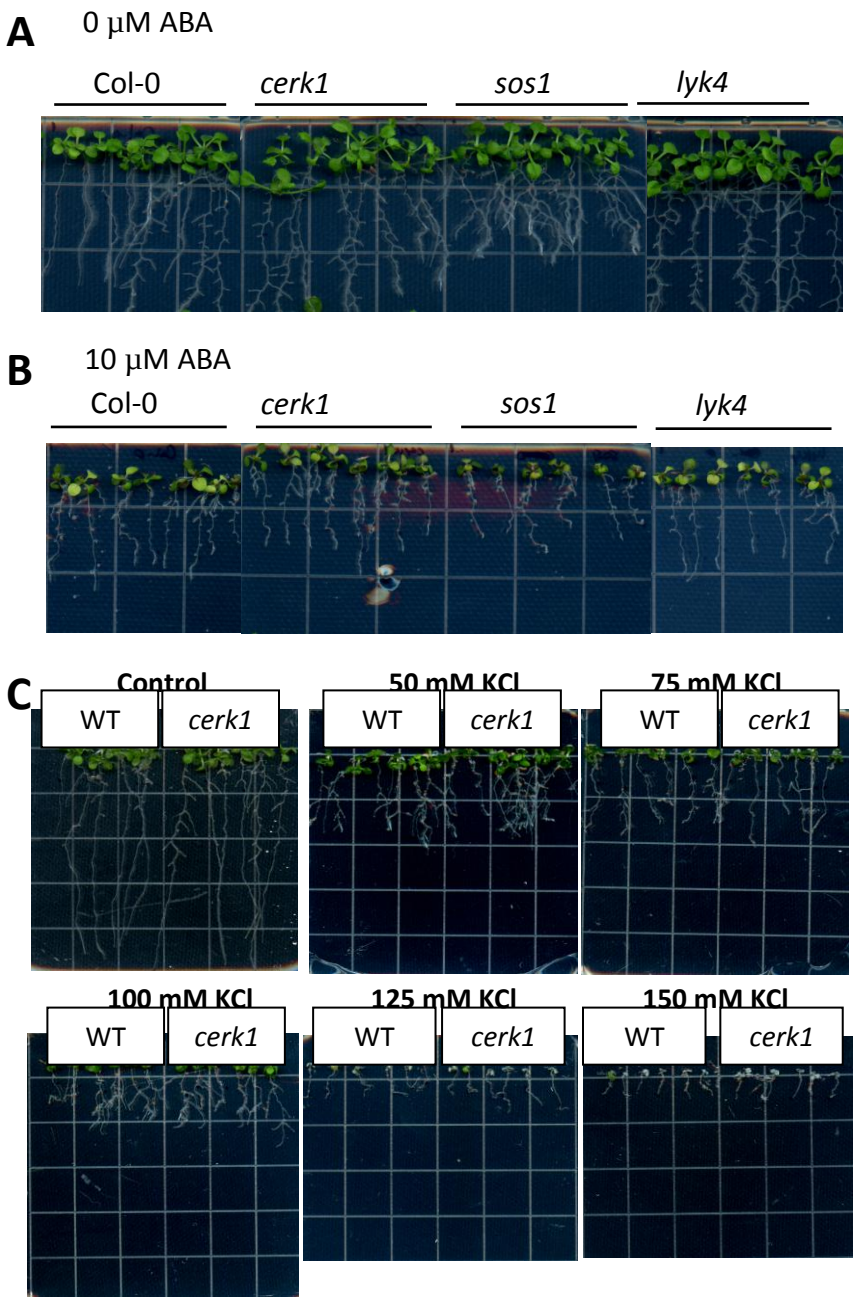

Figure 3.4.*cerk1* and *lyk4* have similar response to ABA and potassium chloride (KCl) than wild type

(A) Growth of WT, *cerk1*, *sos1* and *lyk4* seedlings, 7 days after transfer to control media without ABA. (B) Growth of WT, *cerk1*, *sos1* and *lyk4* seedlings,7 days after transfer to agar media containing 10 µM ABA. C) Growth of WT and *cerk1* seedling, 9 days after transfer to agar media containing indicated concentrations of KCl. Seedlings were germinated on 1/2xMS agar plates for 4 days and then transferred to control, ABA and KCl plates.

Chitin treatment causes similar transcript changes to salt stress

In order to further define the relationship between salinity and chitin, we compared the plant responses at the transcriptome level. Approximately 77% of the genes induced by chitin treatment were also induced by the NaCl treatment (z-value = 52.2), and 42% of the genes decreased by chitin treatment were also decreased by NaCl (z-value = 9.6) (Figure 3.5A and 3.5B).

We compared the transcriptomic datasets of chitin and NaCl treatments versus other abiotic and biotic stress treatments, including treatment with the bacterial PAMP flg22, wounding, and osmotic stress (Table 3.2). Chitin-induced genes were significantly co-expressed with those genes responding to flg22 (z-value = 58.9), wounding (z-value = 52.8) and NaCl (z-value = 52.2), but less co-expressed with genes responding to osmotic stress (z-value = 21) (Figure 3.5C). On the other hand, flg22-induced genes were highly co-expressed with chitin-induced genes (z-value = 59.8), and less significantly with wounding-, NaCl- and osmotic stress-induced genes (z-values = 29.6, 28.6 and 15.7, respectively) (Figure 3.5D). These results suggest a unique cross talk between chitin-mediated plant defenses responses and salt stress responses.

We next analyzed gene expression in WT and *cerk1* plants to test whether *CERK1* is necessary for the induction of genes after NaCl treatment. We hypothesized that genes that were induced by both NaCl and chitin treatments and were also *CERK1*-dependent during chitin induction may also be *CERK1*-dependent in relation to NaCl treatment. We used existing microarray data to guide our selection of genes for analysis and selected genes that were up-regulated with NaCl in different gene expression studies [125-128], as well as up-regulated in a CERK1-dependent manner during chitin treatment [19]. We did not find differences between WT and *cerk1* plants in the expression of 6 selected genes (Figure 3.6), indicating that salt-induced gene expression changes are unlikely solely dependent on CERK1.

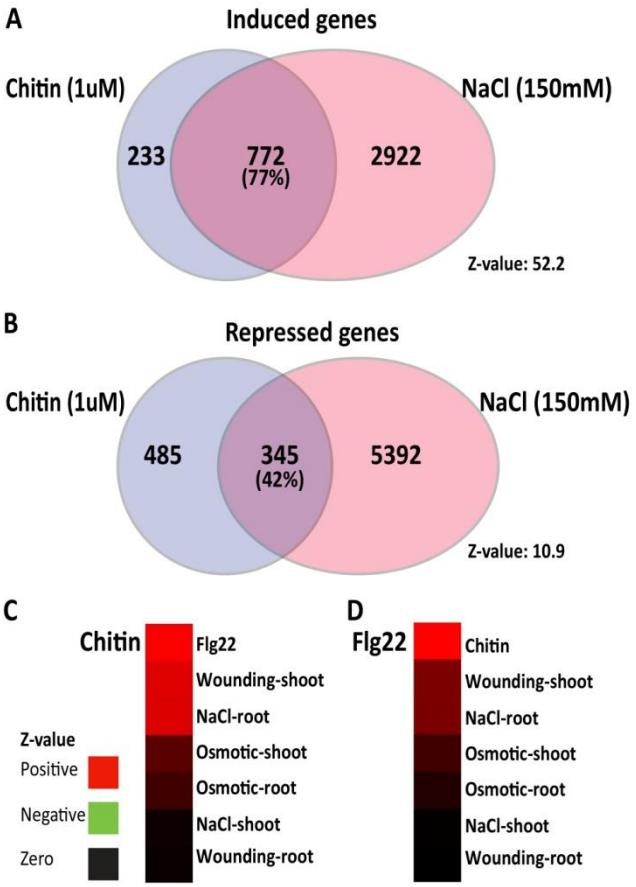

Figure 3.5. Chitin treatment causes similar transcripts changes to salt stress
(A) 77% of the chitin-induced genes were also induced by NaCl. (B) 42% of chitin-repressed genes were also repressed by NaCl. (C) Chitin-induced genes are highly significantly co-expressed with flg22 (z-value = 58.9), wounding (z-value = 52.8) and NaCl (z-value = 52.2), and less significantly with osmotic stress (z-value = 21) (D) Flg22-induced genes were only highly co-expressed with chitin (z-value = 59.8), and less significantly with wounding (z-value = 29.6), NaCl (z-value = 28.6), and osmotic stress (z-value = 15.7). Publicly available trancriptomic data was used for co-expression analysis (See Table 3.2 and Methods).

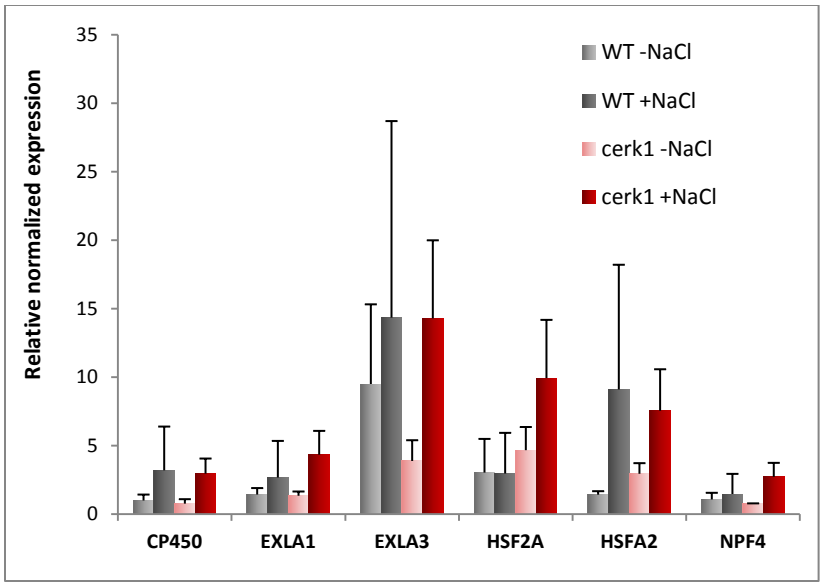

Figure 3.6. Gene expression of selected genes in WT and *cerk1* roots treated with NaCl. Nine day old seedlings grown in 1/2xMS liquid media were treated with 150 mM NaCl for 6 h, and root tissues were collected to extract RNA, synthesize cDNA and perform qRT-PCR. n=3 biological replicates ±SE.

Relationship between NaCl- and Chitin-induced cytosolic calcium increases

Increases in cytosolic calcium ($[Ca^{2+}]_{cyt}$) are common to many stress-activated signaling pathways, including salinity stress [129] and chitin [16]. These specific $[Ca^{2+}]_{cyt}$ increases are formed by the activities of calcium channels and transporters. The shape of the $[Ca^{2+}]_{cyt}$ increase, as measured by aequorin luminescence, was very different between salt and chitin (Figures 3.7C and 3.7E, respectively). The NaCl-induced $[Ca^{2+}]_{cyt}$ response happens fast with a peak 60 secs after application, returning to basal levels after 300 s. On the other hand, the chitin-induced $[Ca^{2+}]_{cyt}$ response is slower with the peak 180 secs after application and also returning to basal levels more slowly.

As another test of a potential interaction between the salt and chitin -triggered $[Ca^{2+}]_{cyt}$ response, we pre-treated Arabidopsis aequorin-expression lines with 150 mM NaCl or 100 μg/ml chitin mixture and then treated again with either NaCl or chitin. Pre-treatment with 150 mM NaCl for 30 minutes significantly reduced the subsequent $[Ca^{2+}]_{cyt}$ increase upon chitin elicitation (38% reduction in comparison to control) (Figures 3.7A and 3.7B). Conversely, pre-treatment with chitin slightly reduced the subsequent $[Ca^{2+}]_{cyt}$ increase in response to 150 mM NaCl (16% reduction in comparison with the control) (Figures 3.7C and 3.7D). Although the mechanism remains unclear, these data support the notion of cross talk between salt and chitin responses. More importantly, the data suggest that the mechanism of crosstalk acts early, during the first steps of stimulus recognition, perhaps mediated at the level of the receptors or, perhaps, through direct action on the calcium permeable channels.

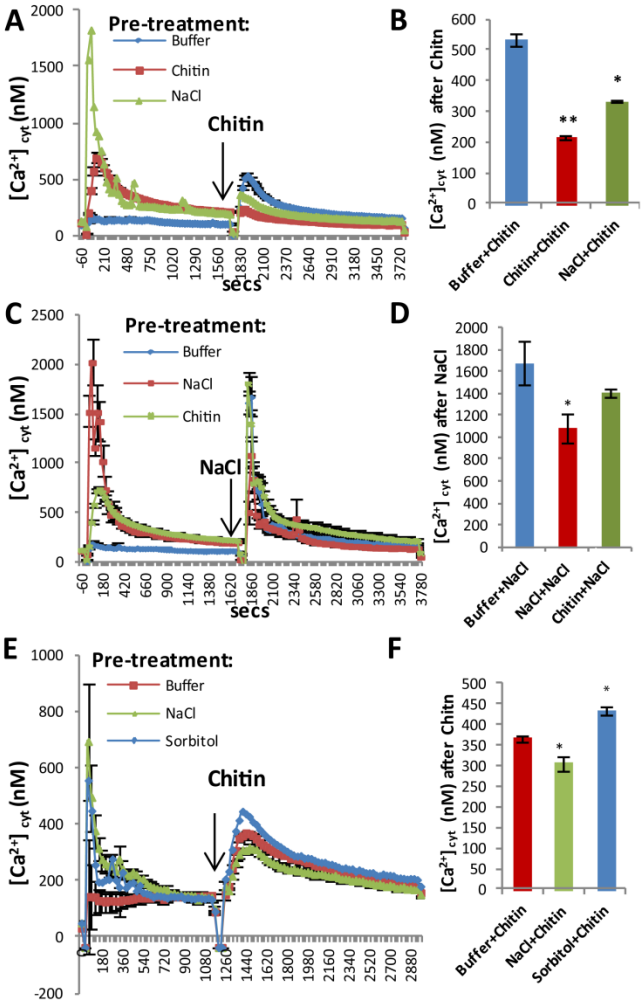

Figure 3.7. NaCl-induced $[Ca^{2+}]_{cyt}$ increases inhibits chitin-induced $[Ca^{2+}]_{cyt}$ increases
(A) Six day old aequorin transgenic lines of WT were pre-treated with buffer, NaCl or chitin, for 30 minutes. Then a second treatment with chitin was applied for 30 min. (B) $[Ca^{2+}]_{cyt}$ values after second treatment with chitin. (C) Seedlings were pre-treated with buffer, NaCl or chitin for 30 min, and after that a second treatment with NaCl was applied for 30 min. (D) $[Ca^{2+}]_{cyt}$ values after second treatment with NaCl. (E) Seedlings were pre-treated with buffer, NaCl or Sorbitol for 30 min, and after that a second treatment with chitin was applied for 30 min. (F) $[Ca^{2+}]_{cyt}$ values after second treatment with chitin. Line graphs in (A), (C) and (E), show kinetic of the $[Ca^{2+}]_{cyt}$ responses. Histograms in (B), (D) and (F), show $[Ca^{2+}]_{cyt}$ at the peak of the second treatment. 150 mM NaCl and 100 µg/ml of chitin mixture was used. Each value shows a mean of 8 seedlings ± SE. Asterisks indicate statistically significant differences compared with control (buffer pre-treatment):*p<0.05, **p<0.01. Experiments were repeated at least three times with similar results.

CERK1 is necessary to correctly modulate the salinity-induced $[Ca^{2+}]_{cyt}$ increases in roots

$[Ca^{2+}]_{cyt}$ increase is one of the earliest responses to a variety of stresses. For example, $[Ca^{2+}]_{cyt}$ increases within a few minutes after chitin recognition, which does not occur in either *cerk1* or *lyk4/lyk5* mutants [16, 20]. Since pretreatment with salt reduced the chitin-induced $[Ca^{2+}]_{cyt}$ increase (Fig. 7B), we hypothesized that CERK1 might also influence NaCl-induced $[Ca^{2+}]_{cyt}$ increases. Indeed, *cerk1* plants showed higher $[Ca^{2+}]_{cyt}$ levels than the wild type (Figure 3.8A) after addition of 150 mM NaCl. We also tested the mutants of the other members of LysM receptor kinases and found that this difference in NaCl-induced $[Ca^{2+}]_{cyt}$ was specific to *cerk1* (Figure 3.9). The response of cerk1 plants was not different when osmotic conditions were changed by addition of 275 mM D-sorbitol (Figure 3.8B). The response of *cerk1* plants was also different than control when using another salt solution containing sodium, 75 mM Na_2SO_4 (Figure 3.8C), but not to another salt solution containing chloride, 75 mM $MgCl_2$ (Figure 3.8D). Roots are the first organs to sense any environmental changes occurring in the soil. Arabidopsis roots show greater $[Ca^{2+}]_{cyt}$ increases after NaCl treatment than shoots [129]. Therefore, we assessed the NaCl- induced $[Ca^{2+}]_{cyt}$ increases in *cerk1* roots and shoots. Roots showed higher $[Ca^{2+}]_{cyt}$ increases than the shoots (Figure 3.8E and 3.8F), corroborating the previous observation from Tracy et al.[129]. The *cerk1* roots had higher $[Ca^{2+}]_{cyt}$ increases than the wild type, but not the shoots (Figure 3.8E and 3.8F). This suggests that *CERK1* may play a role in the NaCl-induced $[Ca^{2+}]_{cyt}$ increases specifically in roots. This idea is supported by the salt-induced *CERK1* expression in roots.

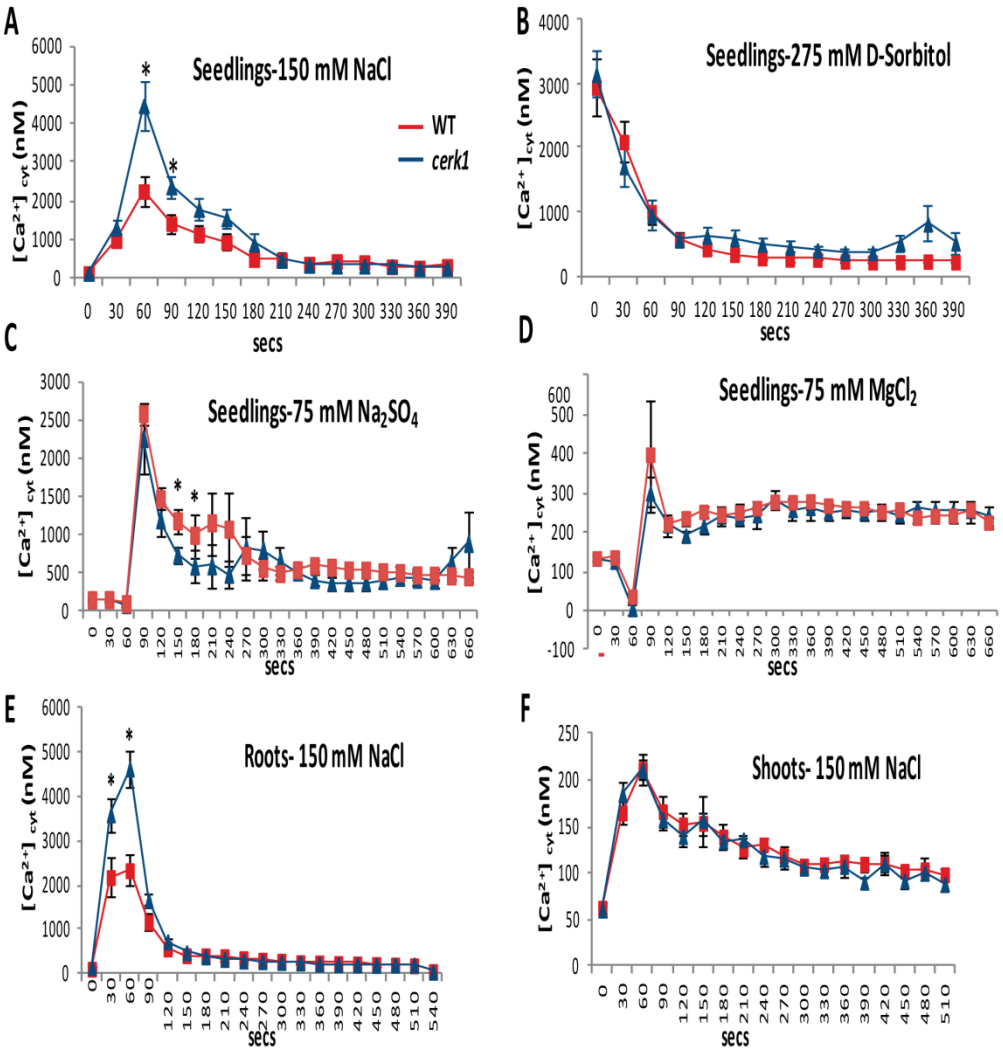

Figure 3.8. *cerk1* showed higher $[Ca^{2+}]_{cyt}$ levels than WT when treated with NaCl
Six day old aequorin transgenic lines of WT and *cerk1* were treated with 150 mM NaCl (A), 275 mM D-Sorbitol (B), 75 mM Na_2SO_4 (C), or 75 mM $MgCl_2$ (D). Excised roots (E) and excised shoots (F) from six days old seedlings of WT and *cerk1* were treated with 150 mM NaCl. Line graphs showed kinetic differences on NaCl-induced $[Ca^{2+}]_{cyt}$ responses for times indicated. Each value shows a mean of 8 seedlings ± SEM; $p<0.05$. Experiments were repeated at least three times with similar results.

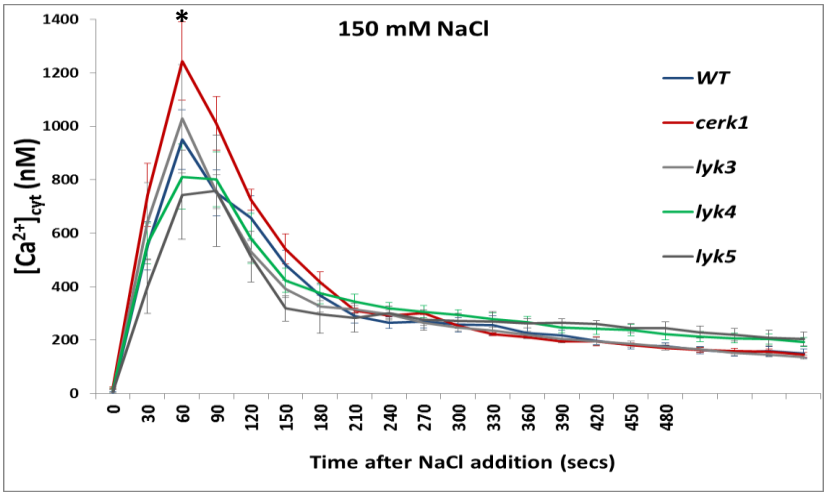

Figure 3.9. Mutants of the other LysM receptor kinase genes (*lyk3*, *lyk4*, and *lyk5*) did not show different increases in $[Ca^{2+}]_{cyt}$ after NaCl treatment in comparison with WT. Six day old aequorin transgenic lines of WT, cerk1, lyk3, lyk4 and lyk5 were treated with 150 mM NaCl. Line graphs showed kinetic difference on NaCl-induced $[Ca^{2+}]_{cyt}$ responses for times indicated Each value shows a mean of 8 seedlings ±SE, *p<0.05. Experiment was repeated twice.

CERK1 associates with ANN1, a NaCl-induced calcium permeable channel in a NaCl-independent manner

The plant salinity response likely involves a variety of plasma membrane channels and transporters of which most have yet to be defined. However, ANN1, a calcium permeable channel, was previously documented as a component of the NaCl-induced $[Ca^{2+}]_{cyt}$ signal. ANN1 was shown to negatively regulate net Na^+ influx when root protoplasts were challenged with 50 mM NaCl, presumably through calcium signaling [38]. *ANN1* is highly expressed in roots and accumulates at the plasma membrane under salinity stress [130]. Previously, ANN1 was found to interact with CERK1 based on a large-scale split-ubiquitin yeast two-hybrid screen [131]. We confirmed that ANN1 was localized at the plasma membrane using transient expression of 35S:ANN1-GFP in *Nicotiana benthamiana* (Figure 3.10). Since CERK1 is localized at the plasma membrane [16, 18], we tested whether CERK1 and LYK4 can associate with ANN1 using bimolecular fluorescence complementation (BiFC) assays in *N. benthamiana* epidermal cells. Since the CERK1 kinase domain causes cell death in *N. benthamiana* [132], we used a kinase dead version, CERK1K349E mutant protein. We found that CERK1K349E associates with ANN1 at the plasma membrane (Figure 3.11A). LYK4 also associates with ANN1 at the plasma membrane (Figure 3.11B). Another plasma membrane receptor, the bacterial MAMP EF-Tu receptor (EFR) failed to interact with ANN1, indicating that ANN1 does not interact with all pathogen response receptors (PRR) (Figure 3.11C). We also tested the CERK1-ANN1 interaction using co-immunoprecipitation (co-IP) assays in *N. benthamiana*. We found that CERK1K349E and LYK4 co-immunoprecipitate with ANN1 in leaf tissues with or without 100 mM NaCl treatment (Figures 3.11E and 3.11F). Together, these results demonstrate that CERK1 and LYK4 interact with ANN1 at the plasma membrane, before and during salt stress. Since ANN1 is a component of the NaCl-induced $[Ca^{2+}]_{cyt}$ signaling, we infer that CERK1 and LYK4 may play an important role during early, salinity stress signaling events.

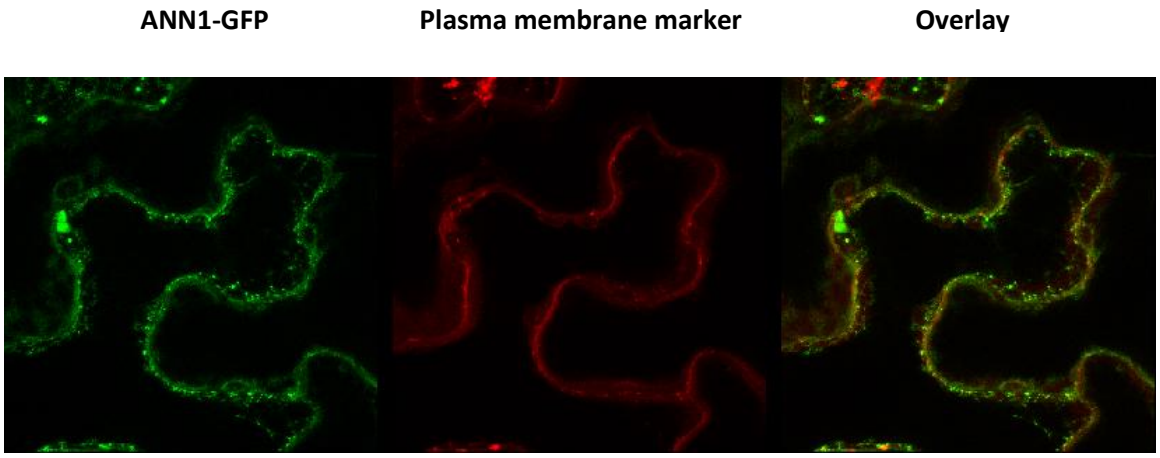

Figure 3.10. ANN1 localizes to the plasma membrane.
GFP epifluorescence (left panel), FM4-64 epifluorescence (plasma membrane marker) (middle panel), overlay of both (right panel). Agrobacterium harboring 35S:ANN1-GFP was infiltrated in *N. benthamiana* leaves for transient expression. FM4-64 was infiltrated in *N. benthamiana* leaves 30 minutes before visualizing the epifluorescence using a confocal microscope.

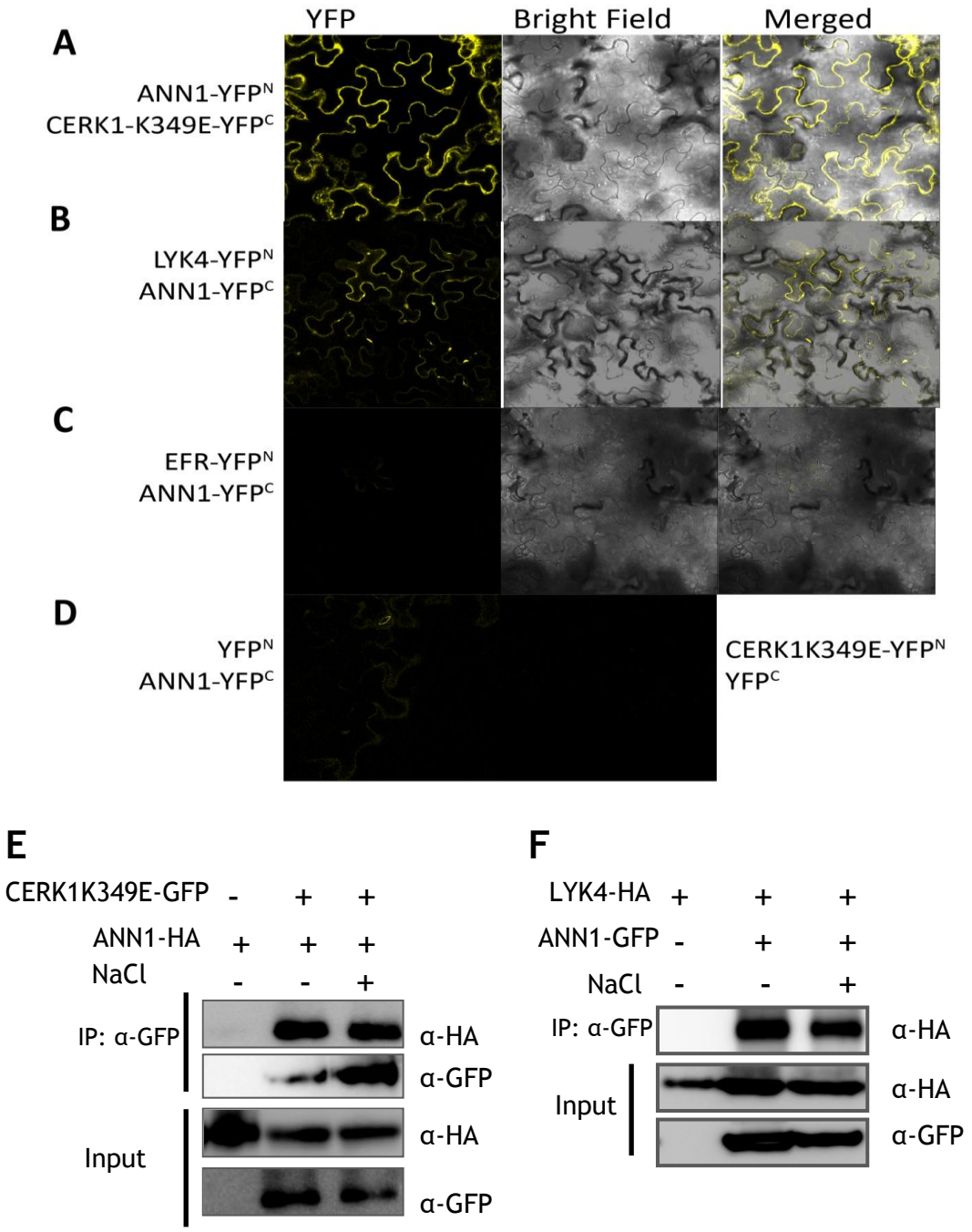

Figure 3.11. CERK1 and LYK4 interact with ANN1, a NaCl-induced calcium permeable channel.

CERK1 and LYK4 interact with ANN1 using bimolecular fluorescence (BiFC) assay in *N. benthamiana* leaves (A and B, respectively). (C) The receptor for bacterial PAMP EF-Tu, EFR, does not interact with ANN1. (D) and (E) Empty vector controls comprising either half of the split YFP molecule do not interact with ANN1 or CERK1. CERK1K349E is an inactive kinase version of CERK1 to overcome cell death in *N.*

benthamiana leaves (see Methods). (E) and (F) CERK1 and LYK4 interacts with ANN1 with or without NaCl treatment. *N. benthamiana* plants were infiltrated with Agrobacterium harbouring 35S:ANN1-HA and 35S:CERK1K349E-GFP or 35S:LYK4-HA and 35S:ANN1-GFP for transient expression. Protein extracts (Input) were immunoprecipitated with anti-GFP magnetic beads and resolved by SDS-PAGE. The shown immunoblots were developed with anti-HA antibody to detect the immunoprecipitate protein (IP), and input were detected with anti-GFP and anti-HA antibodies.

ANN1 is not phosphorylated during salt stress

CERK1 is a protein kinase and given the interaction with ANN1, we examined the possibility that CERK1 can phosphorylate ANN1. However, we first examined the more general question of whether ANN1 is phosphorylated *in planta*. We prepared protein extract from roots expressing a 35S:ANN1-HA construct and analyzed the protein pattern on a 25 μM Phos-tag gel to detect any phosphorylated isoforms of the protein. Phos-tag SDS/PAGE gels contain immobilized metal ions that retard phosphorylated protein mobility allowing gel shifts to be observed. We did not observe any phosphorylated isoforms of ANN1 in response to NaCl, ABA or chitin 8-mer (Figure 3.12). However, we observed an accumulation of ANN1 when treated with NaCl and chitooctaose (Figure 3.12). This result corroborates previous observations that ANN1 protein accumulation in response to NaCl was not dependent on phosphorylation [130]. Previous phosphoproteomics studies found that ANN1 phosphorylation was not induced in response to ABA, dehydration, or osmotic stress [133-135]. These three phosphoproteomic studies each reported a single phosphorylated residue in ANN1 in the untreated samples, but the reported residue was different in each study: S3 [133], S7 [134], and S70 [135], possibly suggesting that the reported phosphopeptides were false positives or the observed phosphorylation was a random event and not biologically significant. We did not observe a band shift in our untreated or treated samples, suggesting that either ANN1 is not phosphorylated under our conditions, or if there is any phosphorylation event it is not causing a shift in its electrophoretic mobility. We conclude that ANN1 is not phosphorylated in untreated conditions or with salt stress, and therefore the possibility of a CERK1-dependent phosphorylation of ANN1 may not be the mechanism of how the LysM receptors are important for salinity stress signaling.

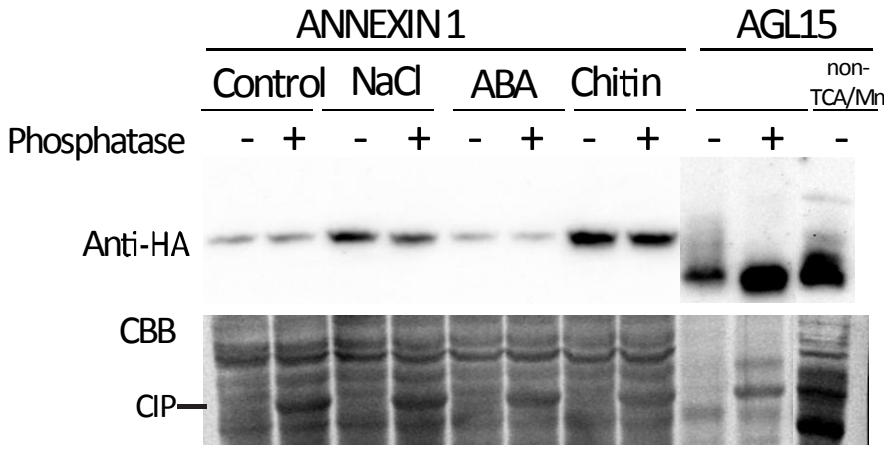

Figure 3.12. ANN1 is not phosphorylated during salt stress.
9 day old seedlings grown in liquid medium were treated with 150 mM NaCl for 2h, with 30 μM ABA for 30 min, or with 100 nM chitin 8-mer for 30 min, and roots were collected. Total protein was split into two tubes, one tube was treated with calf intestinal alkaline phosphatase (CIP) (+) and the other tube was not treated with phosphatase (-). ANN1 in roots runs as one band on 10% SDS/PAGE gels containing 25 μM Phost-tag. AGL15 in stage 15 floral receptacles showed phosphorylated isoforms in the non-phosphatase sample and in the non-TCA/Mn-treated sample as previously reported [136], and a smear of phosphorylated isoforms that could be compressed into a single faster mobility band with phosphatase treatment. Coomasie brilliant blue (CBB) was used for protein loading control and CIP indicates the band corresponding to the phosphatase treatment. Experiments were repeated three times with similar results. All samples were loaded in the same gel but longer exposures are shown for AGL15 due to its reduced abundance.

Role of ANN1 in chitin response

Since we found that ANN1 is interacting with chitin receptors CERK1 and LYK4 (Figures 3.11A and 3.11B), we decided to examine the responses to chitin elicitation in *ann1* mutant plants. Compared to wild type, *ann1* seedlings showed lower $[Ca^{2+}]_{cyt}$ levels (13%) than the wild type in response to chitin (Figure 3.13D). This result is in concordance with a role for ANN1 as a calcium channel and an important component of the cellular calcium signaling response. In addition, *ann1* plants showed hypersensitivity to chitin, as measured by ROS production and MAP kinase phosphorylation (Fig. 3.13A-C). Together, these results suggest a role for ANN1 during chitin response, probably as a negative regulator of chitin signaling.

We observed that ANN1 protein accumulates in response to NaCl and chitin (Figure 3.12). To test if this response was specific to these two stimuli, we assessed the ANN1 protein levels in response to other MAMPs or DAMPs (danger associated molecular pattern). Interestingly, ANN1 protein levels were rapidly reduced in response to the bacterial MAMP flg22 in leaves and to extracellular ATP (a DAMP) in leaves and roots (Figure 3.14). This result suggests that ANN1 degradation might be important during the rapid response to flg22 and extracellular ATP, while ANN1 accumulation might be important in response to salt and chitin.

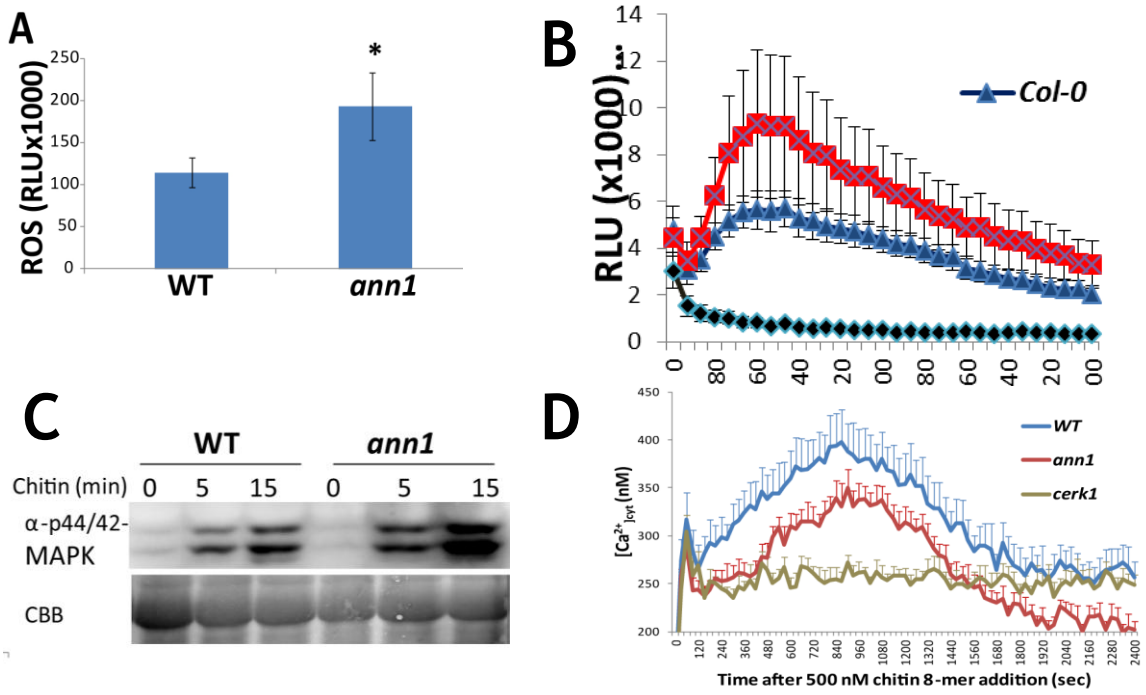

Figure 3.13. *ann1* mutant showed hypersensitivity to chitin-triggered immunity
(A) *ann1* showed hypersensitivity to chitin-triggered ROS production. Leaf discs were treated with or without chitin 8-mer (100nM) and total chemiluminescent signal (relative light units = RLU) was recorded for 30 min. Data are means ± SEM (n=8, **p*<0.05). (B) Kinetic analysis of the samples shown in (A). (C) *ann1* showed hypersensitivity to chitin-triggered MAP kinase phosphorylation. Leaf discs were treated with or without chitin mixture (100ug/ul), and total protein was extracted at indicated times. Immunoblot analysis was performed using anti-p42/p44-MAPK antibody. Coomasie brilliant blue (CBB) was used for protein loading control. (D) Six day old seedlings of Col-0, *ann1* and *cerk1* expressing aequorin gene, were treated with 500 nM chitin 8-mer. Line graphs showed kinetic differences on chitin-induced $[Ca^{2+}]_{cyt}$ responses for times indicated. Each value shows a mean of 8 seedlings ± SEM; $p<0.05$. Experiments were repeated twice with similar results.

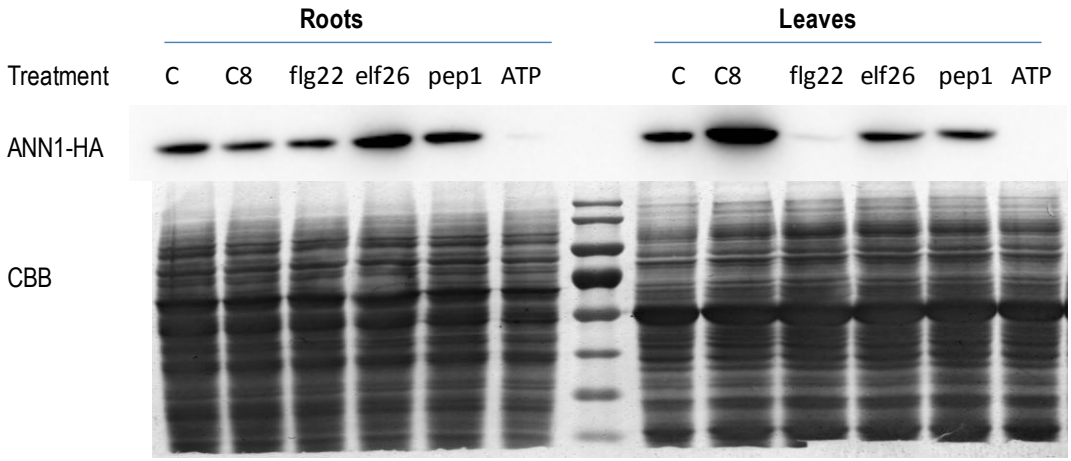

Figure 3.14. ANN1 protein levels in response to PAMPs and DAMPs.
Seedlings were treated with 100 nM chitin 8-mer, 10 nM flg22, 10 nM elf26, 10 nM pep1 and 100 µM ATP or deionized water as a control (C), and tissues were collected after 20 min. Immunoblot analysis was performed using HA-HRP antibody. Coomasie brilliant blue (CBB) was used for protein loading control. Experiments were repeated twice with similar results.

Discussion

Crosstalk between fungal pathogen derived-chitin and salinity stress:

Plants are exposed to different environmental stimuli at once. Several reports indicate that salinity stress can affect the tolerance to pathogens, either repressing or promoting resistance. However current knowledge on its physiological impact on plant resistance is insufficient to provide solid explanations for the contradictory reports. Other study showed that a pre-treatment with chitin increased the tolerance of Arabidopsis to salinity stress, in a CERK1-dependant manner.

Plants have evolved mechanisms that are intimately intertwined with environmental conditions. For example, plants exhibit higher disease resistance during the early hours of the day coincident with the period in which fungal pathogens disperse their spores [137]. Another example of co-evolution of two different stresses is that, when plants undergo submergence, they increase their defense mechanisms in anticipation of a higher probability of pathogen attack [138]. In nature, root fungal pathogens, like *Fusarium sps*, grow optimally in saline conditions [139, 140]. Therefore, plants growing in saline soil could experience both salt stress and fungal pathogen attack. It is possible that root detection of saline soil could serve as an early warning of pathogenic fungal colonies. In addition, plant infection by a fungal pathogen is known to cause significant leakage of sodium ions [141, 142]. This would provide an environment in which both chitin oligomers (released from the fungal cell wall) and elevated salt levels would co-occur. Fungal pathogens have evolved a variety of means to counter plant recognition of chitin [143]. Hence, plants may also use sodium detection resulting from fungal attack as an additional danger signal to respond to pathogen challenge. In this case, while chitin would serve as a MAMP, Na^+ ions would serve as a DAMP (damage associated molecular pattern), both providing the plant a better opportunity to defend against the fungal pathogen (Figure 3.15).

Here, we found a strong relationship between salt- and chitin-induced gene expression patterns, that might explain the cross tolerance phenomenon observed between fungal pathogen defense and salt stress tolerance. In addition, we showed a specific

relationship between salt- and chitin-induced $[Ca^{2+}]_{cyt}$ increases, that indicates a cross-talk occurring during the early signaling events to both stimuli.

CERK1 is necessary for salt tolerance and to correctly modulate $[Ca^{2+}]_{cyt}$ increases

Our results indicate that CERK1 is involved in the response to the ionic stress component of salinity stress (caused by sodium ions) and not to osmotic stress. First, *CERK1* expression is specifically induced by salt stress and not other abiotic stresses, including ABA, drought or osmotic stress using D-sorbitol (Figure 3.1). Second, *cerk1* plants are more susceptible than WT to NaCl treatment but not to D-sorbitol, ABA or KCl (Figures 3.3A-C and Figure 3.4). Third, *cerk1* plants showed increased $[Ca^{2+}]_{cyt}$ increases in the roots, in response to NaCl but not to D-sorbitol (Figures 3.8A and 3.8B).

Our results also indicate that *CERK1* is necessary to correctly modulate $[Ca^{2+}]_{cyt}$ increases when the root senses salt stress. These observations suggest that a correct modulation of $[Ca^{2+}]_{cyt}$ increases mediated by *CERK1* may also be contributing to the whole plant response to salt stress. However, at this point is not possible to link the $[Ca^{2+}]_{cyt}$ increases directly with a whole plant physiological response, since the time it takes to observe a salt-sensitive phenotype is days in comparison to the salt-induced $[Ca^{2+}]_{cyt}$ increases that occur in minutes [40]. For example, *ann1* mutant plants showed less $[Ca^{2+}]_{cyt}$ increases after salt treatment but no salt-sensitive phenotype [38]. In contrast, plants mutated in the ACTIN-RELATED PROTEIN2 (ARP2) gene showed higher $[Ca^{2+}]_{cyt}$ increases and a salt-sensitive phenotype [144]. This indicates that the language of calcium signaling is more complex than simple magnitude and direction. The *lyk4* mutant plants did not display a difference in the salinity induced $[Ca^{2+}]_{cyt}$ increases (Figure 3.9) but did display an increased sensitivity when grown on NaCl-containing agar plates (Figures 3.3D and 3.3E). This suggests that LYK4, which can act as a co-receptor with CERK1 [16, 20], is not directly involved in the salinity induced $[Ca^{2+}]_{cyt}$ increase but apparently does, in some way, influence salinity tolerance, perhaps by impacting a calcium independent salt tolerance pathway. Previously, we reported that LYK4 and LYK5 both interact with CERK1 and appear to be functionally redundant with regard to chitin signaling [20]. Therefore, it was surprising to find that *lyk5* plants showed a

normal NaCl -induced $[Ca^{2+}]_{cyt}$ increases (Figure 3.9). These results suggest that LYK4/CERK1 and LYK5 play different roles in the cross-talk between chitin and salt. Perhaps LYK4/CERK1 mediates cross-talk with different pathways, while LYK5 only functions as a chitin binding protein. This is plausible since CERK1 is also involved in recognition of bacterial PGN [23] and in mediating pathogen-induced cell death [24]. In the same way, another member of the LYK family, LYK3, mediates a cross-talk between ABA and pathogens [50], indicating a theme in which LYSM RLKs are involved in both plant immunity and abiotic stress signaling.

$[Ca^{2+}]_{cyt}$ increases occur very fast after roots sense excess extracellular sodium ions, and generate a quick Ca^{2+} wave from roots to shoots necessary for the gene expression response [40]. This unique salt-specific Ca^{2+} wave propagation is channeled through the cortex and endodermal cell layers of roots [40]. Interestingly, *CERK1* expression is increased in the root cortex and endodermis during salt stress (Figure 1B). This supports a role of CERK1 in salinity-induced $[Ca^{2+}]_{cyt}$ increases. The channels involved in transiently elevating $[Ca^{2+}]_{cyt}$ in response to increasing extracellular NaCl have not been identified [35], but Arabidopsis ANN1 has been reported to form Ca^{2+} permeable channels *in vitro* and mediate both NaCl and ROS-induced Ca^{2+} responses *in vivo* [38, 145]. ANN1 is strongly expressed in roots and moves from the cytosol to the plasma membrane during salinity stress [130]. At the plasma membrane, the ANN1 C-terminal domain interacts with the membrane phospholipids, while its N-terminal domain is exposed in the cytoplasm and available to interact with other proteins [146]. We found that CERK1 interacts with ANN1 at the plasma membrane with or without salt (Figure 3.11A). Similarly, we found that LYK4 also interacts with ANN1 (Figure 11B). Previously, CERK1 and LYK4 were reported to interact in the absence of chitin while, in contrast, CERK1 and LYK5 interaction required chitin elicitation [20]. It is tempting to speculate that this constitutive CERK1-LYK4 complex exists to mediate the response to salt stress with the CERK1-LYK5 receptor more specific to chitin signaling. In both cases, the interaction with ANN1 may contribute to stress induced $[Ca^{2+}]_{cyt}$ increases. Our results also support a role for ANN1 in chitin-innate immunity and showed that ANN1 is

necessary for a normal chitin-induced $[Ca^{2+}]_{cyt}$ increases (Figure 3.13). We also found that *cerk1* and *ann1* plants accumulated more Na^+ ions than the WT (figure 3.3H), which resulted in increased chlorosis in *cerk1* (Figures 3.3F and 3.3G). We hypothesized that the CERK1-ANN1 interaction might be important for controlling salinity-induced $[Ca^{2+}]_{cyt}$ increases which in turn will modulate a mechanism for Na^+ detoxification. Understanding these layers of cross-talk may lead to more sustainable methods to employ innate immunity to protect against both biotic and abiotic stress induced crop losses.

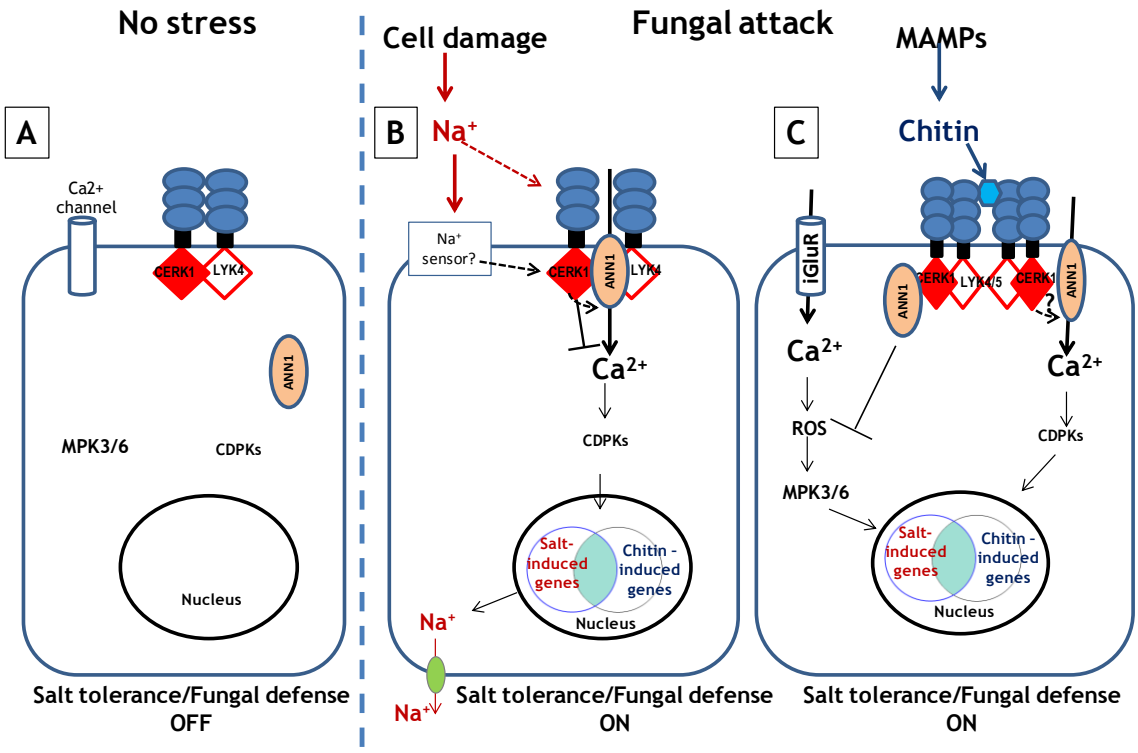

Figure 3.15. Working model

Fungal attack generates both chitin and Na^+ ions that might serve as a danger signal to elicit a fungal triggered immune response and salt stress tolerance in plants. (A) Under no stress, chitin receptors and calcium channels are not activated. (B) Once root cells sense the increase of extracellular Na^+, ANN1 mobilizes to the plasma membrane [130] to form a calcium permeable channel [147] and to interact with chitin receptors CERK1 and LYK4. CERK1 and ANN1 are necessary to correctly modulate the $[Ca^{2+}]_{cyt}$ levels in response to Na^+. Calcium binds CDPKs which activate a transcriptional regulatory program. (C) Chitin is recognized by a receptor complex comprises of CERK1 and LYK4/LYK5 [20] and elicits $[Ca^{2+}]_{cyt}$ increases through iGLUR channels [26], a burst of ROS and activation of MAP kinase cascade. ANN1-formed calcium permeable channels are also activated by chitin and contribute to $[Ca^{2+}]_{cyt}$ increases. ANN1 also plays a negative role in the chitin-induced ROS increases and MPK3/6 activation.

Material and Methods

Plant Material and Growth conditions.

The Columbia ecotype of Arabidopsis was used as wild type (WT=Col-0; ABRC stock no. CS70000). T-DNA mutants were ordered from the Arabidopsis Biological Resources Center (ABRC) at Ohio State University. *cerk1* (GABI-KAT 096F09), *lyk3* (SALK_140374), *lyk4* (WiscDsLox297300_01C), *lyk5-2* (SALK_131911C), *sos1* (CS859742), and *ann1* (SALK_015426C). Complementation lines of CERK1 and LYK4 were generated and characterized previously [16, 19]. Homozygous *ann1* mutant plants were genotyped using primers listed in Table 2.3. For the NaCl and osmotic treatments, Arabidopsis seeds were sterilized in 10% sodium hypochlorite for 10 min, washed thoroughly with sterile water and then evenly distributed on nutrient agar medium [148] containing 150mM NaCl or 275 mM D-Sorbitol, unless other concentrations are mentioned in the text. After sowing, plates were stored at 4^{o}C in the dark for two days, and then transferred to a growth chamber with 16h day/8h night cycle at 22^{o}C. For soil experiments, seeds were cold treated for 2 days at 4 ^{o}C before sowing into Sunshine soil (Premier Horticulture, Dorval, QC, Canada), and grown under 8h day/16h night cycle, 100-150 uEm^{-2}s^{-1}, and 40-70% humidity. Plants were planted in a randomized complete block experimental design for data collection. After 4 weeks, plants were irrigated with 300 mM NaCl solution, and after 14 days plants were photographed and chlorophyll content was analyzed.

Chlorophyll content assay.

20 seedlings per sample were collected, weighed and placed into a 1.5ml Eppendorf tube. In the case of soil-grown plants, three 6 mm leaf discs per plant were collected. Tissues were ground for 90 seconds using a Mini-BeadBeater^{TM} (BioSpec Products Inc., OK, USA). Acetone (250 ul of 80% acetone) was added and the samples were incubated in dark for 15minutes at room temperature. The samples were centrifuged at 3000 rpm for 15 min at 4^{o}C, and the 200 ul of supernatant was transferred to a Costar® 48-well plate (Corning Inc, NY, USA). Light absorption at 663 and 645 was determined using

EnSpire ® Multimode plate reader (Perkin Elmer Inc, USA). The chlorophyll concentration (chlorophyll A, chlorophyll B, and total chlorophyll,) was calculated according to the following formula) [149]: Chlorophyll A = (12.7xA663 - 2.69xA645) x Volume (ml) x Weight (mg); Chlorophyll B = (22.9xA645 - 4.86xA663) x Volume (ml) x Weight (mg); Total chlorophyll = (8.02xA663 + 20.2xA645)* Volume (ml) x Weight (mg).

Gene constructs and transgenics plants.

The full-length cDNA (excluding stop codon) of *ANN1* and *EF-TU RECEPTOR* (EFR) were amplified from cDNA template and cloned into pDNOR-Zeo plasmid by BP cloning (Invitrogen). The resultant plasmids were used for LR cloning (Invitrogen) with destination plasmid pGW14 [150], to form a translational fusion with the 3xHA tag. The 35S:ANN1-HA construct was introduced into *annexin1* and *cerk1* plants by floral dip [151] with EHA105. The 35S:ANN1-HA homozygous T3 lines were screened based on hygromycin resistance and protein expression. For *N. benthamiana* transient expression and co-immunoprecipitation (co-IP), the LYK4 construct was previously described [16, 19], pDNOR-ANN1 and pDONR-EFR, were cloned into the binary vector pMDC83 [152] to form a translational fusion with the GFP sequence, or into selected pSITE-BiFC vectors [153] to create fusions at the C-termini of the full length proteins with split YFP. The constructs were electroporated into *Agrobacterium tumefaciens* GV3101. Because CERK1 kinase activity causes cell death in *N. benthamiana* plants [132], we made an inactive kinase version of CERK1, by inserting a point mutation in the kinase catalytic domain (K349E) using QuikChange II Site-Directed Mutagenesis Kit (Stratagene). Similarly to LYK4 and ANN1, we used CERK1K349E for fustions to GFP, split YFP and HA at the C-terminus of the protein.

Comparative transcriptome analysis.

Publicly available Affymetrix ATH1 data from 5 conditions: osmotic stress, salt stress, chitooctaose, flg22 and wounding were downloaded (Table 3.2), and reanalyzed with RobiNA [154] using the justPlier normalization method, BH p-value correction method, nested multiple testing strategy and a p-value cut-off of 0.05. The number of co-

occurring differentially expressed genes was calculated using the program VennMapper [155] and results were plotted as a heat map using TreeView 1.60 (http://rana.lbl.gov/EisenSoftware.htm).

Calcium influx assay.

Aequorin-expressing transgenic Arabidopsis (Col-0 background) was kindly provided by Marc Knight [156]. *cerk1*, *lyk4*, *lyk3*, *lyk5-2* mutant plantscontaining the aequorin transgene were generated previously [16, 20]. Six-day old seedlings grown vertically on plates containing 1/2x Murashige-Skoog (MS) agar (1/2xMS salts, 0.5% sucrose, 0.6% agar), were transferred to a 96-well white plate and incubated in 50 ul of reconstitution buffer containing 5 mM MES, 1.4 mM $CaCl_2$, 20 mM KCl, and 10uM coelentarazine (Nanolight Technology) overnight in dark at room temperature (23-25^{o}C). After incubation, seedlings, shoots or roots were treated with 50 ul of treatment solution (concentration was double strength to give a set final concentration), and then photon emissions were detected using a Photek CCD camera 216 (Photek Ltd., East Sussex, U.K.). 100uL of discharging buffer containing 2M $CaCl_2$ and 20% (v/v) ethanol was used to estimate the remaining unchelated aequorin. The calcium concentration was calculated as previously described [157, 158]. Treatments used were 150mM NaCl, 275mM D-sorbitol, 75mM Na_2SO_4, 75 mM $MgCl_2$, 100 nM flg22 (GenScript USA Inc. Piscataway, NJ), and 100ug/ml chitin mixture from crab shells (Sigma, St. Louis, MO).

qRT-PCR.

Seedlings were grown for 9 days in a 24-well clear plate containing liquid 1/2xMS medium in a growth chamber with 16h day/8h night cycle at 22^{o}C. After 9 days, seedlings were treated with 150mM NaCl for 6 h. Total RNA from roots was extracted with TRIzol (Ambion) and converted to cDNA with SuperScript III (Invitrogen). qPCR was performed with NEB Taq (NEB) supplemented with 1x buffer, 2.0 mM $MgCl_2$, 0.8 ug/ul BSA, 200 nM dNTPs, 100 nM primers, and 1x EvaGreen (Biotium) [136]. A 1-ng equivalent of total RNA was used as a template for each reaction. Expression levels of genes were determined from three biological replicates. The *ADAPTOR PROTEIN-2*

(At5g46630) gene was used as a reference gene for data normalization [121]. A Bio-Rad CFX96 qPCR machine was used. Data were processed with Bio-Rad CFX Manager and Excel (Microsoft). Primers are listed in Table 3.3.

Transient expression in *N. benthamiana*.

The Agrobacterium strains containing LYK4, CERK1K349E, ANN1 and EFR constructs cultured overnight, pelleted, and re-suspended in activation buffer (10mM MES/KOH (pH5.6), 10mM $MgCl_2$, 150uM acetosyringone), and incubated for 2h in the dark at room temperature [159]. Each strain was adjusted to a final optical density of 0.3 at 600 nm, and the p19 strain was adjusted to a final optical density of 0.1 at 600 nm. Bacterial mixtures were infiltrated into the abaxial side of 5-6 weeks-old *Nicotiana benthamiana* leaves using a needle-less syringe. Two days after infiltration, the infiltrated area was cut and the GFP or YFP fluorescence was observed with a confocal microscope (Leica SP8 spectral confocal microscope). For the BiFC experiments, empty vector controls comprising either half of the split YFP molecule but lacking the protein of interest, were used as a negative control.

Coimmunoprecipitation assay.

To test association of proteins we co-expressed LYK4-HA and ANN1-GFP, or CERK1K349E-GFP and ANN1-HA in *N. benthamiana* plants, as described above. To ensure that CERK1K349E or LYK4 does not bind specifically to anti-GFP magnetic beads, we expressed LYK4-HA and ANN1-HA alone, as negative control. Plants were incubated for 2 days after infiltration. One hour before harvesting the tissue for lysis, half leaf was infiltrated with 100 mM NaCl and the other half was not infiltrated (control). Pull–downs for GFP tag were performed according to the manufacturer's specifications detailed in the uMACS^{TM} Epitope Tag protein isolation kit (Miltenyi Biotec Inc.). The eluted protein (GFP pull-down) and the input protein were separated on 10% SDS-PAGE gel and transferred to PVDF membrane for western blot analysis. Membranes were stained with Coomassie Brilliant Blue R-250 to assess loading and then destained with methanol. Antibodies HA- peroxidase (Roche, Indianapolis, IN) and anti-GFP (Miltenyi Biotec,

Auburn, CA) were diluted 1:1000 for western blots. Both signals were detected using SuperSignal West Pico and Femto chemiluminescent substrate (Thermo Scientific, Rockford, IL) and captured with a FujiFil LAS-3000 camera system (FujiFilm, Minato-ku, Tokyo, Japan).

Analysis of phosphorylation using Phos-Tag and phosphatase treatment.

Seedlings were grown for 9 days in a 24-well clear plate containing liquid 1/2xMS medium in a growth chamber with 16h day/8h night cycle at 22^{o}C. After 9 days, seedlings were treated with 150mM NaCl for 2 h, or 30uM ABA for 30 minutes or 100 nM chitin 8-mer (Sigma, St. Louis, MO) for 30 minutes. Five roots from 35S-ANN1 plants were harvested and ground in liquid nitrogen. Fifteen ul of low salt calf intestinal phosphatase (lsCIP) buffer (50mM Tris pH 8.5, 2 mM $MgCl_2$) with complete proteinase inhibitor (Roche) and 0.5% sarkosyl was added and incubated for 5 min on ice. Ninety ul of lsCIP buffer with complete proteinase inhibitor (Roche) and 0.1% Triton X-100 was added, and then samples were mixed. The lysate was cleared by centrifugation and split into two tubes. A total of 0.75 ul of calf intestinal phosphatase (NEB) was added to one of the aliquots. Both tubes were incubated at 37^{o}C for 30 min, and proteins were precipitated by addition of ¼ vol. 100% trichloroacetic acid (TCA) followed by the addition of 200 ul cold acetone. The protein pellet was dissolved in SDS sample buffer supplemented with 1 mM $MnCl_2$ except where noted, and then samples were resolved on 4%/10% gels with 25 µM Phos-tag (Wako Chemicals) in the separating gel made according to manufacturer's directions, except that SDS was not included in the gel.

Sodium content quantification.

For Na^+ content determination, 4-week-old soil-grown plants were irrigated with 300 mM NaCl solution and rosette leaves were collected at 0 and after 2 days. Elemental analyses were performed using a inductively coupled plasma-optical emission spectroscopy (ICP-OES) (Perkin-Elmer Optima 3000XL; Applied Biosystems) using dried rosette leaves digested for 3 days in trace-metal grade 70% HNO_3.

Table 3.2. Microarray datasets used for transcriptome comparison

Treatment	Reference number/Source	Experimental details
Osmotic stress (300 mM Mannitol)	TAIR-ME00327 AtGenExpress	Shoot and root tissue of 16 days old Arabidopsis thaliana seedlings of Columbia-0 ecotype at several time points after treatment (0,5h; 1h; 3h; 6h; 12h; 24h) [127]
Salt stress (150 mM NaCl)	TAIR-ME00328 AtGenExpress	Shoot and root tissue of 16 days old Arabidopsis thaliana seedlings of Columbia-0 ecotype at several time points after treatment (0,5h; 1h; 3h; 6h; 12h; 24h) [127]
Chitooctaose (chitin)	GSE8319 GEO	Wild type Col-0 and chitin receptor mutants treated with or without 1 µM chitooctaose [19]
Flg22	TAIR-ME00332 AtGenExpress	5 weeks old Arabidopsis Col-0 ecotype leaves infiltrated with 1uM flg22 or water for 1 h
Wounding	GSE5627 AtGenExpress	Punctuation of the leaves by 3 consecutive applications of a custom made pin-tool consisting of 16 needles [127]
Control	GSE5620 AtGenExpress	Shoot and root tissue of 16 days old Arabidopsis thaliana seedlings of Columbia-0 ecotype at several time points after treatment (0,5h; 1h; 3h; 6h; 12h; 24h) [127]
150 mM NaCl	E-MEXP-754 Array Express	Root tissue of 18d-old plants grown in liquid 1/2xMS medium and treated with 150mM NaCl for 6, 24, and 48 h. [128]
140 mM NaCl	GSE46205 and GSE46208 GEO	Roots from 5 d-old seedlings grown vertically were transfer to agar plates containing 140mM NaCl for 0.5, 1, 4, 16 and 32 h. [125]
100 mM NaCl		Roots and leaves from 3 week-old plants grown in hydroponics and treated with 100mM NaCl for 3 and 27 h. [126]

Table 3.3. Primers used in this study.

Objective	5'-sequence-3'
Genotyping	
ann1 (SALK_015426C)	TGTTGTTGGTCTCCCTTTTTG
	AATCTTGGCTCACAGAAGTGC
Cloning	
35S-ANN1-cDNA	GGGGACAAGTTTGTACAAAAAAGCAGGCTatggcgactcttaaggtttct
	GGGGACCACTTTGTACAAGAAAGCTGGGTtagcatcatcttcaccgagaag
35S-EFR-cDNA	GGGGACAAGTTTGTACAAAAAAGCAGGCTatgaagctgtccttttcacttgtt
	GGGGACCACTTTGTACAAGAAAGCTGGGTAcatagtatgcatgtccgtatttaa
Site-direct mutagenesis	
CERK1-K349E-F	AGGAGAAAAAGCTGCGATTGAGAAGATGGA
CERK1-K349E-R	CAATCGCAGCTTTTTCTCCTCTCAGCTCTG
qRT-PCR	
at5g46630-F	TCGATTGCTTGGTTTGGAAGAT
at5g46630-R	GCACTTAGCGTGGACTCTGTTTG^ATC
CP450-qRT-F	AGGGATGGAAAGTACTGCCA
CP450-qRT-R	ACGATTGACCATCTGTACTTAGTG
EXLA1-qRT-F	CTTCTATCTACAAAGACGGTGCT
EXLA1-qRT-R	GTAATCGCAAGGAACTCTTTGGT
EXLA3-qRT-F	CTTCCATTTACAAAGATGGTGC
EXLA3-qRT-R	ATTGCAAGGAACTCTTTGGT
HSF2A-qRT-F	CATCGTCACAAAGATCTATCCCA
HSF2A-qRT-R	TTTGAATCCGTAAGTGTTGAGC
HSFA2-qRT-F	GTTTACTGGTTCTGTAGCGG
HSFA2-qRT-R	GAATCCATAAGTATTGAGCTGACG
NPF4-qRT-F	GGGCATCATTAGCTTAGTCTCC
NPF4-qRT-R	GTCCAAGAACCTGAAACGAG

Acknowledgements

We want to thank Dr. O. R. Patharkar for valuable comments and proofreading and for the AGL15 phosphoprotein positive control, Dr. A. Jurkevich for assistance with confocal

microscopy, Dr. J. Schoelz for providing the BiFC vectors, and Drs. D. Mendoza-Cozatl and N. Castro-Guerrero for assistance with ICP-OES. This work was supported by the Next-Generation BioGreen 21 Program Systems and Synthetic Agrobiotech Center, Rural Development Administration, Republic of Korea (PJ009068 to GS) and the Division of Chemical Sciences, Geosciences, and Biosciences, Office of Basic Energy Sciences (DE-FG02-08ER15309 to GS. We also gratefully acknowledge funding from the University of Missouri Graduate School for fellowship support (to CE).

Appendix 1

An accurate method to assess dehydration tolerance in *Physcomitrella patens*

Abstract

The moss *Physcomitrella patens* is becoming the model of choice for plant functional analysis at the cellular level. *P. patens* can survive moderate osmotic and salt stress conditions but cannot survive complete desiccation. The objective of this study was to develop an accurate method to assess dehydration tolerance in *P. patens* In order to quantify the extent to which our candidate gene expression altered tolerance. We exposed both wild type and transgenic *P. patens* to atmospheres with air water potentials from –4 MPa (97%RH) to –273 MPa (13%RH) and monitored the water loss from the plants until equilibrium. The ability of the plants to survive the different levels of dehydration was assessed by transferring the dried moss onto fresh medium to allow re-growth. *P. patens* did not survive water potentials lower than -13 MPa. In contrast, the desiccation tolerant moss *Tortula ruralis* can survive dehydration levels of less than -100 MPa. Gene discovery efforts in *T. ruralis* have identified candidate genes that may be essential for the expression of desiccation tolerance. We tested our system on transgenic *P. patens* over-expressing an AP2-like transcription factor from *T. ruralis* that resulted in an increase in dehydration tolerance. The use of this strategy for functional analysis of desiccation responsive genes will offer insight on the cellular processes that underlie dehydration tolerance in plants.

This study was a contribution to the publication: Koster, K.L., Balsamo, R. A., Espinoza, C. and M. J. Oliver. 2010. Desiccation sensitivity and tolerance in the moss *Physcomitrella patens*: assessing limits and damage. Plant Growth Regulation Volume 62, Number 3, 293-302.

Introduction

During the transition from water to land, the earliest land plants needed to survive on land and develop mechanisms to tolerate desiccation [5]. Modern vascular plants have evolved different morphological features to maintain water in their cells, e.g. conductive tissues, cuticle, and stomata; and have retained desiccation tolerance only in specialized structures, e.g. seeds. In contrast, modern bryophytes (mosses) lack these morphological adaptations and their tissues rapidly equilibrate with the surrounding air. This also means that mosses experience drying rates faster than those experienced by the more complex plants like ferns and angiosperms. In order to respond to this rapid drying rate, desiccation tolerant mosses developed a different mechanism than desiccation tolerant angiosperms. Desiccation tolerant mosses, like *Tortula ruralis*, exhibit a constitutive cellular protection mechanism instead of the dehydration-induced response seen in resurrection plants like *Craterostigma plantagineum* and *Sporobolus stapfianus*.[5, 73]. In addition, *T. ruralis* possess a repair mechanism that is induced during rehydration [160].

The moss *Physcomitrella patens* has recently emerged as a powerful, genetically tractable model plant system. The availability of a complete genome sequence [161], together with the ability to perform gene targeting efficiently in *P. patens* has allowed the development of methods to perform gene functional analyses [162]. The life cycle of *P. patens* alternates between haploid and diploid generations, where the haploid generation represents most of the tissues present in the moss. Young tissues (called protonemata) are only a single cell layer thick, providing a window into the cellular basis for any observed phenotype [163]. Once the moss gets old, tissues develop into gametophores (the “shoot” of the moss). Both male and female sexual organs form at the top of the gametophores. After fertilization, the zygote develops into the diploid generation (called sporophyte), where haploid spores are produced and released later into the environment [163]. Its simple morphology makes *P. patens* a model of choice for functional genetic studies of plants at the cellular level.

Physcomitrella patens is highly tolerant to drought, salinity and osmotic stress but it is not desiccation tolerant [164]. However, ABA pre-treatment increases their tolerance to desiccation [165-167], and a double mutant of PROTEIN PHOSPHATASE 2C (PP2C), a negative regulator of ABA signaling, showed increased desiccation tolerance [168]. These reports suggest that ABA plays a role in vegetative desiccation tolerance. Another paper claimed that *P. patens* was desiccation tolerant [169] contradicting previous reports. *P. patens* is tolerant only to moderate water deficit; that is, water loss up to around 90% of its fresh weight (-13 MPa), in contrast to desiccation tolerant mosses like *T. ruralis.* which can survive the loss of all bulk water (-540 MPa) [5]. Since *P. patens* has become a model species to study the mechanisms of desiccation tolerance, it was necessary to define a system that allows accurate measurement of the dehydration responses.

We developed a dehydration assay using *P. patens* protonemal filaments and gametophores, to accurately assess any alteration in the dehydration tolerance of the moss resulting from transgene expression [166]. We concluded that *P. patens* cannot be considered desiccation tolerant since it cannot survive water loss of less than -13 MPa. We transfered a desiccation-induced gene from *T. ruralis* into *P. patens* to investigate if it could confer an increase in tolerance to dehydration.

Gene discovery efforts in the desiccation tolerant moss *T. ruralis* have identified candidate genes that may be essential for the expression of vegetative desiccation tolerance [73, 170]. We constitutively expressed a *T. ruralis* AP2-like transcription factor in *P. patens* and tested its effect on dehydration tolerance using our dehydration assay. We found a transgenic line that increased the dehydration tolerance of *P. patens* from -13 MPa to -37.5 MPa. This transgenic line also showed different morphology and ploidy level. Therefore, further characterization is needed to confirm that the increase in desiccation tolerance was conferred by the *T. ruralis* gene.

Results and Discussion

Physcomitrella patens is not a desiccation tolerant moss

P. patens has been proposed to be a model organism to study and elucidate cellular and molecular mechanisms of dehydration tolerance at the cellular level. However these studies depend upon reproducible methods of dehydration and accurate measurement of hydration status of the tissues. Our objective was to establish an accurate method to assess dehydration tolerance in *P. patens*. Previous studies reported that *P. patens* can survive dehydration. However, these studies dried tissues by exposure to ambient air of unknown RH or without quantifying if the tissues equilibrated to the atmospheric RH. Direct measurement of water potential of the plant is difficult and below -10 MPa is out of the range of current instrumentation. We used the equilibrium dehydration method to assess dehydration tolerance. This method dehydrated the moss tissues over a series of oversaturated salt solutions, which provided a theoretical framework to determine the water potential values. This method has been used routinely to assess desiccation tolerance in seeds and in processed foods [171, 172].

P. patens samples lost water when exposed to RH of 97% and lower. The dehydration rate was rapid when samples were exposed to lower RH, equilibrating at 13% RH (-273 MPa) within 24 h, while at 89% RH (-20 MPa), samples equilibrated after 4 days. *P. patens* routinely survived mild dehydration to RH of 94% or greater (water potential of more than -7 MPa) (Figure A.1 A)., as moss tissue retained a green color in the dried state, and also recovered after rehydration in fresh BCD medium (Figure A.1 B). When equilibrated at 89% RH (-15 MPa), the response was variable, some survived and recovered while others became chlorotic and did not recover after rehydration. When WT moss tissue was equilibrated at RH of 85% and lower, it became chlorotic and was not able to recover after rehydration (Figure A.1 B). Our results indicate that *P. patens* is not desiccation tolerant, because it only survived dehydration levels of up to -7 MPa. In contrast, desiccation tolerant mosses like *Tortula ruralis* can be dried to -540 MPa and recover after re-watering [173].

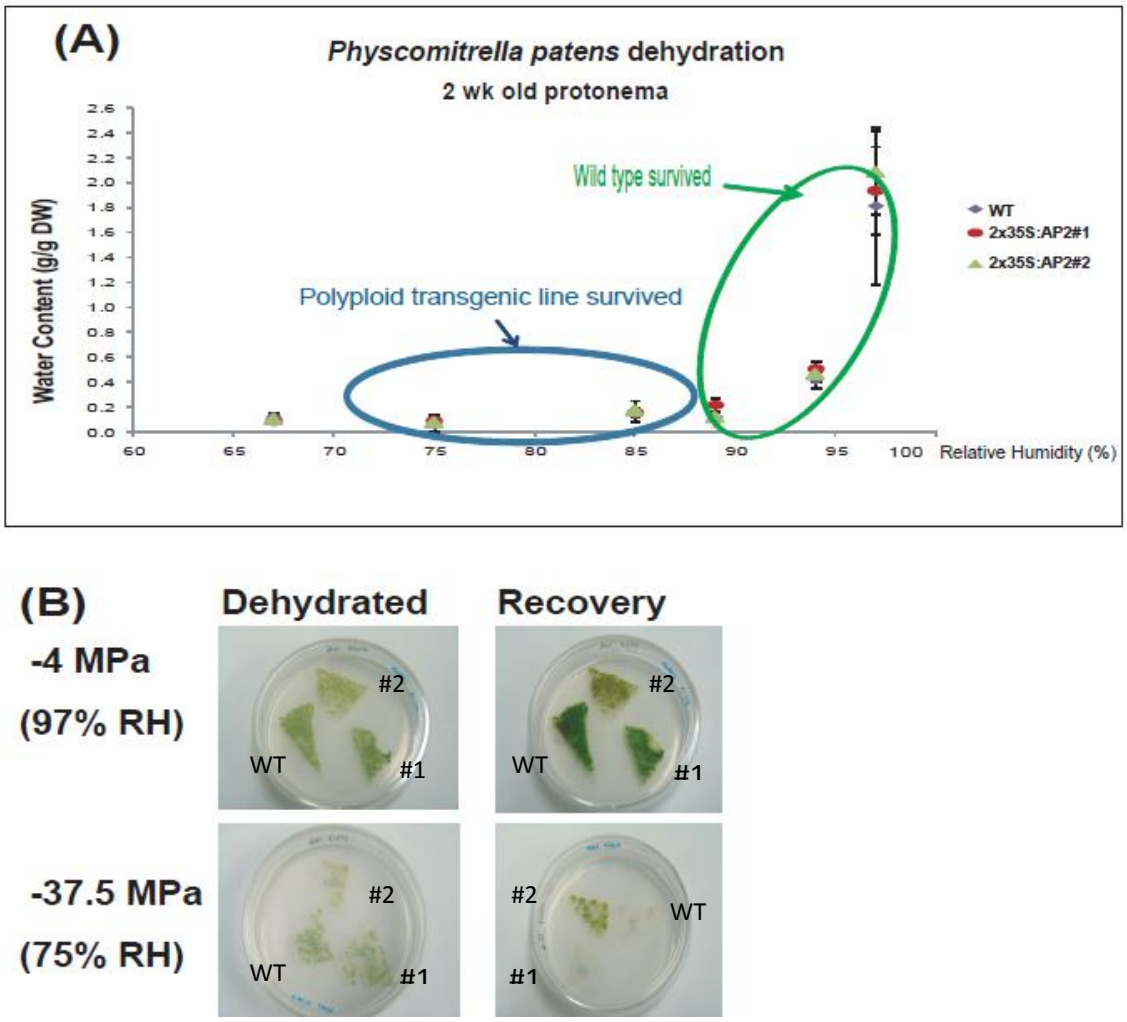

Figure A.1. Dehydration tolerance of *P. patens* dried by equilibration with RH
(A) Moss tissue was exposed to atmospheres with air water potentials from -4 (97%RH) to -57.3 MPa (67% RH) and water content was monitored from the plants until equilibrium. Data shown are means ± SD of four to six replicate samples. (B) Survival was assessed by placement of the treated tissue back on to fresh growth media at full hydration, left pictures show at 0 days after transfer (Dehydrated), and right pictures at 7 days after transfer (Recovery). #1 and #2 represent two independent transgenic lines of moss ectopically expressing a *Tortula rularis* AP2-like TF, WT is wild type.

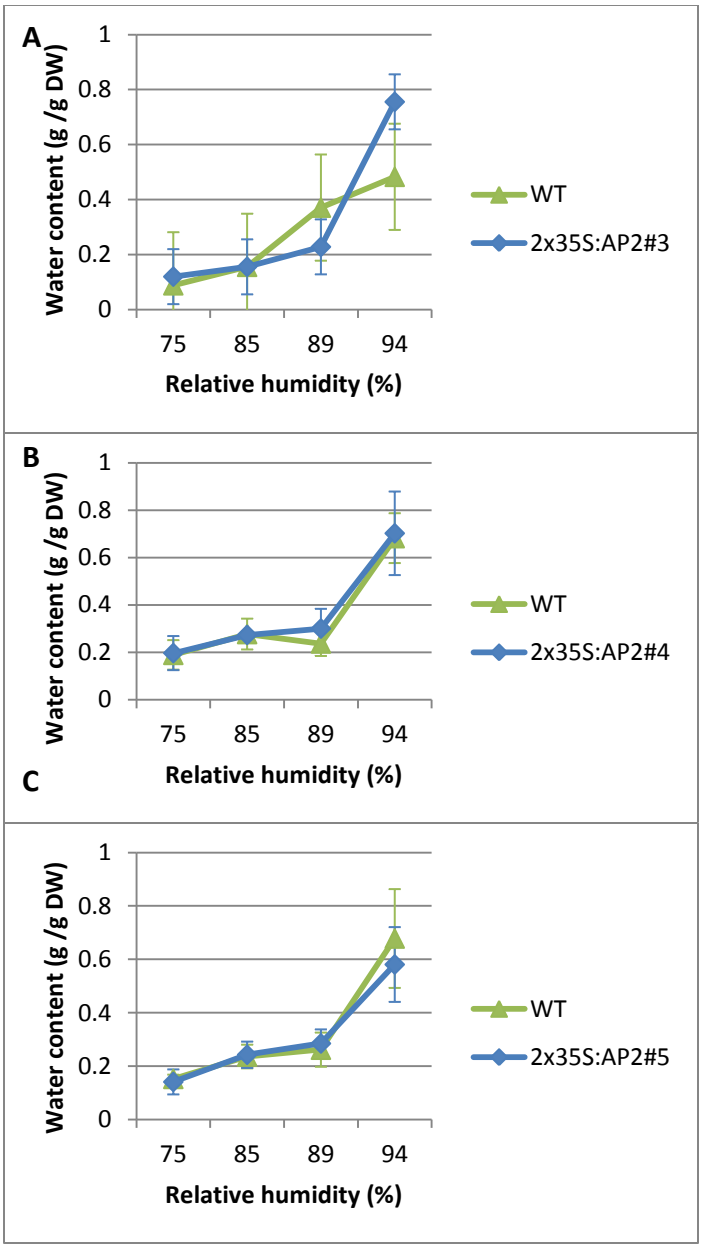

Figure A.2. Water loss comparison of *P. patens* and transgenic lines
Water content on dry matter basis was compared for WT and three independent transgenic lines of moss ectopically expressing a *Tortula ruralis* AP2-like TF. Moss tissue was exposed to atmospheres with air water potentials from -4 (97%RH) to -57.3 MPa (67% RH). Data shown are means ± SD of four to six replicate samples.

A polyploid transgenic line showed enhanced dehydration tolerance

PCR of the splice between the 108 locus of *P. patens* and the sequence of the 2x35S promoter of the transformation vector, confirmed the integration of the vector

containing the TrAP2-like TF into the *P. patens* genome through homologous recombination. (Figures A.3A and A.3B). We also confirmed integration of TrAP2-like TF into *P. patens* by PCR (Figures A.3A and A.3C). We observed two distinct phenotypes in the 2x35S:TrAP2 transgenic lines. The first phenotype, represented by transgenic #1 was similar to wild type, whereas the other phenotype, represented by transgenic #2, showed stunted growth characterized with markedly less production of gametophores, smaller gametophores and also an abnormal leaf shape (Figure A.4).

Transgenic lines dried at the same rate as wild type and there was no difference in water content (g/g DM) (Figures A.1A and Figures A.2A-C). However transgenic line #2, which displayed a different phenotype than WT, was able to recover after drying at RH of 75% (-37.5 MPa) (Figure A.1A-B), this represents a 5-fold increase in dehydration tolerance. Although this increase in dehydration tolerance is greater in comparison to most angiosperms, which survive only to -4 to -6 MPa [174], it is considered desiccation sensitive in bryophytes. Desiccation sensitivity in bryophytes has been defined to maximum limits of dehydration to water potentials of -30 to -48 MPa [175]. Desiccation tolerant bryophytes, as well as their angiosperm counterparts, can survive water potentials less than -100 MPa [176].

In order to understand why only transgenic lines with different morphology were able to survive greater dehydration, we assessed their ploidy level. Polyploid events occur in ~8% of stable regenerants of *P. patens*, and these polyploids can be generated before protoplast isolation or during protoplast regeneration after transformation [177]. Flow cytometry measurements indicated that transgenic #1 (WT-like phenotype) had the same nuclear content as the WT, and transgenic #2 (stunted growth phenotype) had double the nuclear content (Table A.1). These data lead us to think that the observed increased in dehydration tolerance in transgenic #2 may be due to its polyploid nature and not due to expression of the *Tr*AP2-like TF. Both transgenic lines showed the integration of the transgene in the locus 108 of *P. patens* (Figure A.3), but further gene expression and protein synthesis must be assessed to get a conclusion. However there is evidence that polyploidy enhances stress tolerance in plants. Polyploid flowering plants

have undergone one or more whole genome duplications early in their evolution, during times of massive extinction and catastrophic events, which can explain their increased tolerance to environmental stress and higher adaptability [178]. Two different studies suggested that polyploid plants possess a stronger antioxidant defense system which contributes to an increased heat tolerance in a tetraploid *Dioscorea zingiberensis* [179] and to an enhanced adaptability under water stress in the tetraploid and hexaploid species of the grass *Cenchrus* [180].

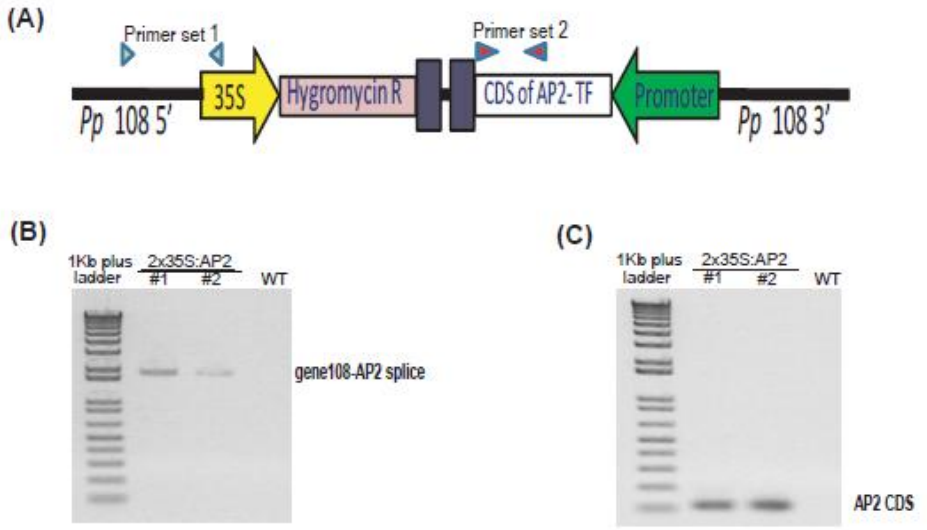

Figure A.3. Targeted insertion of the *Tortula* AP2 gene in *P. patens*
(A)We constructed transgenic lines of *P. patens* that overexpress the *Tortula* AP2-like transcription factor under the control of constitutive promoter 2x35S promoter. Gene targeting at the 108 genomic locus and insertion of AP2 were confirmed by PCR using primer set 1 (B) and primer set 2(c), respectively. Location of the primer sets used is shown by arrowheads.

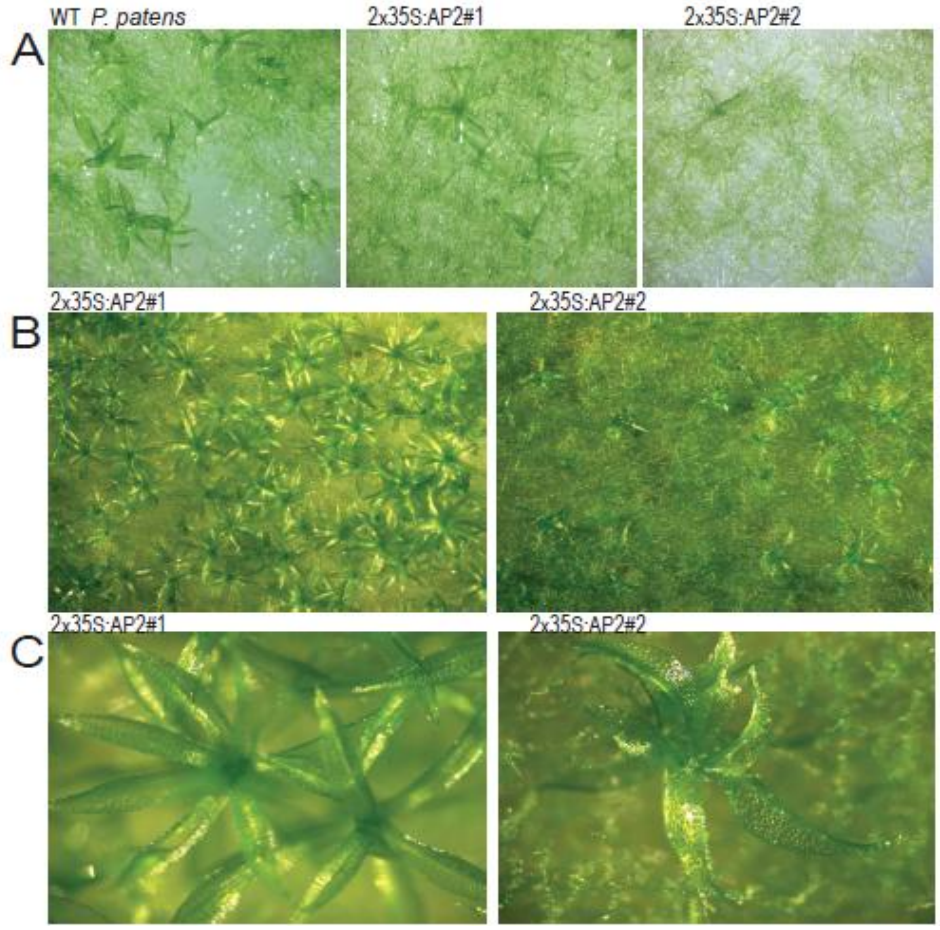

Figure A.4. Phenotypes observe in *P. patens* ectopically expressing *T.ruralis* AP2-like TF
Phenotype of 2x35S:AP2 transgenic #1 is similar to wild type *P. patens*, whereas 2x35S:AP2 transgenic #2 shows markedly less production of gametophores, smaller gametophores and abnormal leaf shape. (A) Morphology of wild type, 2x35S:AP2 #1 and 2x35S:AP2 #2 *P. patens* colonies after 2 weeks of growth (20x). (B) Morphology of 2x35S:AP2 #1 and 2x35S:AP2 #2 *P. patens* colonies after 5 weeks (20x). (C) Close-up view of gametophores shown in (B) (40x).

Table A.1. Ploidy analysis of WT and transgenic lines of *P. patens*

Flow cytometric estimation of nuclear DNA content of tissue samples of wild type *Physcomitrella patens* and 2x35S:AP2 transgenic lines #1 and #2.

Genotype	DNA content (pg/2C)	St. Dev ±
Physcomitrella patens WT (wildtype)	1.52	
	1.54	
	1.49	
	1.50	
	average=1.5	**0.02**
Physcomitrella patens 2x35S:AP2 #1	1.72	
	1.71	
	1.69	
	1.70	
	average=1.7	**0.01**
Physcomitrella patens 2x35S:AP2 #2	2.93	
	2.88	
	2.86	
	2.98	
	average=2.9	**0.06**

Materials and methods

Moss culture.

Physcomitrella patens (Gransden) (kindly provided by R.S. Quatrano and D. Cove at Washington University in St. Louis) was grown on cellophane discs overlaying 0.7% agar in Petri dishes containing minimal medium plus 0.5 g/L (di)ammonium tartrate (BCD medium) ([181]. Cultures were maintained at 24 ^{o}C under a long-day light cycle (16h light [100 µmol $m^{-2}s^{-1}$]/8 h dark).

Gene constructs.

For this study, we selected an AP2/ERF like-transcription factor gene that was shown to be up-regulated in response to desiccation and rehydration in a previous study using the desiccation tolerant moss *Tortula ruralis* [182]. The complete coding sequence of *T. ruralis* AP2-like transcription factor (TF) was amplified from the ATG to the STOP codon (375 bp) and cloned into TOPO T/A (Invitrogen). The resulting construct was verified by PCR and transferred via LR clonase to a PT2x35SGate destination vector (kindly provided by P.F. Perroud and R.S. Quatrano, Washington University in St. Louis), which drives gene expression using the constitutive 2x35S promoter and contains a hygromycin resistance cassette flanked by the *P. patens* 108 genomic locus used as targeting sequence [183]. *P. patens* has the natural ability to integrate foreign sequences by homologous recombination [162, 177]. The final vector was cut with *Swa*I restriction enzyme to linearize the construct prior to transformation. Cloning was performed by J. Elder, a technician at USDA.

Moss transformation.

P. patens protoplasts were transformed using polyethylene glycol (PEG)-mediated DNA uptake [184]. In order to obtain protoplasts, 1-week-old protonema were treated with 0.5% disrelase in 8.5% mannitol for 45 minutes, passed through a 100-µm sieve, incubated for 15 minutes, and passed through a 50-µm sieve. Protoplasts were washed twice in 8.5% mannitol, centrifuged and re-suspended in MMM solution (9.1% mannitol, 10% MES, 15 mM $MgCl_2$) at concentration of $1.6x10^6$ protoplasts/ml. Transformation

was performed by adding 30ug linearized DNA to 300 uL of protoplast suspension, using 300 uL of polyethylene glycol solution and heating at 45^{o}C for 5 minutes. Protoplasts were resuspended in 500 uL 8.5% mannitol and 2.5 mL of molten BCD medium supplemented with 10mM $CaCl_2$ and 8% mannitol, and cultured 90-mm Petri dish containing BCD medium supplemented with 10mM $CaCl_2$ and 6% mannitol. Protoplasts were regenerated in BCD medium for 7 days and then transferred to BCD medium containing hygromycin (30ug/mL) to select for transformants. After 2 rounds of selection, a line was considered stable if both the plate without selection and the plate with selection grew equally well. DNA from transgenic lines and wild type was isolated using CTAB method. Insertion of transgene was confirmed by PCR using 2 sets of primers: Set 1 to verify TrAP2 gene insertion (forward primer 5'-GCATCTGGCTGGGCTCCTTCT-3'; reverser primer 5'-GTACGTGGAGCCGGGGAAGTT-3', expected size band 150 bp); and Set 2 to verify that TrAP2 was inserted into 108 genomic locus (forward primer 5'-CTGGGGGAGTTTTGCTTTCA-3'; reverse primer 5'-AACATAGTATCGTCACCTTCACC-3', expected size band 1669 bp).

Dehydration assay.

P. patens were grown on cellophane discs placed on top of BCD medium for 2 weeks, when most of the tissue comprises protonemal filaments and fewer gametophores. Cellophane discs covered with moss tissue were cut into 2 cm diameter-sections, fresh weight (FW) measured, and transferred to petri dishes. Petri dishes were sealed in chambers containing atmospheres of known relative humidity (RH), and placed in a 20^{o}C incubator, with 16 h light, 8 h dark cycle. Different RH treatments (and their corresponding water potential expressed in MPa) were achieved using saturated salt solutions: 97% RH (-4 MPa) with K_2SO_4; 94% RH (-7 MPa) with KNO_3; 89% RH (-15 MPa) with $MgSO_4$; 85% RH (-21.5 MPa) with KCl; 75% RH (-37.5 MPa) with NaCl; and 67% RH (-57.3 MPa) with NH_4NO_3. Water loss in tissues was monitored daily until samples equilibrated to the RH of the chamber. Dehydrated samples were transferred to fresh BCD medium and maintained under above growth conditions for 7 days. Survival was

scored when more than 30% of tissue remained green and further protonemal growth was observed.

Water content.

After samples had equilibrated to a given RH, dehydrated moss tissue was quickly scraped from its cellophane substrate and transferred into a pre-weighed aluminum dish. Samples were weighed to obtain fresh weight (FW) and oven-dry weight (DW) was measured after drying for 48 hours at 70^{o}C. Water content, expressed on a dry matter basis, was calculated as: (FW –DW)/DW.

Nuclear content estimation.

Flow cytometric estimation of nuclear content of the WT and two transgenic lines was measured using the services of Flow Cytometry and Imaging Core laboratory, Virginia Mason Research Center (Seattle, Washington).

Microscopy.

P. patens protonemal filaments and gametophores were imaged digitally using a Leica MZFLIII stereoscope (Heerbrugg, Switzerland).

Acknowledgements

We want to acknowledge Dr. Karen Koster at University of South Dakota for her guidance, Dr. Ralph Quatrano and Dr. Pierre-Francois Perroud at Washington University, St. Louis, for providing the *P. patens* transformation vectors and training, and staff at Molecular Cytology Core at University of Missouri for assistance with microscopy.

References

1. Schroeder, J.I., et al., *Using membrane transporters to improve crops for sustainable food production.* Nature, 2013. **497**(7447): p. 60-66.

2. Fisher, M.C., et al., *Emerging fungal threats to animal, plant and ecosystem health.* Nature, 2012. **484**(7393): p. 186-94.

3. Oliver, M.J., J.C. Cushman, and K.L. Koster, *Dehydration tolerance in plants.* Methods Mol Biol, 2010. **639**: p. 3-24.

4. Illing, N., et al., *The Signature of Seeds in Resurrection Plants: A Molecular and Physiological Comparison of Desiccation Tolerance in Seeds and Vegetative Tissues.* Integr. Comp. Biol., 2005. **45**(5): p. 771-787.

5. Oliver, M.J., J. Velten, and B.D. Mishler, *Desiccation Tolerance in Bryophytes: A Reflection of the Primitive Strategy for Plant Survival in Dehydrating Habitats?* Integr. Comp. Biol., 2005. **45**(5): p. 788-799.

6. Oliver, M., Z. Tuba, and B. Mishler, *Evolution of desiccation tolerance in land plants.* Plant Ecol, 2000. **151**: p. 85 - 100.

7. Farrant, J.M. and J.P. Moore, *Programming desiccation-tolerance: from plants to seeds to resurrection plants.* Current Opinion in Plant Biology, 2011. **14**(3): p. 340-345.

8. Gaff, D.F., *The desiccation tolerant higher plants of Southern Africa.* Science, 1971. **174**: p. 1033-1034.

9. Gaff, D.F. and R.P. Ellis, *Southern African grasses with foliage that revives after dehydration.* Bothalia, 1974. **11**: p. 305-308.

10. Oliver, M.J., et al., *Proteome analysis of leaves of the desiccation-tolerant grass, Sporobolus stapfianus, in response to dehydration.* Phytochemistry, 2011. **72**(10): p. 1273-1284.

11. Oliver, M.J., et al., *A Sister Group Contrast Using Untargeted Global Metabolomic Analysis Delineates the Biochemical Regulation Underlying Desiccation Tolerance in Sporobolus stapfianus.* The Plant Cell Online, 2011. **23**(4): p. 1231-1248.

12. Jones, J.D. and J.L. Dangl, *The plant immune system.* Nature, 2006. **444**(7117): p. 323-9.

13. Shinya, T., et al., *Chitin-mediated plant-fungal interactions: catching, hiding and handshaking.* Curr Opin Plant Biol, 2015. **26**: p. 64-71.

14. Tanaka, K., et al., *Role of LysM receptors in chitin-triggered plant innate immunity.* Plant Signaling & Behavior, 2013. **8**(1): p. e22598.

15. Petutschnig, E.K., et al., *The Lysin Motif Receptor-like Kinase (LysM-RLK) CERK1 Is a Major Chitin-binding Protein in Arabidopsis thaliana and Subject to Chitin-induced Phosphorylation.* Journal of Biological Chemistry, 2010. **285**(37): p. 28902-28911.

16. Wan, J., et al., *LYK4, a Lysin Motif Receptor-Like Kinase, Is Important for Chitin Signaling and Plant Innate Immunity in Arabidopsis.* Plant Physiology, 2012. **160**(1): p. 396-406.

17. Liu, T., et al., *Chitin-Induced Dimerization Activates a Plant Immune Receptor.* Science, 2012. **336**(6085): p. 1160-1164.

18. Miya, A., et al., *CERK1, a LysM receptor kinase, is essential for chitin elicitor signaling in Arabidopsis.* Proceedings of the National Academy of Sciences, 2007. **104**(49): p. 19613-19618.

19. Wan, J., et al., *A LysM Receptor-Like Kinase Plays a Critical Role in Chitin Signaling and Fungal Resistance in Arabidopsis.* The Plant Cell Online, 2008. **20**(2): p. 471-481.

20. Cao, Y.R., et al., *The kinase LYK5 is a major chitin receptor in Arabidopsis and forms a chitin-induced complex with related kinase CERK1.* Elife, 2014. **3**.

21. Narusaka, Y., et al., *Presence of LYM2 dependent but CERK1 independent disease resistance in Arabidopsis.* Plant Signaling & Behavior, 2013. **8**(9): p. e25345.

22. Faulkner, C., et al., *LYM2-dependent chitin perception limits molecular flux via plasmodesmata.* Proceedings of the National Academy of Sciences, 2013. **110**(22): p. 9166-9170.

23. Willmann, R., et al., *Arabidopsis lysin-motif proteins LYM1 LYM3 CERK1 mediate bacterial peptidoglycan sensing and immunity to bacterial infection.* Proceedings of the National Academy of Sciences, 2011. **108**(49): p. 19824-19829.

24. Petutschnig, E.K., et al., *A novel Arabidopsis CHITIN ELICITOR RECEPTOR KINASE 1 (CERK1) mutant with enhanced pathogen-induced cell death and altered receptor processing.* New Phytologist, 2014. **204**(4): p. 955-967.

25. Wan, J., X.-C. Zhang, and G. Stacey, *Chitin signaling and plant disease resistance.* Plant Signaling & Behavior, 2008. **3**(10): p. 831-833.

26. Kwaaitaal, M., et al., *Ionotropic glutamate receptor (iGluR)-like channels mediate MAMP-induced calcium influx in Arabidopsis thaliana.* Biochem J, 2011. **440**(3): p. 355-65.

27. Wan, J., S. Zhang, and G. Stacey, *Activation of a mitogen-activated protein kinase pathway in Arabidopsis by chitin.* Molecular Plant Pathology, 2004. **5**(2): p. 125-135.

28. Libault, M., et al., *Identification of 118 Arabidopsis Transcription Factor and 30 Ubiquitin-Ligase Genes Responding to Chitin, a Plant-Defense Elicitor.* Molecular Plant-Microbe Interactions, 2007. **20**(8): p. 900-911.

29. Son, G.H., et al., *Ethylene-responsive element-binding factor 5, ERF5, is involved in chitin-induced innate immunity response.* Mol Plant Microbe Interact, 2012. **25**(1): p. 48-60.

30. Meng, X., et al., *Phosphorylation of an ERF Transcription Factor by Arabidopsis MPK3/MPK6 Regulates Plant Defense Gene Induction and Fungal Resistance.* The Plant Cell, 2013. **25**(3): p. 1126-1142.

31. Kadota, Y., et al., *Direct Regulation of the NADPH Oxidase RBOHD by the PRR-Associated Kinase BIK1 during Plant Immunity.* Molecular Cell, 2014. **54**(1): p. 43-55.

32. Li, L., et al., *The FLS2-Associated Kinase BIK1 Directly Phosphorylates the NADPH Oxidase RbohD to Control Plant Immunity.* Cell Host & Microbe, 2014. **15**(3): p. 329-338.

33. Zhang, J., et al., *Receptor-like cytoplasmic kinases integrate signaling from multiple plant immune receptors and are targeted by a Pseudomonas syringae effector.* Cell Host Microbe, 2010. **7**(4): p. 290-301.

34. Munns, R. and M. Tester, *Mechanisms of Salinity Tolerance.* Annual Review of Plant Biology, 2008. **59**(1): p. 651-681.

35. Deinlein, U., et al., *Plant salt-tolerance mechanisms.* Trends in Plant Science, 2014. **19**(6): p. 371-379.

36. Yuan, F., et al., *OSCA1 mediates osmotic-stress-evoked Ca2+ increases vital for osmosensing in Arabidopsis.* Nature, 2014. **514**(7522): p. 367-371.

37. Haswell, E.S. and P.E. Verslues, *The ongoing search for the molecular basis of plant osmosensing.* J Gen Physiol, 2015. **145**(5): p. 389-94.

38. Laohavisit, A., et al., *Salinity-induced calcium signaling and root adaptation in Arabidopsis thaliana require the calcium regulatory protein annexin1.* Plant Physiology, 2013.

39. Hasegawa, P.M., *Sodium (Na+) homeostasis and salt tolerance of plants.* Environmental and Experimental Botany, 2013. **92**(0): p. 19-31.

40. Choi, W.-G., et al., *Salt stress-induced Ca2+ waves are associated with rapid, long-distance root-to-shoot signaling in plants.* Proceedings of the National Academy of Sciences, 2014. **111**(17): p. 6497-6502.

41. Kissoudis, C., et al., *Enhancing crop resilience to combined abiotic and biotic stress through the dissection of physiological and molecular crosstalk.* Frontiers in Plant Science, 2014. **5**.

42. Triky-Dotan, S., et al., *Development of crown and root rot disease of tomato under irrigation with saline water.* Phytopathology, 2005. **95**(12): p. 1438-44.

43. Mohr, P.G. and D.M. Cahill, *Abscisic acid influences the susceptibility of Arabidopsis thaliana to Pseudomonas syringae pv. tomato and Peronospora parasitica.* Functional Plant Biology, 2003. **30**(4): p. 461.

44. Tippmann, H.F.S., U.; Collinge, D. B., *Common themes in biotic and abiotic stress signalling in plants*, in *Floriculture, ornamental and plant biotechnology*, J.A. Teixeira da Silva, Editor 2006. p. 52-67.

45. Wiese, J., T. Kranz, and S. Schubert, *Induction of pathogen resistance in barley by abiotic stress.* Plant Biol (Stuttg), 2004. **6**(5): p. 529-36.

46. Achuo, E.A., E. Prinsen, and M. Hofte, *Influence of drought, salt stress and abscisic acid on the resistance of tomato to Botrytis cinerea and Oidium neolycopersici.* Plant Pathology, 2006. **55**(2): p. 178-186.

47. Reusche, M., et al., *Verticillium infection triggers VASCULAR-RELATED NAC DOMAIN7-dependent de novo xylem formation and enhances drought tolerance in Arabidopsis.* Plant Cell, 2012. **24**(9): p. 3823-37.

48. Mengiste, T., et al., *The BOTRYTIS SUSCEPTIBLE1 Gene Encodes an R2R3MYB Transcription Factor Protein That Is Required for Biotic and Abiotic Stress Responses in Arabidopsis.* The Plant Cell Online, 2003. **15**(11): p. 2551-2565.

49. Luo, H., et al., *The Arabidopsis Botrytis Susceptible1 Interactor Defines a Subclass of RING E3 Ligases That Regulate Pathogen and Stress Responses.* Plant Physiology, 2010. **154**(4): p. 1766-1782.

50. Paparella, C., et al., *The Arabidopsis LYSIN MOTIF-CONTAINING RECEPTOR-LIKE KINASE3 regulates the cross talk between immunity and abscisic acid responses.* Plant Physiol, 2014. **165**(1): p. 262-76.

51. Liang, Y., et al., *Nonlegumes respond to rhizobial Nod factors by suppressing the innate immune response.* Science, 2013. **341**(6152): p. 1384-7.

52. Brotman, Y., et al., *The LysM Receptor-Like Kinase LysM RLK1 Is Required to Activate Defense and Abiotic-Stress Responses Induced by Overexpression of Fungal Chitinases in Arabidopsis Plants.* Molecular Plant, 2012. **5**(5): p. 1113-1124.

53. Suzuki, N., et al., *Abiotic and biotic stress combinations.* New Phytologist, 2014. **203**(1): p. 32-43.

54. Pandey, P., V. Ramegowda, and M. Senthil-Kumar, *Shared and unique responses of plants to multiple individual stresses and stress combinations: physiological and molecular mechanisms.* Frontiers in Plant Science, 2015. **6**.

55. Boyer, J.S., *Plant productivity and environment.* Science, 1982. **218**: p. 443-448.

56. Eckardt, N.A., et al., *The Future of Science: Food and Water for Life.* The Plant Cell Online, 2009. **21**(2): p. 368-372.

57. Battisti, D.S. and R.L. Naylor, *Historical Warnings of Future Food Insecurity with Unprecedented Seasonal Heat.* Science, 2009. **323**(5911): p. 240-244.

58. Proctor, M. and V. Pence, *Vegetative Tissues: bryophytes, vascular resurrection plants and vegetative propagules.* In: Desiccation and Survival in Plants: Drying without dying, 2002: p. 207 - 238.

59. Dinakar, C., D. Djilianov, and D. Bartels, *Photosynthesis in desiccation tolerant plants: Energy metabolism and antioxidative stress defense.* Plant Science, 2012. **182**(0): p. 29-41.

60. Leprince, O. and J. Buitink, *Desiccation tolerance: From genomics to the field.* Plant Science, 2010. **179**: p. 554-564.

61. Moore, J.P., et al., *Towards a systems-based understanding of plant desiccation tolerance.* Trends in Plant Science, 2009. **14**(2): p. 110-117.

62. Martinelli, T., et al., *Amino acid pattern and glutamate metabolism during dehydration stress in the â€˜resurrectionâ€™ plant Sporobolus stapfianus: a comparison between desiccation-sensitive and desiccation-tolerant leaves.* Journal of Experimental Botany, 2007. **58**(11): p. 3037-3046.

63. Moore, J.P.V.-G., Mäite; Farrant, Jill M., and Driouich, Azeddine, *Adaptations of higher plant cell walls to water loss: drought vs desiccation.* Physiologia Plantarum, 2008. **134**(2): p. 237-245.

64. Jones, L. and S. McQueen-Mason, *A role for expansins in dehydration and rehydration of the resurrection plant Craterostigma plantagineum.* FEBS Letters, 2004. **559**(1-3): p. 61-65.

65. Farrant, J.M., W.F. Brandt, and G.C. Lindsey, *An overview of mechanisms of desication tolerance in selected angiosperm resurrection plants.* Plant Stress, 2007(1): p. 72-84.

66. Toldi, O., Tuba, Z., and Scott, P., *Vegetative desiccation tolerance: Is it a goldmine for bioengineering crops?* Plant Science, 2009. **176**: p. 187-199.

67. Yobi, A., et al., *Comparative metabolic profiling between desiccation-sensitive and desiccation-tolerant species of Selaginella reveals insights into the resurrection trait.* Plant J, 2012. **72**(6): p. 983-99.

68. Hilbricht, T., et al., *Retrotransposons and siRNA have a role in the evolution of desiccation tolerance leading to resurrection of the plant Craterostigma plantagineum.* New Phytologist, 2008. **179**(3): p. 877-887.

69. Furini, A., *CDT retroelement: The stratagem to survive extreme vegetative dehydration.* Plant Signal Behav, 2008. **3**(12): p. 1129-31.

70. Frank, W., et al., *Water Deficit Triggers Phospholipase D Activity in the Resurrection Plant Craterostigma plantagineum.* The Plant Cell Online, 2000. **12**(1): p. 111-123.

71. Gaff, D.F., *Desiccation tolerant plants of southern Africa. Oecologia*, 1977. **31**: p. 95-109.

72. Gaff, D.F., et al., *Sporobolus stapfianus, a model desiccation-tolerant grass.* Functional Plant Biology, 2009. **36**: p. 589-599.

73. Oliver, M., et al., *The rehydration transcriptome of the desiccation-tolerant bryophyte Tortula ruralis: transcript classification and analysis.* BMC Genomics, 2004. **5**(1): p. 89.

74. Suarez-Rodriguez, M.C., et al., *Transcriptomes of the desiccation-tolerant resurrection plant Craterostigma plantagineum.* The Plant Journal, 2010. **63**(2): p. 212-228.

75. Collett, H., et al., *Towards transcript profiling of desiccation tolerance in Xerophyta humilis: Construction of a normalized 11 k X. humilis cDNA set and microarray expression analysis of 424 cDNAs in response to dehydration.* Physiologia Plantarum, 2004. **122**(1): p. 39-53.

76. Iturriaga, G., M.A.F. Cushman, and J.C. Cushman, *An EST catalogue from the resurrection plant Selaginella lepidophylla reveals abiotic stress-adaptive genes.* Plant Science, 2006. **170**(6): p. 1173-1184.

77. Gechev, T.S., et al., *Molecular mechanisms of desiccation tolerance in the resurrection glacial relic Haberlea rhodopensis.* Cell Mol Life Sci, 2013. **70**(4): p. 689-709.

78. Altschul, S.F.M., Thomas L.; Schäffer, Alejandro A.; Zhang, Jinghui; Zhang, Zheng; Miller, Webb and Lipman, David J., *Gapped BLAST and PSI-BLAST: a new generation of protein database search programs.* Nucleic Acids Research, 1997. **25**: p. 3389-3402.

79. Emrich, S.J., Barbazuck, W. Brad; Li, Li; and Schnable, Patrick S., *Gene discovery and annotation using LCM-454 transcriptome sequencing.* Genome Research, 2007. **17**: p. 69-73.

80. Doust, A., *Architectural Evolution and its Implications for Domestication in Grasses.* Annals of Botany, 2007. **100**(5): p. 941-950.

81. Conesa, A., et al., *Blast2GO: a universal tool for annotation, visualization and analysis in functional genomics research.* Bioinformatics, 2005. **21**(18): p. 3674-3676.

82. Benjamini, Y. and Y. Hochberg, *Controlling the false discovery rate: a practical and powerful approach to multiple testing.* J Roy Stat Soc Ser B (Stat Method), 1995. **57**: p. 289-300.

83. Thimm, O., et al., *MAPMAN: a user-driven tool to display genomics data sets onto diagrams of metabolic pathways and other biological processes.* Plant J, 2004. **37**(6): p. 914-39.

84. Grandbastien, M.-A., *Activation of plant retrotransposons under stress conditions.* Trends in Plant Science, 1998. **3**(5): p. 181-187.

85. Naito, K., et al., *Unexpected consequences of a sudden and massive transposon amplification on rice gene expression.* Nature, 2009. **461**(7267): p. 1130-1134.

86. Ito, H., et al., *An siRNA pathway prevents transgenerational retrotransposition in plants subjected to stress.* Nature, 2011. **472**(7341): p. 115-119.

87. Battaglia, M., et al., *The Enigmatic LEA Proteins and Other Hydrophilins.* Plant Physiology, 2008. **148**(1): p. 6-24.

88. Hand, S.C., et al., *LEA proteins during water stress: not just for plants anymore.* Annual Review of Physiology, 2011. **73**: p. 115-134.

89. Battista, J., M. Park, and A. McLemore, *Inactivation of two homologues of proteins presumed to be involved in the desiccation tolerance of plants sensitizes Deinococcus radiodurans R1 to desiccation.* Cryobiology, 2001. **43**: p. 133-139.

90. Gal, T., I. Glazer, and H. Koltai, *A LEA group 3 family member is involved in survival of C. elegans during exposure of stress.* FEBS Letters, 2004. **577**: p. 21-26.

91. Liu, Y., et al., *ZmLEA3, a Multifunctional Group 3 LEA Protein from Maize (Zea mays L.), is Involved in Biotic and Abiotic Stresses.* Plant and Cell Physiology, 2013. **54**(6): p. 944-959.

92. Amara, I., et al., *Insights into Maize LEA Proteins: From Proteomics to Functional Approaches.* Plant and Cell Physiology, 2012. **53**(2): p. 312-329.

93. van der Schoot, C., et al., *Plant lipid bodies and cell-cell signaling: A new role for an old organelle?* Plant Signaling & Behavior, 2011. **6**(11): p. 1732-1738.

94. Aubert, Y., et al., *RD20, a Stress-Inducible Caleosin, Participates in Stomatal Control, Transpiration and Drought Tolerance in Arabidopsis thaliana.* Plant and Cell Physiology, 2010. **51**(12): p. 1975-1987.

95. Harb, A., et al., *Molecular and physiological analysis of drought stress in Arabidopsis reveals early responses leading to acclimation in plant growth.* Plant Physiol, 2010. **154**(3): p. 1254-71.

96. Lu, G., et al., *Transcription factor veracity: is GBF3 responsible for ABA-regulated expression of Arabidopsis Adh?* The Plant Cell Online, 1996. **8**(5): p. 847-57.

97. Bartels, D. and S.S. Hussain, *Resurrection Plants: Physiology and Molecular Biology*, in *Plant Desiccation Tolerance*, U. Lüttge, E. Beck, and D. Bartels, Editors. 2011, Springer-Verlag: Berlin Heidelberg. p. 339-364.

98. Gechev, T., et al., *Molecular mechanisms of desiccation tolerance in resurrection plants.* Cellular and Molecular Life Sciences, 2012. **69**(19): p. 3175-3186.

99. Pomeranz, M., J. Finer, and J.-C. Jang, *Putative molecular mechanisms underlying tandem CCCH zinc finger protein mediated plant growth, stress and gene expression responses.* Plant Signaling & Behavior, 2011. **6**(5): p. 647-651.

100. Raffaele, S., et al., *Genome-Wide Annotation of Remorins, a Plant-Specific Protein Family: Evolutionary and Functional Perspectives.* Plant Physiology, 2007. **145**(3): p. 593-600.

101. Tóth, K., et al., *Functional Domain Analysis of the Remorin Protein LjSYMREM1 in Lotus japonicus.* PLos One, 2012. **7**(1): p. e30817.

102. Lefebvre, B., et al., *A remorin protein interacts with symbiotic receptors and regulates bacterial infection.* Proceedings of the National Academy of Sciences, 2010. **107**(5): p. 2343-2348.

103. Raffaele, S., et al., *Remorin, a Solanaceae Protein Resident in Membrane Rafts and Plasmodesmata, Impairs Potato virus X Movement.* The Plant Cell Online, 2009. **21**(5): p. 1541-1555.

104. Checker, V. and P. Khurana, *Molecular and functional characterization of mulberry EST encoding remorin (MiREM) involved in abiotic stress.* Plant Cell Reports, 2013. **32**(11): p. 1729-1741.

105. Yue, J., et al., *A remorin gene SiREM6, the target gene of SiARDP, from foxtail millet (Setaria italica) promotes high salt tolerance in transgenic Arabidopsis.* PLos One, 2014. **9**(6): p. e100772.

106. Guo, W.-J. and T.-H. David Ho, *An Abscisic Acid-Induced Protein, HVA22, Inhibits Gibberellin-Mediated Programmed Cell Death in Cereal Aleurone Cells.* Plant Physiology, 2008. **147**(4): p. 1710-1722.

107. Chen, C.-N., et al., *AtHVA22 gene family in Arabidopsis: phylogenetic relationship, ABA and stress regulation, and tissue-specific expression.* Plant Molecular Biology, 2002. **49**: p. 633-644.

108. Quartacci, M.F., et al., *Desiccation-tolerant Sporobolus stapfianus: lipid composition and cellular ultrastructure during dehydration and rehydration.* Journal of Experimental Botany, 1997. **48**(6): p. 1269-1279.

109. Rossini, S., et al., *Suppression of Both ELIP1 and ELIP2 in Arabidopsis Does Not Affect Tolerance to Photoinhibition and Photooxidative Stress.* Plant Physiology, 2006. **141**(4): p. 1264-1273.

110. Alamillo, J.M. and D. Bartels, *Effects of desiccation on photosynthesis pigments and the ELIP-like dsp 22 protein complexes in the resurrection plant Craterostigma plantagineum.* Plant Science, 2001. **160**(6): p. 1161-1170.

111. Araújo, S.S., et al., *Water deficit and recovery response of Medicago truncatula plants expressing the ELIP-like DSP22.* Biologia Plantarum, 2012: p. 1-5.

112. Zeng, Q., X. Chen, and A.J. Wood, *Two early light-inducible protein (ELIP) cDNAs from the resurrection plant Tortula ruralis are differentially expressed in response to desiccation, rehydration, salinity, and high light.* Journal of Experimental Botany, 2002. **53**(371): p. 1197-1205.

113. Eriksson, S.K. and P. Harryson, *Dehydrins: Molecular Biology, Structure and Function.* 2011. **215**: p. 289-305.

114. Guo, J., et al., *Involvement of Arabidopsis RACK1 in Protein Translation and Its Regulation by Abscisic Acid.* Plant Physiology, 2011. **155**(1): p. 370-383.

115. Barrs, H.D. and P.E. Weatherley, *A re-examination of the relative turgidity technique for estimating water deficits in leaves.* Aust. J. Biol. Sci., 1962. **15**: p. 413-428.

116. Margulies, M., Egholm, M., Altman, W.E., Attiya, S., Bader, J.S., Bemben, L.A., Berka, J., Braverman, M.S., Chen, Y.J., Chen, Z., et al., *Genome sequencing in microfabricated high-density picolitre reactors.* Nature, 2005. **437**: p. 376-380.

117. Pertea, G., et al., *TIGR Gene Indices clustering tools (TGICL): a software system for fast clustering of large EST datasets.* Bioinformatics, 2003. **19**(5): p. 651-652.

118. Childs, K.L., Hamilton, John P.; Zhu, Wei; Ly, Eugene; Cheung, Foo; Wu, Hank; Rabinowicz, Pablo D.; Town, Chris D.; Buell, C. Robin and Chan, Agnes P., *The TIGR Plant Transcript Assemblies database.* Nucleic Acids Research, 2007. **Vol. 35**((Database issue): D846–D851).

119. Singh-Gasson, S., et al., *Maskless fabrication of light-directed oligonucleotide microarrays using a digital micromirror array.* Nat Biotech, 1999. **17**(10): p. 974-978.

120. Neale, A.D., C. K. Blomstedt, P. Bronson, T.-N. Le, K. Guthridge, J. Evans, D. F. Gaff, J. D. Hamill,, *The isolation of genes from the resurrection grass Sporobolus stapfianus which are induced during severe drought stress.* Plant, Cell & Environment, 2000. **23**(3): p. 265-277.

121. Czechowski, T., et al., *Genome-Wide Identification and Testing of Superior Reference Genes for Transcript Normalization in Arabidopsis.* Plant Physiology, 2005. **139**(1): p. 5-17.

122. Ji, H., et al., *The Salt Overly Sensitive (SOS) Pathway: Established and Emerging Roles.* Molecular Plant, 2013.

123. Liang, Y., et al., *Lipochitooligosaccharide recognition: an ancient story.* New Phytol, 2014. **204**(2): p. 289-96.

124. Ayres, P.G., *The Interaction Between Environmental Stress Injury and Biotic Disease Physiology.* Annual REview of Phytopathology, 1984. **22**(1): p. 53-75.

125. Geng, Y., et al., *A Spatio-Temporal Understanding of Growth Regulation during the Salt Stress Response in Arabidopsis.* The Plant Cell Online, 2013. **25**(6): p. 2132-2154.

126. Kreps, J.A., et al., *Transcriptome Changes for Arabidopsis in Response to Salt, Osmotic, and Cold Stress.* Plant Physiology, 2002. **130**(4): p. 2129-2141.

127. Kilian, J., et al., *The AtGenExpress global stress expression data set: protocols, evaluation and model data analysis of UV-B light, drought and cold stress responses.* The Plant Journal, 2007. **50**(2): p. 347-363.

128. Jiang, Y. and M.K. Deyholos, *Comprehensive transcriptional profiling of NaCl-stressed Arabidopsis roots reveals novel classes of responsive genes.* BMC Plant Biol, 2006. **6**: p. 25.

129. Tracy, F.E., et al., *NaCl-induced changes in cytosolic free Ca2+ in Arabidopsis thaliana are heterogeneous and modified by external ionic composition.* Plant, Cell & Environment, 2008. **31**(8): p. 1063-1073.

130. Lee, S., et al., *Proteomic Identification of Annexins, Calcium-Dependent Membrane Binding Proteins That Mediate Osmotic Stress and Abscisic Acid Signal Transduction in Arabidopsis.* The Plant Cell Online, 2004. **16**(6): p. 1378-1391.

131. Jones, A.M., et al., *Border Control—A Membrane-Linked Interactome of Arabidopsis.* Science, 2014. **344**(6185): p. 711-716.

132. Pietraszewska-Bogiel, A., et al., *Interaction of Medicago truncatula lysin motif receptor-like kinases, NFP and LYK3, produced in Nicotiana benthamiana induces defence-like responses.* PLos One, 2013. **8**(6): p. e65055.

133. Umezawa, T., et al., *Genetics and phosphoproteomics reveal a protein phosphorylation network in the abscisic acid signaling pathway in Arabidopsis thaliana.* Sci Signal, 2013. **6**(270): p. rs8.

134. Wang, P., et al., *Quantitative phosphoproteomics identifies SnRK2 protein kinase substrates and reveals the effectors of abscisic acid action.* Proc Natl Acad Sci U S A, 2013. **110**(27): p. 11205-10.

135. Xue, L., et al., *Quantitative Measurement of Phosphoproteome Response to Osmotic Stress in Arabidopsis Based on Library-Assisted eXtracted Ion Chromatogram (LAXIC).* Molecular & Cellular Proteomics, 2013. **12**(8): p. 2354-2369.

136. Patharkar, O.R. and J.C. Walker, *Floral organ abscission is regulated by a positive feedback loop.* Proc Natl Acad Sci U S A, 2015. **112**(9): p. 2906-11.

137. Wang, W., et al., *Timing of plant immune responses by a central circadian regulator.* Nature, 2011. **470**(7332): p. 110-4.

138. Hsu, F.C., et al., *Submergence confers immunity mediated by the WRKY22 transcription factor in Arabidopsis.* Plant Cell, 2013. **25**(7): p. 2699-713.

139. Mohamed, H.A.-L.A. and W.M. Haggag, *Biocontrol potential of salinity tolerant mutants of Trichoderma harzianum against Fusarium oxysporum.* Brazilian Journal of Microbiology, 2006. **37**: p. 181-191.

140. Türkkan, M., *Antifungal effect of various salts against Fusarium oxysporum f.sp. cepae, the causal agent of fusarium basal rot of onion.* Journal of Agricultural Sciences, 2013. **19**(2013): p. 178-187.

141. Kunoh, H., *Ultrastructure and Mobilization of Ions Near Infection Sites.* Annual REview of Phytopathology, 1990. **28**(1): p. 93-111.

142. Park, P., et al., *Leakage of sodium ions from plasma membrane modification, associated with permeability change, in host cells treated with a host-specific toxin from a Japanese pear pathotype ofAlternaria alternata.* Canadian Journal of Botany, 1987. **65**(2): p. 330-339.

143. Sanchez-Vallet, A., J.R. Mesters, and B.P. Thomma, *The battle for chitin recognition in plant-microbe interactions.* FEMS Microbiol Rev, 2015. **39**(2): p. 171-83.

144. Zhao, Y., et al., *The Actin-Related Protein2/3 Complex Regulates Mitochondrial-Associated Calcium Signaling during Salt Stress in Arabidopsis.* The Plant Cell Online, 2013. **25**(11): p. 4544-4559.

145. Laohavisit, A., et al., *Arabidopsis Annexin1 Mediates the Radical-Activated Plasma Membrane Ca2+- and K+-Permeable Conductance in Root Cells.* The Plant Cell Online, 2012. **24**(4): p. 1522-1533.

146. Konopka-Postupolska, D., G. Clark, and A. Hofmann, *Structure, function and membrane interactions of plant annexins: An update.* Plant Science, 2011. **181**(3): p. 230-241.

147. Laohavisit, A., et al., *Zea mays Annexins Modulate Cytosolic Free Ca2+ and Generate a Ca2+-Permeable Conductance.* The Plant Cell Online, 2009. **21**(2): p. 479-493.

148. van der Weele, C.M., et al., *Growth of Arabidopsis thaliana seedlings under water deficit studied by control of water potential in nutrient-agar media.* J Exp Bot, 2000. **51**(350): p. 1555-62.

149. Ni, Z., E.-D. Kim, and Z.J. Chen, *Chlorophyll and starch assays.* Protocol Exchange, 2009.

150. Nakagawa, T., et al., *Development of series of gateway binary vectors, pGWBs, for realizing efficient construction of fusion genes for plant transformation.* J Biosci Bioeng, 2007. **104**(1): p. 34-41.

151. Clough, S.B., AF, *Floral dip: a simplified method for Agrobacterium-mediated transformation of Arabidopsis thaliana.* Plant J, 1998. **16**(6): p. 735-43.

152. Curtis, M.D. and U. Grossniklaus, *A Gateway Cloning Vector Set for High-Throughput Functional Analysis of Genes in Planta.* Plant Physiology, 2003. **133**(2): p. 462-469.

153. Martin, K., et al., *Transient expression in Nicotiana benthamiana fluorescent marker lines provides enhanced definition of protein localization, movement and interactions in planta.* Plant J, 2009. **59**(1): p. 150-62.

154. Lohse, M., et al., *Robin: An Intuitive Wizard Application for R-Based Expression Microarray Quality Assessment and Analysis.* Plant Physiology, 2010. **153**(2): p. 642-651.

155. Smid, M., L.C.J. Dorssers, and G. Jenster, *Venn Mapping: clustering of heterologous microarray data based on the number of co-occurring differentially expressed genes.* Bioinformatics, 2003. **19**(16): p. 2065-2071.

156. Knight, H. and M.R. Knight, *Recombinant aequorin methods for intracellular calcium measurement in plants.* Methods Cell Biol, 1995. **49**: p. 201-16.

157. Tanaka, K., et al., *Extracellular Nucleotides Elicit Cytosolic Free Calcium Oscillations in Arabidopsis.* Plant Physiology, 2010. **154**(2): p. 705-719.

158. Knight, H., Trewavas, A.J., Knight, M.R., *Cold calcium signaling in Arabidopsis involves two cellular pools and a change in calcium signature after acclimation.* Plant Cell, 1996. **8**(3): p. 489-503.

159. Voinnet, O., et al., *An enhanced transient expression system in plants based on suppression of gene silencing by the p19 protein of tomato bushy stunt virus.* The Plant Journal, 2003. **33**(5): p. 949-956.

160. Oliver, M.J., *Influence of Protoplasmic Water Loss on the Control of Protein Synthesis in the Desiccation-Tolerant Moss Tortula ruralis : Ramifications for a Repair-Based Mechanism of Desiccation Tolerance.* Plant Physiology, 1991. **97**(4): p. 1501-1511.

161. Rensing, S.A., et al., *The Physcomitrella Genome Reveals Evolutionary Insights into the Conquest of Land by Plants.* Science, 2008. **319**(5859): p. 64-69.

162. Schaefer, D.G., *A NEW MOSS GENETICS: Targeted Mutagenesis in Physcomitrella patens.* Annual Review of Plant Biology, 2002. **53**(1): p. 477-501.

163. Prigge, M.J. and M. Bezanilla, *Evolutionary crossroads in developmental biology: Physcomitrella patens.* Development, 2010. **137**(21): p. 3535-43.

164. Frank, W., D. Ratnadewi, and R. Reski, *Physcomitrella patens is highly tolerant against drought, salt and osmotic stress.* Planta, 2005. **220**(3): p. 384-394.

165. Khandelwal, A., et al., *Role of ABA and ABI3 in Desiccation Tolerance.* Science, 2010. **327**(5965): p. 546.

166. Koster, K.L., et al., *Desiccation sensitivity and tolerance in the moss Physcomitrella patens: assessing limits and damage.* Plant Growth Regulation, 2010. **62**(3): p. 293-302.

167. Oldenhof, H., et al., *Freezing and desiccation tolerance in the moss Physcomitrella patens: An in situ Fourier transform infrared spectroscopic study.* Biochimica et Biophysica Acta (BBA) - General Subjects, 2006. **1760**(8): p. 1226-1234.

168. Komatsu, K., et al., *Group A PP2Cs evolved in land plants as key regulators of intrinsic desiccation tolerance.* Nat Commun, 2013. **4**: p. 2219.

169. Wang, X.Q., et al., *Exploring the Mechanism of Physcomitrella patens Desiccation Tolerance through a Proteomic Strategy.* Plant Physiology, 2009. **149**(4): p. 1739-1750.

170. Oliver, M.J., et al., *A combined subtractive suppression hybridization and expression profiling strategy to identify novel desiccation response transcripts from Tortula ruralis gametophytes.* Physiol Plant, 2009. **136**(4): p. 437-60.

171. Liang, Y., *Desiccation tolerance of recalcitrant Theobroma cacao embryonic axes: the optimal drying rate and its physiological basis.* Journal of Experimental Botany, 2000. **51**(352): p. 1911-1919.

172. Labuza, I.P., *Moisture Sorption: Practical aspects of isotherm measurement and use.*1984, St Paul, MN: American Association of Cereal Chemists.

173. Wood, A. and M. Oliver, *Molecular biology and genomics of the desiccation tolerant moss Tortula ruralis.* In New Frontiers in Bryology: Physiology, Molecular Biology and Functional Genomics, 2004: p. 71 - 89.

174. Oliver, M.J., *Lessons on Dehydration Tolerance from Desiccation-Tolerant Plants.* 2007: p. 11-50.

175. Wood, A.J., *The nature and distribution of vegetative desiccation-tolerance in hornworts, liverworts and mosses.* The Bryologist, 2007. **110**(2): p. 163-177.

176. Alpert, P. and M.J. Oliver, *Drying without dying*, in *In: Desiccation and Survival in Plants: Drying without dying*, M.B.a.H.W.P. (eds.), Editor 2002, CABI publishing: Wallingford and New York. p. pp. 3 - 43.

177. Cove, D., *The moss Physcomitrella patens.* Annu Rev Genet, 2005. **39**(1): p. 339-58.

178. Fawcett, J.A., S. Maere, and Y. Van de Peer, *Plants with double genomes might have had a better chance to survive the Cretaceous-Tertiary extinction event.* Proc Natl Acad Sci U S A, 2009. **106**(14): p. 5737-42.

179. Zhang, X.-Y., C.-G. Hu, and J.-L. Yao, *Tetraploidization of diploid Dioscorea results in activation of the antioxidant defense system and increased heat tolerance.* Journal of Plant Physiology, 2010. **167**(2): p. 88-94.

180. Chandra, A. and A. Dubey, *Effect of ploidy levels on the activities of delta(1)-pyrroline-5-carboxylate synthetase, superoxide dismutase and peroxidase in Cenchrus species grown under water stress.* Plant Physiol Biochem, 2010. **48**(1): p. 27-34.

181. Ashton, N.W.D.J.C., *The isolation and preliminary characterisation of auxotrophic and analogue resistant mutants of the moss, Physcomitrella patens.* Molec Gen Genet, 1977. **154**: p. 87-95.

182. Oliver, M.J., et al., *A combined subtractive suppression hybridization and expression profiling strategy to identify novel desiccation response transcripts from Tortula ruralis gametophytes.* Physiologia Plantarum, 2009. **136**(4): p. 437-460.

183. Schaefer, D.G. and J.-P. Zryd, *Efficient gene targeting in the moss Physcomitrella patens.* The Plant Journal, 1997. **11**(6): p. 1195-1206.

184. Cove, D.J., et al., *Transformation of the moss Physcomitrella patens using direct DNA uptake by protoplasts.* Cold Spring Harb Protoc, 2009. **2009**(2): p. pdb prot5143.

VITA

Catherine G. Espinoza was born March 10th, 1978 in Lima, Peru. She received her Bachelor of Science degree in Biology from Universidad Federico Villarreal, Lima, Peru in 2001. She joined the International Potato Center (CIP), Lima, Peru, to conduct an undergraduate research thesis under the guidance of Dr. William Roca, to get her Licentiate in Biology in 2003. After that, she joined CIP as a Research Assistant at the Division of Plant Genetic Resources (2003-2008). She received her PhD in Plant, Insect and Microbial Sciences from the University of Missouri-Columbia in December 2015, under the guidance of Dr. Gary Stacey.